Acquisition Directorate

Research & Development Center

Report No. CG-D-01-21

Freshwater In-situ Oil Burning

February 2021

Homeland Security

N O T I C E

This document is disseminated under the sponsorship of the Department of Homeland Security in the interest of information exchange.

For use outside the United States Government, the Government assumes no liability for its contents or use thereof.

The United States Government does not endorse products or manufacturers. Trade or manufacturers' names appear herein solely because they are considered essential to the objective of this report.

M. J. Lewandowski
Environment & Waterways Branch Chief
United States Coast Guard
Research & Development Center
1 Chelsea Street
New London, CT 06320

Technical Report Documentation Page

1. Report No.	2. Government Accession Number	3. Recipient's Catalog No.
CG-D-01-21	AD1124052	

4. Title and Subtitle	5. Report Date
Freshwater In-situ Oil Burning	February 2021
	6. Performing Organization Code Project No. 47041

7. Author(s)	8. Performing Report No.
Murphy, E. A., Adewale, B. S., Pham, H. V., Aurell, J., Gullett, B. K., Arsava, K. S., Lamie, N. J., Wurl, M. A., Cisternelli, M. M., Fitzpatrick, M.	RDC UDI 1835

9. Performing Organization Name and Address	10. Work Unit No. (TRAIS)
U.S. Coast Guard Research and Development Center 1 Chelsea Street New London, CT 06320	11. Contract or Grant No. EPA GLNPO IAA DW-070-95926401-0

12. Sponsoring Organization Name and Address	13. Type of Report & Period Covered
Commander (dr) Ninth Coast Guard District 1240 E 9th Street Cleveland, OH 44199-2001 U.S. Environmental Protection Agency Great Lanes National Program Office 77 West Jackson Blvd Chicago, IL 60604-3507	Interim
	14. Sponsoring Agency Code CGD NINE (dr) EPA/GLNPO

15. Supplementary Notes

The R&D Center's technical point of contact is LT Elizabeth Murphy, 860-271-2866, email: Elizabeth.A.Murphy@uscg.mil.

16. Abstract (MAXIMUM 200 WORDS)

This report documents the background, planning, preparation for, and conduct of a series of in-situ burning (ISB) tests using crude, residual fuel and "bunker" oil in freshwater. Various governments and governmental agencies use ISB to mitigate the effect of oil spills in marine or brackish environments. The Great Lakes provide drinking water to seven states and the most-populated area of Canada. Federal On-Scene Coordinators and Regional Response Teams require more information about ISB in freshwater before considering it a viable oil-spill response tool. The U. S. Coast Guard Research and Development Center (RDC) undertook this effort to gain information on the physical and chemical processes involved in freshwater ISB. RDC conducted this work with material and technical support from the U. S. Army Cold Regions Research and Engineering Lab, the U.S. Naval Research Lab, and the Environmental Protection Agency. The intent is to provide Coast Guard operational commanders and Regional Response Teams information to consider in future discussions on whether ISB is a feasible action to mitigate the threat of large oil quantities spilled in a freshwater environment.

17. Key Words	18. Distribution Statement
In-situ Burning (ISB), Freshwater Oil Spill Response, Great Lakes, Marshland, Burn Efficiency, Burn Residue, Remote Air Monitoring	Distribution Statement A: Approved for public release; distribution is unlimited.

19. Security Class (This Report)	20. Security Class (This Page)	21. No of Pages	22. Price
UNCLAS\\Public	UNCLAS\\Public	108	

(This page intentionally left blank.)

ACKNOWLEDGEMENTS

The project team thanks the following organizations and individuals. The National Oceanic and Atmospheric Administration (NOAA) provided detailed weather reports to ensure safe and effective field testing. The U.S. Coast Guard (USCG) Auxiliary provided professional videography. The USCG Gulf and Atlantic Strike Teams provided ground-based air quality monitoring and emergency medical support during field tests. USCG Sector Mobile provided logistical and field personnel support. The Research and Development Center's (RDC's) Joint Maritime Test Facility (JMTF) staff – Chief Machinery Technician (MKC) Darrel Boyles and Mr. Mike Hering – were instrumental in execution of all phases of field testing. This research was partially funded by the EPA Great Lakes National Program Office through the Great Lakes Restoration Initiative (GLRI).

(This page intentionally left blank.)

EXECUTIVE SUMMARY

In-situ burning (ISB) is an applied response technology to minimize adverse environmental effects of oil spilled on water. The objectives of this research were to: 1) assess the feasibility of ISB as an oil spill response option in freshwater environments such as the Great Lakes, which are in close proximity to population centers; 2) assess the feasibility of ISB for heavy oils such as those identified by Great Lakes stakeholders as commonly transported by pipeline (crude oil) and carried by vessel as fuel (residual marine fuel/"bunker" oil) in the Great Lakes region, and 3) assess the feasibility of ISB in a freshwater marshland environment, such as that found along Great Lakes shorelines, and measure the impact of vegetation on oil consumption during ISB.

The U.S. Coast Guard (USCG) Research and Development Center (RDC) designed a series of ISB tests to begin to address these issues. RDC conducted a total of twenty oil burns (5 small-scale burns, 11 mesoscale burns, and 4 large-scale burns) over a nine-month period (March 2019 to October 2019), including:

1. Small-scale burns at the RDC's Joint Maritime Test Facility (JMTF) on Little Sand Island, Mobile, AL 25-26 March 2019.
2. Mesoscale burns at U.S. Army Engineer Research and Development Center (ERDC), Cold Regions Research and Engineering Laboratory (CRREL) in Hanover, NH 15-19 July 2019.
3. Large-scale burns at JMTF on Little Sand Island, Mobile, AL 17-18 September and 21-22 October 2019.

Tests confirmed ignitability of residual marine grade (RMG) 380 fuel oil and that ten millimeters (10 mm) was a thick enough slick for ignition of this oil, without addition of an accelerant such as diesel fuel. ISB at all test scales resulted in oil boil over outside of the burn containment area. Presence of marshland vegetation resulted in lower peak flame temperatures and burn efficiencies of 10 mm slicks of RMG 380 and Number (No.) 6 Bunker Oil (i.e., Bunker C), another heavy fuel oil similar in characteristics to RMG 380. Vegetation did not affect burn efficiency in tests conducted with crude oil. The large-scale test of RMG 380 with vegetation resulted in a large quantity of sunken residue. All other test scenarios resulted in primarily floating residue immediately after ISB. Furthermore, ISB of RMG 380 yielded more emissions of particulates, black carbon, and volatile organic compounds than crude oil ISB.

In general, burn efficiencies for the mesoscale test burns of Bunker C were in the mid-80% range for conditions without vegetation, and for the large-scale burns of medium crude and RMG 380, in the high-90% ranges, except for the burn with RMG 380 and vegetation. Overall, tests suggested that ISB may be a viable response option for certain crude oils, or for Bunker C oil and RMG 380 in freshwater, within a relatively short period after a spill. However, variability of the results call for additional large-scale burns to better quantify and evaluate burn behavior.

The large-scale tests provided valuable experience using a small unmanned aerial system (sUAS) for air emission monitoring during ISB. The capability of sUAS for remote monitoring may necessitate air monitoring protocol revisions to keep up with advances in technology, developments in techniques, and improvements in understanding.

(This page intentionally left blank.)

TABLE OF CONTENTS

TABLE OF CONTENTS (Continued)

LIST OF FIGURES

LIST OF FIGURES (Continued)

LIST OF TABLES

LIST OF ACRONYMS, ABBREVIATIONS, AND SYMBOLS

=	Equals
<	Less than
–	Minus
#	Number
%	Percent
ºC	Degree(s) Celsius
ºF	Degree(s) Fahrenheit
µg	Microgram(s)
µm	Micron/micrometer
API	American Petroleum Institute
BC	Black carbon
BrC	Brown carbon
BSEE	Bureau of Safety and Environmental Enforcement
BTEX	Benzene, toluene, ethylbenzene, xylenes
C	Carbon
CDC	Center for Disease Control
CFR	Code of Federal Regulations
CG-MER	Coast Guard Office of Marine Environmental Response
cm	Centimeter(s)
CO	Carbon monoxide
CO_2	Carbon dioxide
cP	Centipoise
CRREL	Cold Regions Research and Engineering Laboratory
D9	Ninth Coast Guard District
DRAT	District Response Advisory Team
EC	Elemental carbon
EPA	Environmental Protection Agency
ERDC	Engineer Research and Development Center
FID	Flame ionization detector
FOSC	Federal On-scene Coordinator
ft	Foot or Feet (imperial measurement)
GC	Gas chromotograph(y)
GLRI	Great Lakes Restoration Initiative
GST	Gulf Strike Team
h	Hour(s)
H_20	Water
HRR	Heat release rate
IAA	Interagency Agreement
IARC	International Agency for Research on Cancer
i	Iso (i.e., iso-alkane)
i.e.	“Id est”/in other words
in	Inch(es)

LIST OF ACRONYMS, ABBREVIATIONS, AND SYMBOLS (Continued)

IR	Infrared
ISB	In-situ burning
JMTF	Joint Maritime Test Facility
kg	Kilogram(s)
kn	Knot(s) (nautical mile per hour)
kW	Kilowatt(s)
L	Liter(s)
LOC	Level of Concern
LSI	Little Sand Island
m	Meter(s)
m^3	Cubic meter
M600 Pro	Matrice 600 Pro
MCE_T	Modified combustion efficiency
mg	Milligram(s)
min	Minute(s)
MKC	Chief Machinery Technician
ml	Milliliter(s)
mm	Millimeter(s)
MS	Mass spectrometry
MSD	Mass selective detector
MW	Megawatt
n	Normal (i.e., n-alkane)
n/a	Not applicable
NAAQS	National Ambient Air Quality Standard
ND	Not determined
No.	Number
NOAA	National Oceanic and Atmospheric Administration
NRC	Nuclear Regulatory Commission
NRL	Naval Research Laboratory
NRT	National Response Team
OC	Organic carbon
ORD	Office of Research and Development
OR&R	Office of Response and Restoration
ρ	Density
PAH	Polycyclic aromatic hydrocarbon
PCDD	Polychlorinated dibenzo-*para*-dioxin
PCDF	Polychlorinated dibenzofuran
PM	Particulate matter
PM1.0	Particulates less than one micrometer in diameter
PM2.5	Particulates less than 2.5 micrometers in diameter
PM4.0	Particulates less than four micrometers in diameter
PM10	Particulates less than ten micrometers in diameter

LIST OF ACRONYMS, ABBREVIATIONS, AND SYMBOLS (Continued)

R&D	Research and development
RDC	Research and Development Center
RMG 380	Residual marine grade fuel oil with viscosity up to 380 centistokes
RRT	Regional Response Team
s	Second(s)
SG	Specific gravity
SMART	Special Monitoring of Applied Response Technologies
SOP	Standard operating procedure(s)
SSC	Scientific Support Coordinator
sUAS	Small unmanned aerial system
T	Time
TC	Thermocouple or Total carbon
THFG	Total heat flux gauge
TPH	Total petroleum hydrocarbons
TT	Thermocouple tree
TWA	Time weighted average
UNCLAS	Unclassified
USCG	U.S. Coast Guard
VOC	Volatile organic compound(s)
WHO	World Health Organization
x	Multiplied by

1 INTRODUCTION

In-situ burning (ISB) is a response technology used to minimize the adverse environmental effects of oil spilled on water. It constitutes controlled burning at the spill site for rapid removal of oil from the surface of water (NOAA, 2019). Responders conducted over 400 ISB events to help mitigate the Deepwater Horizon Macondo spill of April 2010. Afterwards, researchers assembled several groups to determine how to address ISB knowledge and capability gaps. While some early efforts contributed to the development of new manuals and guidelines, technical issues for temperate and colder regions, as well as fresh/inland waters, remained outstanding.

ISB is now a generally accepted option for offshore oil spill response, as approved in Area Contingency Plans. The carriage of heavy fuel oil and aging pipelines in the Great Lakes has led regulators and responders to address the feasibility of ISB as a response option closer to shore, in freshwater and marshlands. The decision to consider ISB as a feasible response option in these conditions requires specific information, including:

1. The burn behavior, including ignitability, burn rate, and burn efficiency, of medium to heavy oil spilled on freshwater;
2. The chemical components of the burn residue; whether it floats or sinks, and whether it is more or less toxic to the environment than the original oil (also includes the toxicity of the water);
3. The nature of the air emissions associated with ISB and potential effect on nearby populations; and
4. The effect of vegetation on the burn process, including efficiency, residue, and emissions.

The U.S. Coast Guard (USCG) Research and Development Center (RDC) designed a series of ISB tests to analyze these criteria. This report includes a discussion of test procedures, test data and results, and findings and conclusions regarding the feasibility of ISB as a response option for medium to heavy oil spilled in freshwater, with and without vegetation.

2 BACKGROUND

Most ISB to date, both research and actual field response, occurred in offshore marine (saltwater) and remote brackish environments (Fingas, 2011; Mabile, 2012). This is largely because freshwater bodies tend to be closer to population centers where public safety is a concern (APPENDIX A). The result is a response community knowledge gap about ISB in freshwater. In the wetland environment, the alternative to ISB – mechanical cleanup of oil spills –is problematic due to constricted access and the potential to cause more damage to the ecosystem during response efforts (McCauley & Harrel, 1981; DLaune, Smith, Patrick Jr., Fleeger, & Tolley, 1984; Kiesling, Alexander, & Webb, 1988). Previous wetland ISB research focused on the regrowth and recovery of burnt vegetation, but not the influence of vegetation on burn efficiency. Additionally, understanding the environmental fate of burn residue is important in comparing costs and benefits of different response options.

RDC staff consulted with Ninth Coast Guard District (D9) District Response Advisory Team (DRAT) and the National Oceanic and Atmospheric Administration (NOAA) Great Lakes Scientific Support Coordinator (SSC) to understand Great Lakes region research priorities for ISB response technologies and techniques. The stakeholders identified medium crude oil (37-41 American Petroleum Institute [API] gravity), which is

transported through pipelines, and “bunker oil” or RMG 380 fuel oil, which is carried in large vessel fuel tanks (Figure 1) as priority test oils for ISB research (Table 2). The DRAT identified crude oil having 37-41 API gravity as a Great Lakes worst case spill vulnerability and preparedness priority, and aligned with a pipeline operator’s crude oil commodity map and commodity routing summary. The second priority oil – “bunker oil” – refers to residual fuel oil that powers large vessels. Residual fuel oil is the material remaining after refining the more valuable cuts of crude oil. The designation of 380 identifies oil as having a viscosity up to 380 centistokes – thick and highly viscous. Although residual fuel oil is difficult to pump and may contain pollutants such as sulfur, it is inexpensive and still used to fuel large vessels. Since it does not degrade rapidly, environmental fate of residue remaining after ISB is an important question.

Figure 1. Great Lakes bulk carrier (representative of large commercial ships that use heavy "bunker oil").

3 EXPERIMENT EXECUTION AND RESULTS

RDC researchers designed a series of three experiments to address the feasibility of using ISB as a response to freshwater and marshland oil spills. RDC conducted twenty oil burns over a nine-month period (March 2019 to October 2019), including:

1. Five small-scale burns at the RDC’s Joint Maritime Test Facility (JMTF) on Little Sand Island, Mobile, AL 25-26 March 2019;
2. Eleven mesoscale burns at U.S. Army Engineer Research and Development Center (ERDC), Cold Regional Research and Engineering Laboratory (CRREL) in Hanover, NH 15-19 July 2019; and
3. Four large-scale burns at JMTF AL 17-18 September and 21-22 October 2019.

Because ISB in freshwater research has been limited, researchers planned the tests in terms of increasing size and duration. As such, the small pan tests provided a rudimentary degree of information such as ignitability, action at the oil-water interface, and boil-over or splatter. The team followed up with the mesoscale burns to increase oil amounts and burn time, and to begin experimenting with vegetation, and concluded with the large-scale burns. Researchers kept the relative dimensions of the burn area the same as size increased from small-scale to large-scale to control for any variation in burn behavior related to ISB burn-area shape. Table 1 summarizes the burn tests and provides their basic parameters. Figure 2 shows the relative size of the three burn areas.

Table 1. List of test burns.

Test #	Date	Oil Type	Target Initial Slick Thickness (mm)	Slick Area	Vegetation Coverage (%)
S1	3/25/2019	RMG 380	20	0.18 x 0.36 m (7 x 14 in)	0
S2	3/25/2019	RMG 380	20		0
S3	3/26/2019	RMG 380	10		0
S4	3/25-26/2019	RMG 380	10		0
S5	3/26/2019	RMG 380	10		0
M1	7/15/2019	Bunker C	12.1	0.7 x 1.4 m (2.3 x 4.6 ft)	0
M2	7/16/2019	Bunker C	13.0		0
M3	7/16/2019	Bunker C	13.3		0
M4	7/16/2019	Bunker C	15.1		50
M5	7/16/2019	Bunker C	15.2		50
M6	7/17/2019	Bunker C	15.2		50
M7	7/17/2019	Bunker C	13.3		0
M8	7/17/2019	Bunker C	23.4		0
M9	7/18/2019	Bunker C	18.0		100
M10	7/18/2019	Bunker C	23.8		0
M11	7/18/2019	Bunker C	23.4		100
L1	9/17/2019	Medium Crude	10	2.1 x 4.3 m (7 x 14 ft)	0
L2	9/18/2019	Medium Crude	10		50
L3	10/21/2019	RMG 380	10		0
L4	10/22/2019	RMG 380	10		50

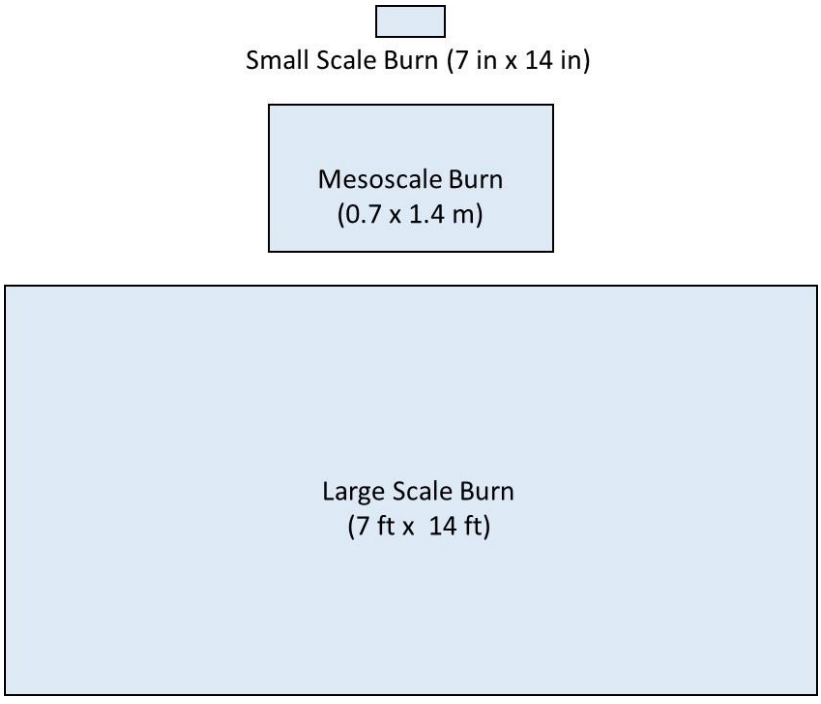

Figure 2. Relative areas of the three burn sets.

Researchers used residual heavy oil (RMG 380) for the small-scale tests. For two of these tests, they added diesel oil to the heavy oil as an accelerant to determine if the diesel made a difference in the ease of ignition. For the mesoscale tests, researchers used Bunker C fuel oil, a heavy oil with similar properties to RMG 380. For the large-scale tests, researchers used RMG 380 and medium petroleum crude oil. Table 2 provides the physical characteristics of the oils used in the tests. APPENDIX B contains specification sheets for the oils.

Table 2. Test oil physical properties.

Test Oil	Density (ρ) at 15ºC (kg/m^3)	API Gravity at 15.5ºC (ºC)	Viscosity (cP)	Flash Point (°C)	Pour Point (°C)
RMG 380	984	12	22,800	80	-21
Bunker C*	974	14	45,030	<132	15
Medium Crude	817	42	93.48	<40	<-30

Table 3 summarizes the parameters and measurements addressed for each scale.

Table 3. Test parameters by scale.

Research Parameters and Measurements	Scale		
	Small	Meso-	Large
Ignitability with and without Accelerant	X		
Starting Slick Thickness	X	X	
Vegetation Coverage		X	X
Burn Efficiency	X	X	X
Flame Spread and Burn Rate		X	X
Temperature and Heat Flux	X	X	X
Visual Observations	X	X	X
Chemical Analysis of Raw Oil			X
Chemical Analysis of Burn Residue	X	X	X
Chemical Analysis of Water			X
Air Emissions			X

Researchers designed the small-scale tests to collect information on heavy oil ignitability, boil-over[1], burn sustainability, and residue characteristics. The small-scale results helped the researchers design the mesoscale and large-scale tests by providing the following input:

- Oil thickness needed for ignition
- Need for additives such as diesel for ignition and sustained burn
- Interaction between the oil and water at their interface and how this affects burn feasibility, boil-over and efficiency

[1] Boil-over is an event in the burning of certain oils in an open top tank when, after a long period of quiescent burning, there is a sudden increase in fire intensity associated with the expulsion of burning oil from the tank (National Fire Protection Association 30).

Researchers designed the mesoscale test of heavy fuel oil in freshwater with and without marshland vegetation to determine the following:

- Burn efficiency
- Effects of boil-over phenomenon
- Characteristics of burn residue
- Influence of vegetation on oil spread rate
- Influence of the vegetation on burn efficiency in terms of mass loss rate, burn rate, and flame spread rate
- Change in heat transfer from the flame to the oil slick when vegetation is present

Researchers designed the large-scale tests of medium crude and RMG 380 oil in freshwater with and without marshland vegetation to determine the following:

- Burn efficiency
- ISB consumption rate of medium crude and RMG 380
- The quantity, fate, and physical and chemical properties of burn residue
- The particulates and emissions concentrations in the smoke plume, and how they move and/or dissipate in time and space

For all ISBs, chemists used gas chromatography-mass spectrometry (GC-MS) to measure polycyclic aromatic hydrocarbons (PAHs), short chain alkanes (C_4-C_9), long chain alkanes (C_{10}-C_{35}), and benzene from samples of raw oil (large-scale only), burn residue, and pre/post burn water. Alkanes are a group of hydrocarbons composed of only carbon and hydrogen. Examples of short alkanes include methane, ethane and propane. PAHs are a class of organic compounds with hydrogen and carbon that contain two or more aromatic rings fused together (Gullet et al., 2017) and include cycloaromatics, diaromatics, triaromatics and quadaromatics. These chemicals release when coal, oil, gas, wood, garbage, or other organic substances burn incompletely and can be harmful to the environment and humans.

3.1 Small-scale Tests

3.1.1 Small-scale Design

RDC conducted small-scale tests at JMTF (Figure 3). The burn area was 0.18 by 0.36 meters (m) (7 x 14 inches). The depth of the freshwater layer was 120 mm (4.72 inches) for all tests. The RDC test team installed the small-scale test apparatus inside a 2.4 m x 2.4 m x 0.71 m (8.25 x 8.25 x 2.4 foot) portable, hinged-steel-frame, emergency spill-containment storage bin. They lined the barrier with fire blankets to reduce the risk of fire spread or environmental contamination. The test apparatus included a 24-gauge stainless steel water pan with overall dimensions of 52.7 cm x 32.4 cm x15.2 cm (20 ¾ in x 12 ¾ in x 6 in) and a fuel oil containment carbon steel ring with dimensions 35.6 cm x 17.8 cm x 5.0 cm (14 in x 7 in x 2 in) (Figure 4).

Figure 3. Joint Maritime Test Facility (JMTF) field site.

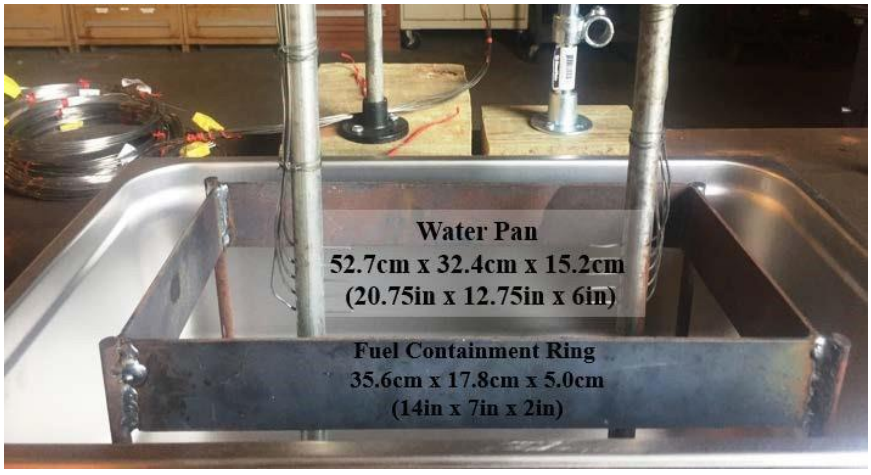

Figure 4. Small-scale test apparatus.

Small-scale test design included processes and instrumentation to determine the following:

- Mass measurements for calculating burn efficiency
- Temperature and heat flux
- Residue chemical analyses
- Visual documentation

3.1.1.1 Mass Measurements for Calculating Burn Efficiency

Burn efficiency is the percent of oil removed from the water surface during burning. Researchers calculated burn efficiency after each completed burn experiment. A digital scale positioned under the burn pan (Figure 5) measured the initial mass of fuel oil added. Researchers weighed residue (unconsumed oil) recovered from the test apparatus after the burns.

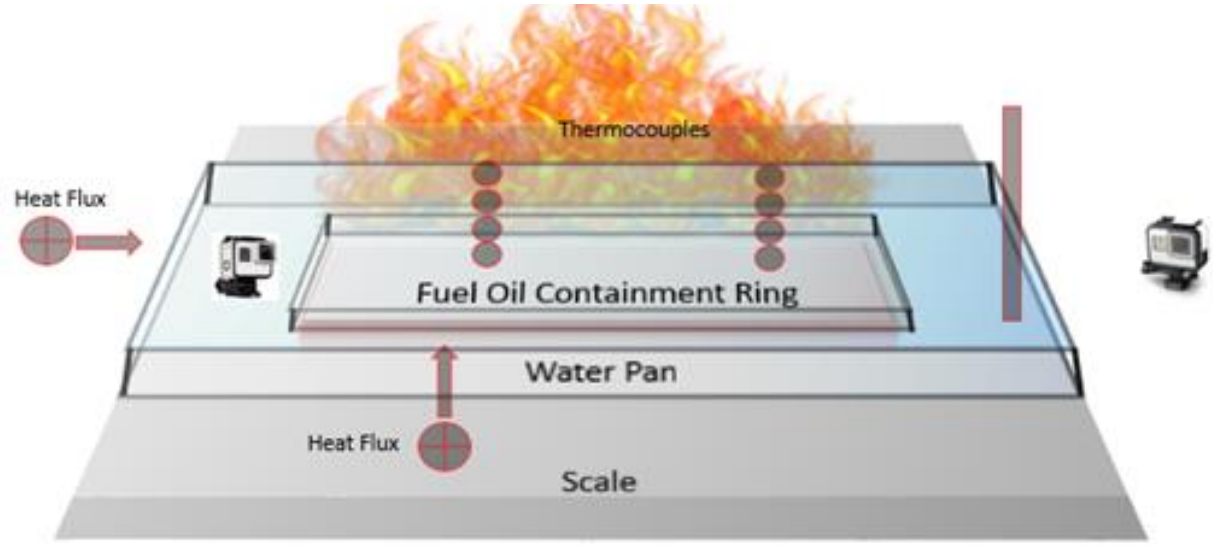

Figure 5. Sketch of small-scale pretest set-up showing scale, thermocouple, and heat flux instrument placement.

3.1.1.2 Temperature and Heat Flux

Researchers used thermocouples to measure flame, fuel, and surface water temperatures. Two Inconel-sheathed Type-K thermocouple trees inside the fuel containment ring measured flame, fuel, and surface water temperature (Figure 5). Each thermocouple tree contained one thermocouple at the water surface to measure water temperature, and five thermocouples staggered above the water surface to measure fuel and flame temperatures. Researchers placed thermocouples at the following heights above the water: 10, 20, 30 and 200 mm (Figure 6). Trees were adjustable vertically and horizontally. Two Medtherm 64-Series total heat flux gauges (THFGs) installed 0.75 m (2.5 ft) to the South and East of the burn pan center, at a height of 51 cm (20 in) measured total heat flux emitted from the flame (Figure 6).

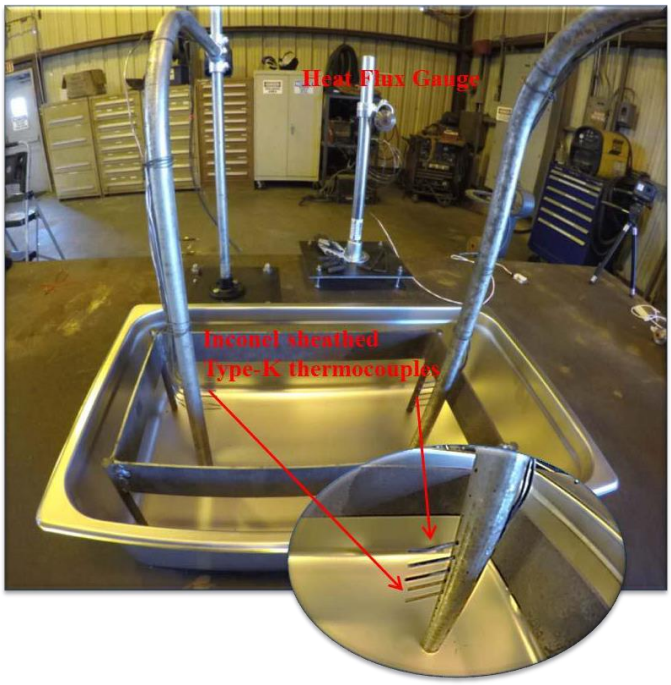

Figure 6. Small-scale instrumentation layout of thermocouples and heat flux gauges.

3.1.1.3 Visual Documentation

The research team estimated pre-boil over and boil over events during the small-scale test by visual and audio observations but did not capture measurement for fuel oil and/or water lost via splashing and vaporizing caused by boil over phenomena.

The test team digitally recorded and manually timed the burns to estimate burn rate. Both infrared (IR) and stationary visual video cameras (GoPro) recorded burn activity. Test technicians reviewed footage in conjunction with instrumentation data to reconcile precision timing.

3.1.2 Small-scale Execution

JMTF and RDC researchers conducted five (5) small-scale ISB tests of RMG 380 in freshwater to determine the oil slick thickness needed for ignition, if additives such as diesel are required for ignition and sustained burn, and behavior of oil and water at their interface during ISB and how this may affect burn feasibility and efficiency. Table 4 lists the small-scale ISB tests and their parameters.

Table 4. Small-scale ISB test matrix and parameters.

Test #	Date	Test Oil Quantity (kg)	Target Test Oil Slick Thickness (mm)	Diesel Accelerant (mm)	Delayed Ignition	Burn Time (min:s)	Wind (kn)	Ambient Temperature
S1	3/25/2019	1.23	20	n/a	No	11:57	0.4	16ºC/60ºF
S2	3/25/2019	1.26	20	20	No	8:32	6.6	19ºC/66ºF
S3	3/26/2019	0.62	10	20	No	5:49	4.0	16ºC/60ºF
S4	3/25-26/2019	0.63	10	n/a	24 hours	3:54	3.0	14ºC/57ºF
S5	3/26/2019	0.62	10	n/a	No	4:47	3.0	14ºC/57ºF

While API ISB guidelines reported ten millimeters (10 mm) as sufficient surface slick thickness for ignition and sustained burn of heavy oils, this guideline was not specific for RMG 380, which did not spread evenly during JMTF lab scale evaluations (API, 2015; NOAA, 2013). Therefore, the team tested two different target oil thicknesses for ignitability – 10 mm and 20 mm. To assess ignitability and optimized burn behavior, the team executed two (2) burns with diesel fuel accelerant.

Additionally, the team delayed ignition of one test iteration (S4) for 24 hours to assess ignitability representative of real world response time. Researchers placed the apparatus under a carport overnight to protect against rain. They placed an expanded metal sheet on top the apparatus to prevent wildlife from interacting with the fuel oil.

Figure 7 shows one of the small-scale tests in progress. Figure 8 shows visual screenshots and associated infrared images of the fire spreading. Figure 9 shows mounted stationary video capture of the small-scale burn activity.

Figure 7. Small-scale test.

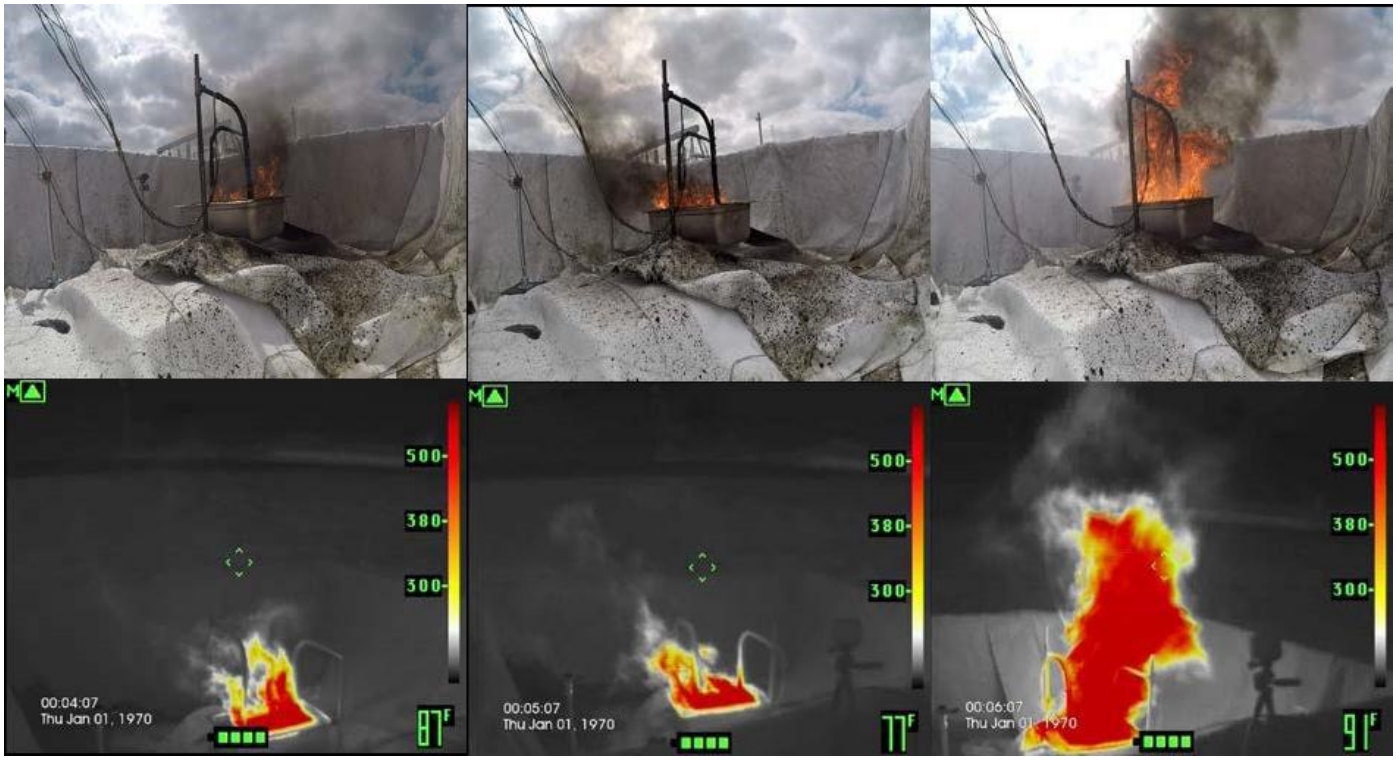

Figure 8. Visual screenshots and associated infrared images of fire spreading.

Figure 9. Mounted stationary video capture of small-scale test.

Researchers used pre-weighed oleophilic/hydrophobic (attract oil only/do not collect water) sorbent pads to collect and measure remaining oil residue by mass. For laboratory quantification of total petroleum hydrocarbon (TPH) in each sample, oiled sorbent pads underwent four (4) liquid-liquid extractions with dichloromethane, then GC-MS injection. Chemical analysis of oiled sorbent pads and freshwater extracts via GC-MS quantified alkanes and aromatics in the samples. Figure 10 shows example post-burn residue sample collection and preparation for chemical analysis.

Figure 10. Post-burn residue sample collection (a) and preparation (b) for chemical analysis.

3.1.3 Small-scale Test Results

3.1.3.1 Ignitability

The small-scale tests provided information about the ignitability of RMG 380 and confirmed that ten millimeters is sufficient surface oil thickness for ignition and sustained burn, in concurrence with API ISB guidelines for heavy oils (API, 2015; NOAA, 2013). Additionally, tests without added diesel accelerant ignited and sustained burn equal in time to those with accelerant. Figure 11 shows ignition of small-scale test without diesel accelerant.

Therefore, the research team concluded diesel accelerant was not necessary for subsequent tests. After 24 hours weathering, small-scale test number four (S4) took 64 seconds longer to ignite, but ultimately did ignite and sustain burn, indicating that RMG 380 could possibly sustain ISB under real world response times.

Figure 11. Propane torch ignition stages over time (T) of RMG 380, 10 mm thickness with no diesel accelerant.

3.1.3.2 Small-scale Burn Efficiency

Researchers calculated the burn efficiency for all three scales using Equation 1.

Equation 1. Burn efficiency.

$$Burn\ Efficiency\ (\%) = \left[\frac{Initial\ Oil\ Mass - Residue\ Mass}{Initial\ Oil\ Mass}\right] \times 100$$

Table 5 shows the mass of unburned residue that remained, and burn efficiency for each small-scale test iteration. Post-test visual inspection showed a black viscous and dense liquid hydrocarbon layer that remained on top of the water surface. Researchers found a hard, tar-like product attached around the lip of the pan and small spherical droplets (tar balls) at the bottom of the pan (Figure 12), which researchers were unable to measure. Omission of this unmeasured residue may have skewed burn efficiency calculations to be higher than they actually were. Researchers also found splashed, oily residue approximately 0.5 m around the pan perimeter (Figure 13), and precipitated soot that lay beyond the exterior of the containment berm.

For tests with accelerant, efficiency calculations included diesel mass. The addition of diesel did not appear to increase burn efficiency.

Table 5. Small-scale ISB residue mass and burn efficiencies.

Test #	Average Wind Speed (kn)	Target Initial Slick Thickness (mm)	RMG 380 Mass In (kg)	Diesel Accelerant Mass In (kg)	Residue Mass Out (kg)	Burn time (min:s)	Burn Efficiency (%)
S1	0.4	20	1.230	n/a	0.180	11:57	85
S2	6.6	20	1.260	0.116	0.430	8:32	66
S3	6.0	10	0.620	0.120	0.260	5:49	58
S4	6.0	10	0.625	n/a	0.200	3:54	68
S5	3.0	10	0.620	n/a	0.140	4:47	77

Figure 12. Hardened residue around pan lip and small tar balls immediataly following small-scale ISB.

Figure 13. Splattered oily residue around the perimeter of the small-scale burn pan.

The fire blanket enclosure used to protect the environment from fire and contamination hazard may have affected burn characteristics by creating a chimney effect under windier conditions, contributing to swirling or turbulent flames, or other impact to air circulation around the fire (Figure 14). It is uncertain if this caused burn efficiency results unrepresentative of open area ISB.

Figure 14. Violent fire growth and swirling behavior observed during small-scale test (S3).

3.1.3.3 Temperature and Heat Flux

As described in section 3.1.1.2, researchers used thermocouples to measure flame, fuel, and surface water temperatures during the small-scale test to determine a correlation between flame temperature and burn efficiency. Table 6 provides a temperature data summary for small-scale tests. Test S1 had equipment calibration errors and did not measure temperature or heat flux. Temperature profiles and heat flux plots for each test are in APPENDIX C.

Table 6. Small-scale ISB temperature data summary.

Test #	Target Initial Slick Thickness (mm)	RMG 380 Mass In (kg)	Diesel Accelerant Mass In (kg)	Burn time (min:s)	Peak Temperature (ºC)	Peak Heat Flux (kW/m^2)
S1	20	1.230	n/a	11:57	n/a	n/a
S2	20	1.260	0.116	8:32	850	12
S3	10	0.620	0.120	5:49	850	21
S4 (delayed ignition)	10	0.625	n/a	3:54	800	17
S5	10	0.620	n/a	4:47	820	20

3.1.3.4 Residue Chemical Analyses

The focus of the chemical analysis was to examine PAH and alkane mass percentages in the post-burn residue, which showed trace levels of hydrocarbons in both weathered and non-weathered samples. For all small-scale tests, the concentration of total i-alkanes was about seven to ten percent greater than total n-alkanes in burn residue, as shown in Figure 15. Neither the addition of diesel (S2 and S3), nor 30 days weathering (S4), had notable influence on the mass percent of total alkanes in the burn residue.

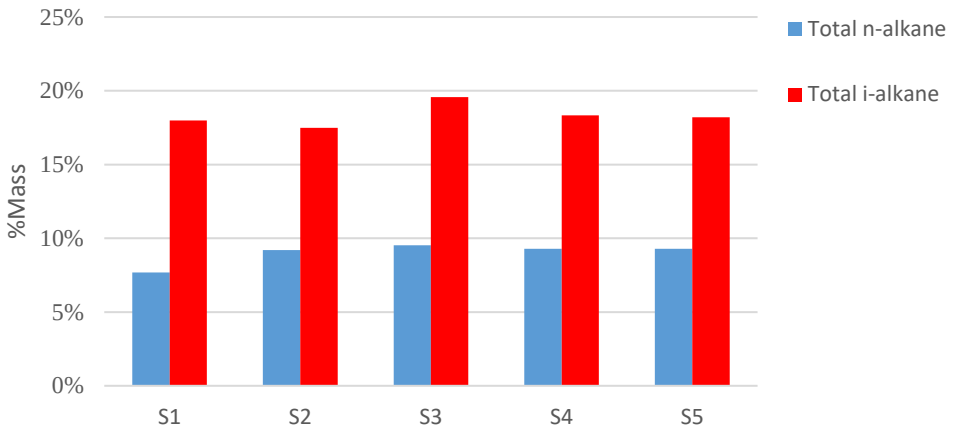

Figure 15. Total n- and i-alkane (C_5-C_{10}) mass percentages in residue from small-scale ISB of RMG 380.

Figure 16 shows PAH concentrations for oil residue from each of the small-scale burns. Thicker (20 mm) starting slicks resulted in more highly concentrated PAH in post-burn residue than thinner (10 mm) starting slicks. S3 (thin slick with diesel) had the lowest concentrations of PAHs.

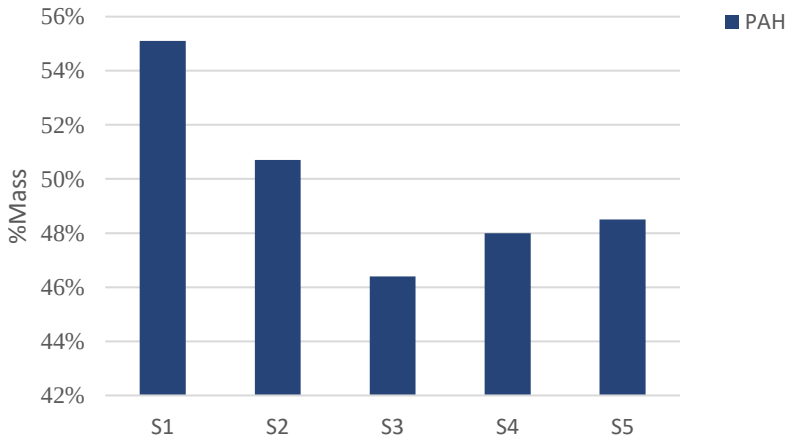

Figure 16. PAH concentrations in post-burn residue

3.1.3.5 Visual Documentation

During all small-scale test iterations, boil-over occurred and resulted in an oiled splatter zone beyond the primary containment of the burn area (Figure 17). During the small-scale burn, as the fire steadily consumed the RMG 380 light chemical components and the fire continued to develop, observers noted crackling sounds approximately three minutes after ignition. Researchers attributed the sounds to water droplets suspended in the fuel rapidly boiling and causing the fuel to splatter (Figure 18).

Figure 17. Boil-over and resultant splatter during small-scale ISB.

Figure 18. Steam eruptions and fuel oil splatter events during small-scale tests.

3.1.3.6 Weathering

Researchers conducted a weathering experiment on the S4 oil residue. Weathering changes the oil's physical and chemical properties. As oil weathers, it can become more viscous and more likely to clump together. Understanding the fate of ISB oil residue may help oil spill responders determine the necessity and/or the timeline for mechanical collection of ISB residue.

Researchers left the burn pan outside in direct/non-direct sunlight for 30 days after the burn. Figure 19, Figure 20, and Figure 21 show the progression of physical weathering of the oil burn residue over 30 days. Immediately after completion of the S4 test, all measureable residue floated. For the first two days (Figure 19), the residue remains afloat.

Figure 19. Oil residue after two days of weathering.

On Day 9 (Figure 20), quarter-sized sunken tar balls began to develop. Researchers removed the metal containment ring (which mimickes the boom) after they observed the sunken tar balls. The containment boom may have affected residue floatation, as some residue appeared to adhere to the metal edge.

Figure 20. Oil residue and tar balls after nine days and sixteen days of weathering.

On day ten, researchers placed the pan inside a carport due to heavy rain but moved the pan back out to direct sunlight on day 16. On day 28, the floating residue turned to thin dried flakes with no liquid/soft residue found on the surface. Rust from the pan clouded the water. Heavy precipitation on day 30 accumulated three centimeters of rain water in the test pan (Figure 21).

Figure 21. Oil residue and tar balls after thirty days of weathering.

3.1.4 Small-scale Summary

The small-scale test yielded the following results that informed design of the mesoscale and large-scale tests.

- Ten millimeters is thick enough for ignition and sustained burn of RMG 380 oil
- Diesel accelerant is unnecessary for ignition and sustained burn of RMG 380 oil and does not appear to increase burn efficiency
- Weathered RMG 380 oil ignited after a 24 hours and then sustained burning
- RMG 380 burn residue remained afloat for up to nine days, after which it began to sink
- Peak burn temperature reached 850°C
- Thicker (20 mm) starting slicks resulted in more highly concentrated PAH in post-burn residue
- Boil over occurs, resulting in an oiled splatter zone beyond the primary containment of the burn area

3.2 Mesoscale Tests

The research team conducted 11 mesoscale tests at CRREL to address three fundamental concepts: baseline burn efficiencies for bunker oil in freshwater at two starting thicknesses, the effect of vegetation on heat transfer from the flame to the oil slick, and the effect of the vegetation on burn efficiency in terms of flame spread, oil-mass loss rate, and post burn residue.

3.2.1 Mesoscale Design

Researchers conducted the mesoscale experiments in CRREL's 12 m (40 ft) long, 2.4 m (8 ft) wide and 2.25 m (7.4 ft) deep tank (Figure 22). Researchers proportionately scaled the actual burn pan area (0.7 m x 1.4 m) between the small-scale and large-scale set-ups (Figure 2). Figure 23 shows a sketch and picture of the mesoscale burn experimental setup, including burn pan area and thermocouple (TC) towers.

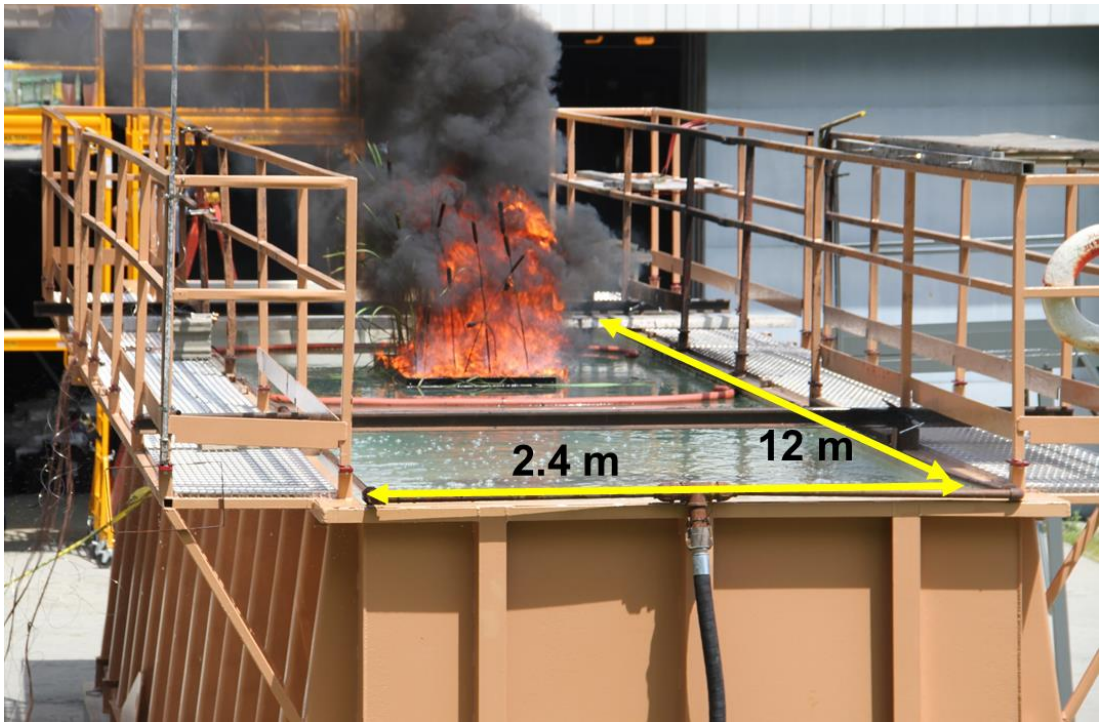

Figure 22. Mesoscale burn in CRREL test tank.

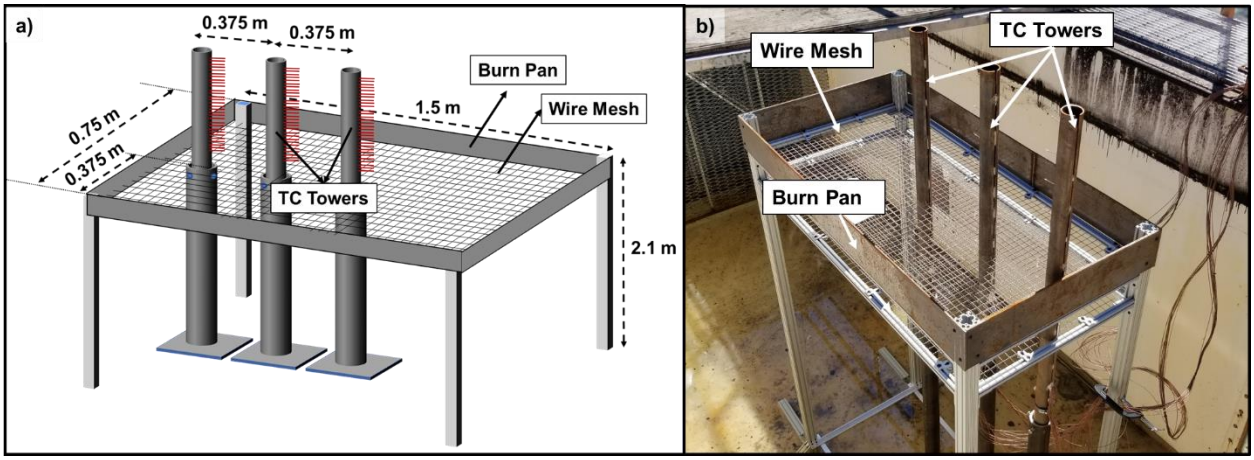

Figure 23. Mesoscale experimental setup a) sketch and b) picture.

Mesoscale test design included instrumentation and processes to determine the following:

- Mass measurements for calculating oil thickness and burn efficiency
- Flame spread and burn rate
- Temperature and heat flux
- Residue chemical analyses
- Visual Documentation

3.2.1.1 Mass Measurements for Calculating Oil Thickness and Burn Efficiency

To calculate burn removal efficiency, researchers compared the pre-burn mass of oil poured into the burn area to the mass of residue recovered after ISB. Researchers determined pre-burn mass by multiplying the burn area size by the desired thickness of the oil divided by oil density. Filter fabric atop the submerged wire mesh captured sunken post-burn residue.

After each burn, researchers allowed the residue to cool. Using pre-weighed sorbent pads and collection bags, they then collected residue and weighed it immediately after. They collected and weighed residue inside and outside of the burn pan separately. Researchers followed this process except for mesoscale burn number ten (M10). Prior to collection, researchers allowed burn residue from M10 to weather 12 hours overnight.

3.2.1.2 Flame Spread and Burn Rate

Researchers determined flame spread rates by recording the ignition time (t_i), times of 50% (t_{50}) and 100% (t_{100}) flame coverage, and self-extinction time ($t_{extinguish}$). Researchers digitally recorded and manually timed each burn to estimate burn rate, and estimated burn rate using the area integration method (APPENDIX D). For this analysis, the burn rate is in terms of 'regression rate' in millimeters per minute (mm/min), or equivalently, a mass loss rate per unit area (Hu, 2017).

3.2.1.3 Temperature and Heat Flux

Researchers used thermocouples (TCs) to measure flame, oil, and water temperatures at different locations as shown in Figure 24. Technicians constructed the TCs with thermocouple wire and fused them using a specialized fine wire welder. Researchers placed three 50 cm high TC towers holding 15 TCs each in the burn pan, one in the center, one 0.375 m away from the side wall, and one on the inside of the north side wall of the burn pan. Technicians designed the towers with telescopic joints for fine vertical adjustment for accurately targeting the burn profile. As shown in Figure 24, researchers placed three total heat flux gauges (HFGs) (orange circles) and three radiometers (light blue circles) 1.3 m away from the burn pan center to measure the total and radiative heat flux emitted from the flame.

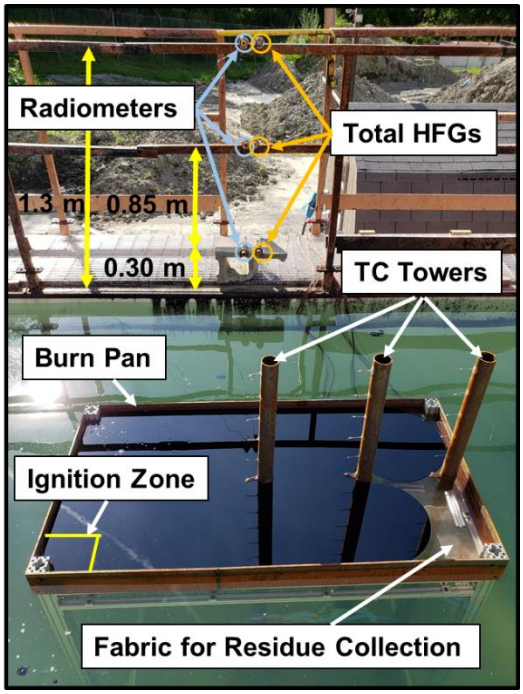

Figure 24. Instrumentation used in mesoscale experiments.

3.2.2 Mesoscale Execution

Table 7 provides details of the mesoscale experimental matrix. Researchers conducted four baseline burns (M1, M2, M3 and M7) with initial oil thickness between 12.1 – 13.3 mm, three burns (M4, M5 and M6) with vegetation covering 50 percent of the burn area (Figure 25), and one burn (M9) with 100 percent vegetation coverage (Figure 26). For the vegetated burns, the study team harvested cattails (*Typha lotifolia)* and stood them upright in the burn area at a density of two stalks per square foot over either 50 or 100 percent of the burn area. Researchers performed three additional tests – two baseline with double the fuel mass (referred to in this report as "double oil mass") (M8 and M10) and one double oil mass with 100 percent vegetation coverage (M11).

Figure 27 shows a fully engulfed mesoscale burn with vegetation, and Figure 28 shows burn residue collection after a mesoscale test.

Table 7. Mesoscale ISB test matrix and parameters.

Test #	Date	Description	Initial Oil Slick Thickness (mm)	Vegetation		Weather	
				Surface Coverage (%)	Density (stems/m²)	Wind Speed (kn)	Rain (mm)
M1	7/15/2019	Baseline	12.1	0	0	2.04	0
M2	7/16/2019	Baseline	13.0			1.40	
M3	7/16/2019	Baseline	13.3			2.60	
M4	7/16/2019	50% vegetation	15.1	50	26	1.17	
M5	7/16/2019	50% vegetation	15.2		30	2.18	
M6	7/17/2019	50% vegetation + rain	15.2		25	1.44	0.51
M7	7/17/2019	Baseline	13.3	0	0	1.61	0
M8	7/17/2019	Baseline double oil mass	23.4			4.06	
M9	7/18/2019	100% vegetation	18.0	100	26	3.98	
M10	7/18/2019	Baseline double oil mass	23.8	0	0	1.77	
M11	7/18/2019	100% vegetation, double oil mass	23.4	100	26	1.46	

Figure 25. Mesoscale ISB with 50 percent vegetation coverage.

Figure 26. Mesoscale ISB with 100 percent vegetation coverage.

Figure 27. Fully engulfed mesoscale ISB with vegetation.

Figure 28. Burn residue collection after mesoscale ISB.

3.2.3 Mesoscale Test Results

The mesoscale tests provided information on ISB of bunker fuel in freshwater, including the effect of vegetation on burn characteristics. Analysts also quantified the change in heat transfer from the flame to the oil slick and the influence of vegetation on burn efficiency in terms of mass loss rate, flame spread, and post burn residue.

3.2.3.1 Mesoscale Burn Efficiency

Table 8 shows the burn efficiencies for bunker oil in freshwater, including two oil thicknesses (standard baseline and baseline double oil mass) and two amounts of vegetation cover.

Table 8. Mesoscale ISB residue mass and burn efficiencies.

Test #	Description	Mass In (kg)		Residue Mass Out (kg)		Burn Efficiency (%)
		Oil	Vegetation	Inside Burn Pan	Outside Burn Pan	
M1	Baseline	11.02	n/a	0.63	1.32	82.30
M2	Baseline	10.96	n/a	0.36	0.96	87.96
M3	Baseline	11.22	n/a	0.73	0.91	85.38
M4	50% vegetation	10.95	3.36	2.09	0.89	79.18
M5	50% vegetation	11.09	1.30	1.83	0.95	77.56
M6	50% vegetation + rain	11.02	2.22	2.28	1.07	73.26
M7	Baseline	11.25	n/a	1.16	1.29	78.22
M8	Baseline double oil mass	22.70	n/a	1.21	2.21	84.93
M9	100% vegetation	11.34	2.80	2.62	1.13	73.48
M10	Baseline double oil mass	23.10	n/a	1.95	1.29	85.97
M11	100% vegetation, double oil mass	21.75	3.15	2.67	1.25	84.26

The mesoscale tests fell into one of five conditions (Table 9): baseline (thin layer); baseline double oil mass (thick layer), 50% vegetation (thin layer); 100% vegetation (thin layer); and 100% vegetation, double oil mass (thick layer).

Table 9. Average mesoscale ISB burn efficiencies.

Description	Number of Trials	Average Burn Efficiency (%)	Standard Deviation (%)
Baseline “thin slick”	4	83	2.83
Baseline double oil mass “thick slick”	2	85	n/a
50% vegetation, “thin slick”	3	77	3.06
100% vegetation, “thin slick”	1	73	n/a
100% vegetation, double oil mass “thick slick”	1	84	n/a

The experiments indicate for the most part, baseline thin layer (M1, M2, M3 and M7) efficiencies (83%) compare to baseline double-mass thick layer (M8 and M9) efficiencies (85%). NOTE: This average includes one baseline thin layer burn (M7) where burn efficiency was 78%.

Three thin layer tests with vegetation covering 50% of the burn area (M4, M5 and M6) had an average burn efficiency of 76%, including where light rain occurred during burn M6. The full vegetation (100% covered) thin slick (M9) burn efficiency was 73%. For the tests performed with higher oil mass (M8, M10 and M11), the vegetation did not have a measured effect on burn efficiency (approximately 85%).

3.2.3.2 Flame Spread and Burn Rate

The flame spread rates in the second half of the burn pan were about two to three times higher than the spread rates in the first half (side of ignition) of the pan. When the flame reached the midpoint, heat feedback from flame to fuel was sufficient to heat the oil surface to a point where its viscosity decreased significantly. Less viscous, heated fuel spread and evaporated rapidly, allowing the flame front to advance.

The average burn rate of the four baseline tests was about 2.4 mm/min, while the average burn rate of the 50% (M4 and M5) and 100% vegetation burns was 2.37 mm/min. For the increased double oil mass tests,

the burn rate of the baseline and 100% vegetation was about 2 mm/min. The results indicated the vegetation had no significant influence on the burn rate (Table 10).

Table 10. Average mesoscale ISB flame spread and burn rates.

Description	Number of Trials	Flame spread rate through 1st 50% of pan (mm/min)	Flame spread rate through 2nd 50% of pan (mm/min)	Burn Rate (mm/min)
Baseline "thin slick"	4	330.9	867.5	2.4
Baseline double oil mass "thick slick"	2	340.9	804.6	2.0
50% vegetation, "thin slick"	3	328.5	884.2	2.4
100% vegetation, "thin slick"	1	357.0	652.0	2.4
100% vegetation, double oil mass "thick slick"	1	245.9	737.7	2.1

3.2.3.3 Temperature and Heat Flux

Figure 29 shows the vertical temperature distribution from the central TC tree for a baseline (M3), 50% vegetation (M4), and 100% vegetation (M9) test one minute after reaching 100% flame coverage (t_{100}). During the mesoscale tests, flame temperature inversely related to vegetation coverage. In other words, when vegetation was greater, flame temperature was lower. With 100% vegetation, the temperature ten centimeters above the fuel layer reached up to 680°C, which is around 200°C lower than the baseline case. This difference appeared to dissipate around 20 cm above the fuel layer, possibly due to greater separation of hot gas from the vegetation. See APPENDIX D for comprehensive temperature and heat flux profiles from mesoscale tests.

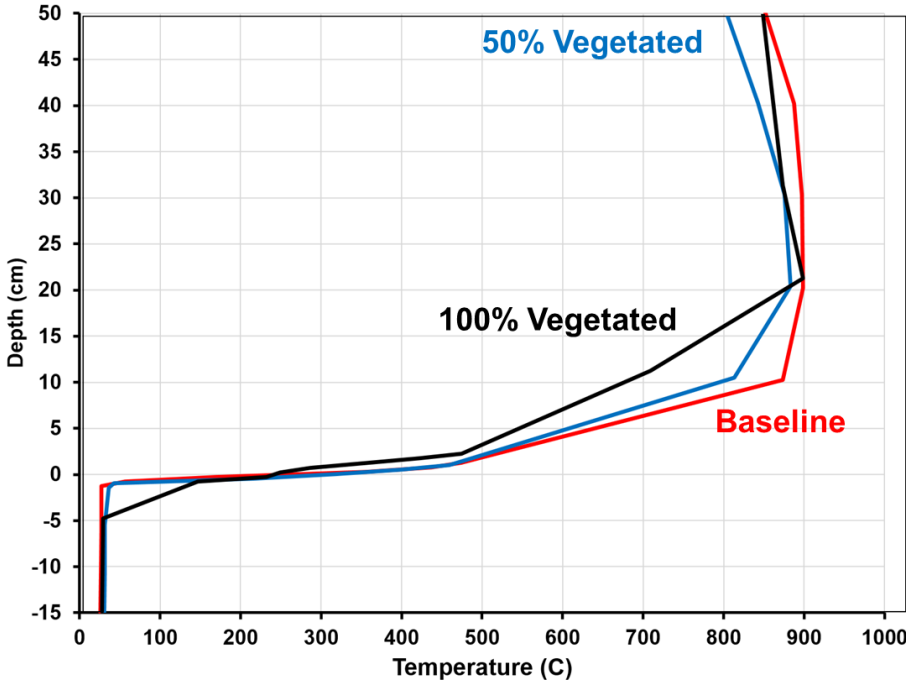

Figure 29. Temperature profiles at the pan center for one minute after reaching t_{100}.

3.2.3.4 Residue Chemical Analyses

The focus of the chemical analysis was to examine the percent of alkanes and PAHs in the burn residue with and without vegetation. Figure 30 shows the summary of the post-burn chemical analysis for n- and i- short chain alkanes and PAH for the mesoscale tests. Tests M5 (50% vegetation), M8 (baseline double oil mass) and M9 (100% vegetation) had the highest total i-alkanes mass percentages.

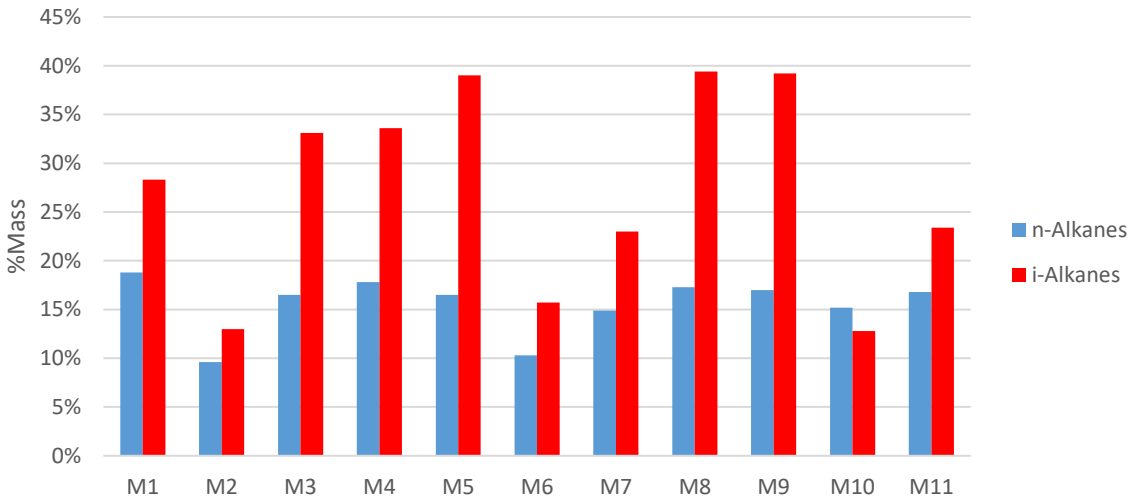

Figure 30. Total n- and i-alkane mass percentages in residue from mesoscale ISB of Bunker C Oil.

The post-burn residue in the full vegetation test (M9) had substantially decreased concentrations of cycloaromatics and diaromatics compounds when compared with baseline tests (M1, M2, M3 and M7). Triaromatic and quadaromatic compounds were highest for full vegetation (M9) and partial vegetation (M4 and M5) tests, as shown in Table 11.

Table 11. Mesoscale ISB residue concentrations of PAH (mass percent).

Compound	Test #										
	M1	M2	M3	M4	M5	M6	M7	M8	M9	M10	M11
Cycloaromatics	4%	11%	3%	1%	3%	9%	6%	7%	0%	6%	5%
Diaromatics	25%	29%	24%	20%	22%	24%	21%	18%	12%	17%	21%
Triaromatics	28%	16%	30%	35%	35%	14%	21%	26%	35%	19%	23%
Quadaromatics	17%	6%	16%	23%	23%	4%	10%	23%	32%	9%	16%
Total PAH	**74%**	**62%**	**72%**	**80%**	**83%**	**51%**	**58%**	**74%**	**78%**	**50%**	**74%**

3.2.3.5 Visual Documentation

During the mesoscale test of Bunker C oil, boil over occurred and resulted in an oiled splatter zone beyond the primary containment of the burn area (Figure 31) and boil over splatter remained within a radius 1.7 m secondary containment. Figure 32 shows splatter outside of the burn area from boil over during a mesoscale test.

Figure 31. Boil over visible during mesoscale ISB.

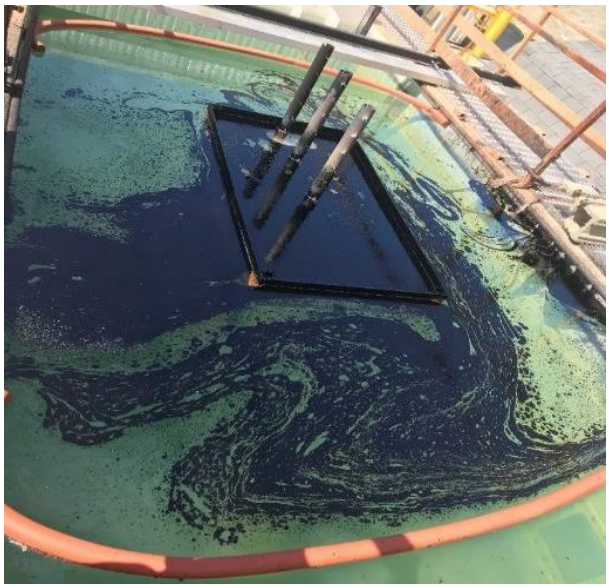

Figure 32. Splatter outside of the burn area from boil over during mesoscale ISB.

3.2.4 Mesoscale Summary

The mesoscale test provided the following results that informed the design of the large-scale tests.

- The average burn efficiency of Bunker C in freshwater without vegetation was approximately 85%
- There was a decrease in burn efficiency of thin oil slicks with vegetation
- The influence of vegetation on burn efficiency was minimal for the tests performed with thick oil slicks
- Vegetation had no significant influence on the burn rate
- There was decreased hot gas temperatures in vegetation tests
- Residue from burns with vegetation had higher concentrations of PAHs

- In all cases, boil over occurred, resulting in an oiled splatter zone beyond the primary containment of the burn area

3.3 Large-scale Tests

Researchers conducted four (4) large-scale ISB tests at JMTF on Little Sand Island (LSI) in Mobile Bay, AL. The team executed two burns of medium crude oil (37-41 API gravity) in freshwater, one without vegetation (baseline) and one with vegetation on 17-18 September 2019. Due to unfavorable wind conditions, RDC could not complete all large-scale burns during the same timeframe. The team conducted two burns of RMG 380 in freshwater, one baseline and one with vegetation on 21-22 October 2019.

In planning the large-scale test, the research team used information gained during the small-scale and mesoscale tests: (1) boil over resulted in a splatter zone beyond the primary burn area containment; (2) 10 millimeters (mm) was a sufficient surface oil thickness for ISB of RMG 380; (3) diesel accelerant was unnecessary to ignite and sustain a burn.

The large-scale ISB tests addressed four fundamental concepts: ISB consumption rate and burn efficiency of heavier crude and fuel oils in freshwater, effects of vegetation on ISB, the quantity, fate and physical and chemical properties of burn residue, and particulate and emission concentrations in the smoke plume.

Large-scale tests included processes and instrumentation to collect the following:

- Mass measurements for calculating burn efficiency
- Flame spread and burn rate
- Temperature and heat flux
- Residue and water chemical analyses
- Emissions inside the smoke plume
- Ground-based air quality monitoring
- Visual documentation

3.3.1 Large-scale Design

Researchers used the JMTF 30 m (100 ft) long, 9.1 m (30 ft) wide and 1.5 m (5 ft) deep tank. Following the size-scaling previously discussed in Section 3.2.1, researchers made the approximately 2.1 x 4.3 m (7 x 14 feet) burn area with a fire boom as primary containment. A secondary containment boom collected splatter from boil over and the test team installed fire blankets on the east and west side of the burn area to minimize risk of environmental contamination (Figure 33).

Figure 33. Large-scale burn-pan layout at JMTF.

3.3.1.1 Fuel Rate

The large-scale burn design included target burn length of 20-30 minutes to allow for flame engagement replicative of full-scale field response efforts. This would require each burn sample to consist of 155-170 gallons of oil according to the U.S. Nuclear Regulatory Commission (NRC) Handbook burn duration/fuel consumption calculations for heavy fuel, an industry accepted source for burn science standards (NRC, 2004). The researchers used a continuous oil feed system to deliver the crude and RMG 380 oils to the burn pan. Figure 34 shows the flowing fuel delivery system used for the large-scale ISB.

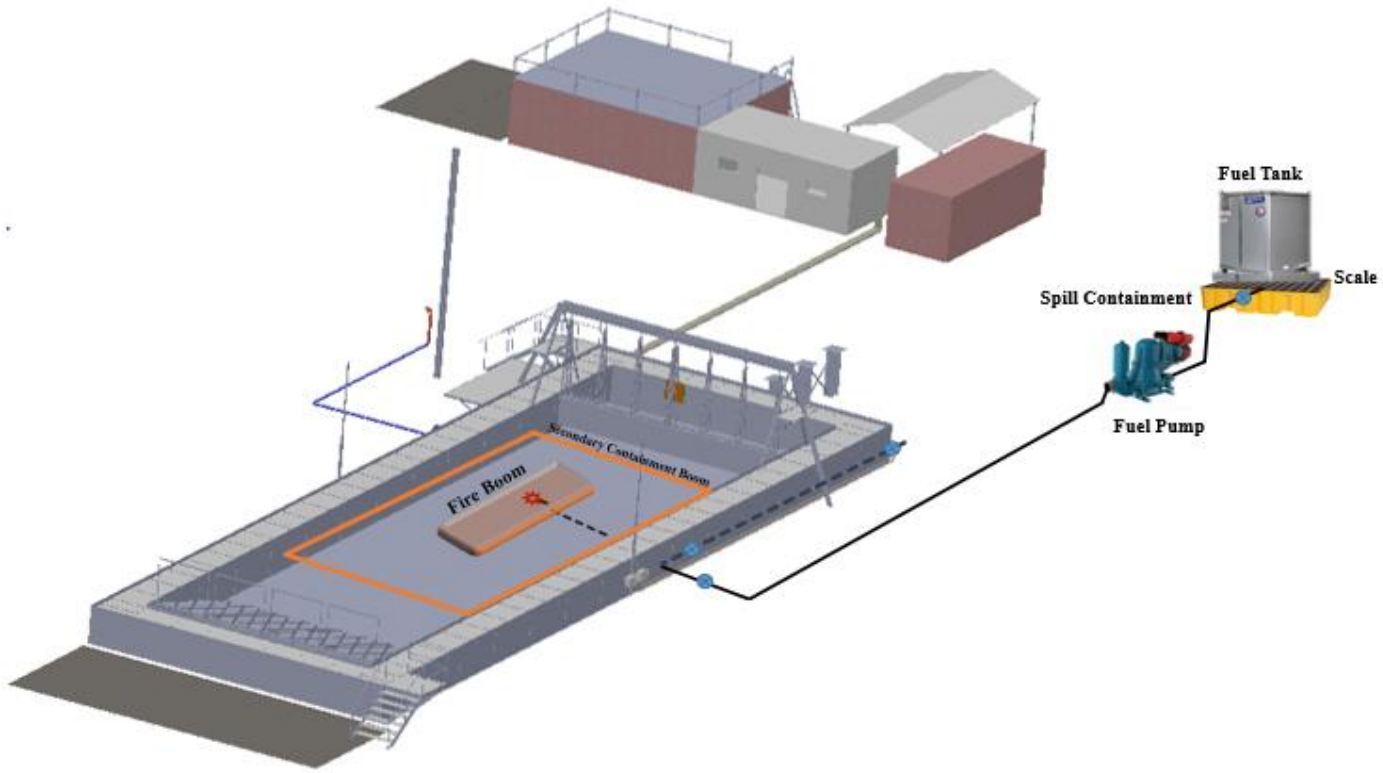

Figure 34. Flowing fuel system large-scale ISB.

The research team planned to achieve estimated desired initial oil thickness by multiplying target thickness by the surface area within the fire boom to determine the initial volume to pump prior to ignition. Pumping stops once the surface oil reaches the relative target oil thickness of 10 millimeters. After ignition and the flame engulfs the oil, researchers control a continuous flow to the burn area to maintain the relative target thickness until the sample size is consumed. The test team attempted to maintain an approximation of the desired thickness throughout the burn according to expected burn rate per the NRC Handbook and published pump rate for the motor and material density, a target flow rate of roughly five gallons per minute. At about eight and a half pounds per gallon, this equates to about 40 pounds per minute of flowing fuel to the burn area.

3.3.1.2 Large-scale ISB Vegetation

The study team harvested 200 cattails (*Typha lotifolia)* for two burns (100 stalks of cattails for each vegetation burn) covering 50% of the burn area (Figure 35). This equates to 50 square feet at a density of two stalks per square foot.

Figure 35. Vegetative coverage within large-scale test burn area.

3.3.1.3 Mass Measurements for Calculating Burn Efficiency

To calculate burn efficiency, researchers measured the total mass of fuel oil added to the burn area before and during the burn, and total residue recovered from the test area and apparatus after the burn. A pre-weighed netting secured below the water surface in the burn area collected sunken residue. Researchers weighed the sunken residue separately, and added it to mass of total unburned product for each test.

3.3.1.4 Flame Spread and Burn Rate

Researchers calculated flame spread and burn rates for large-scale ISB using the same methods described in section 3.2.1.2 and APPENDIX D. As with mesoscale ISB, burn rates are a mass loss rate per unit area.

3.3.1.5 Temperature and Heat Flux

As in small-scale tests, Inconel-sheathed, Type-K thermocouples measured flame temperature directly in the test fire, and the temperature of the water at various depths. Three thermocouple trees (TTs) stood in the boomed burn area (Figure 36, Figure 37, and Figure 38). Each TT consisted of 16 thermocouples (eight thermocouples positioned below the water surface to provide a temperature profile of the water and eight positioned above the water level to measure fuel and flame temperatures). Each tree had thermocouples positioned at the following depths below, and elevations above, the water surface: -300, -200, -150, -100, -60, -30, -10, 0, 10, 30, 60, 100, 150, 99, 1500, 2100 mm. Fittings allowed for vertical and horizontal adjustments of the trees.

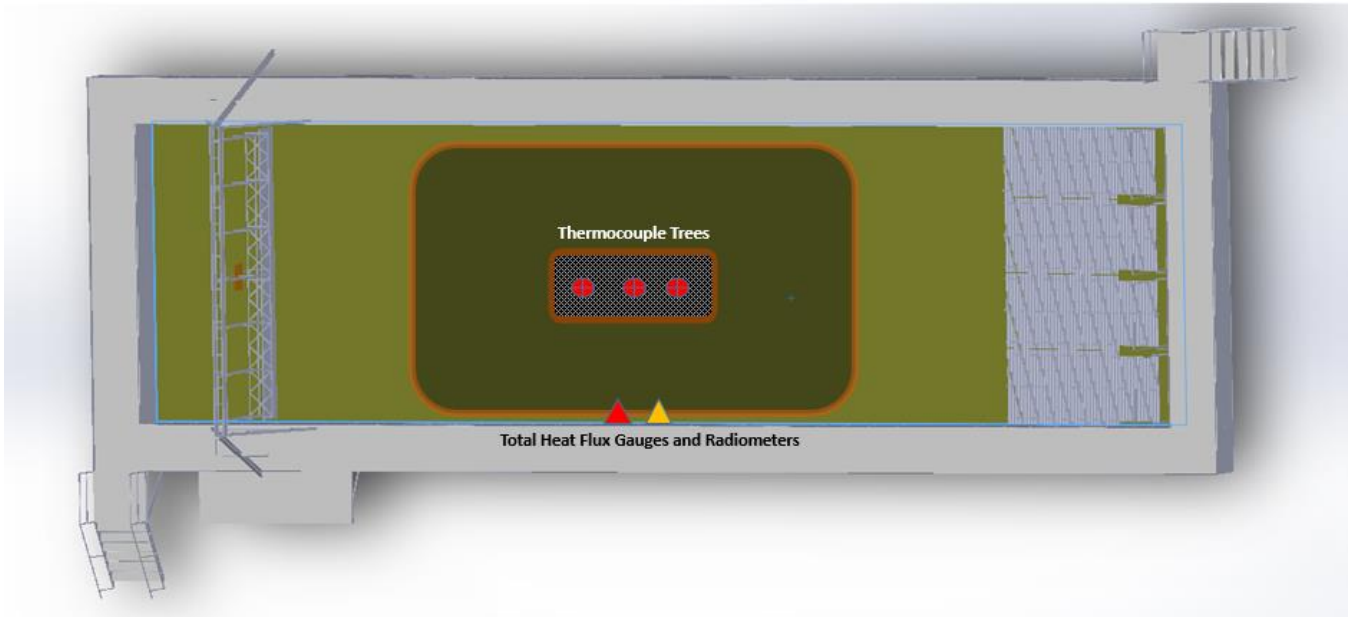

Figure 36. Overview of temperature instrumentation placement for ISB tests. Red circles depict thermocouple trees inside the burn area (primary containment). Heat flux and radiometers are outside the secondary containment.

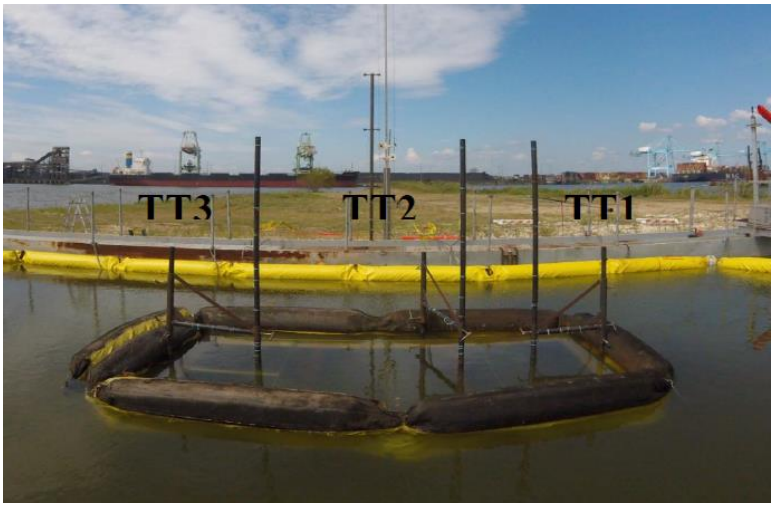

Figure 37. Placement of thermocouple trees during large-scale ISB tests.

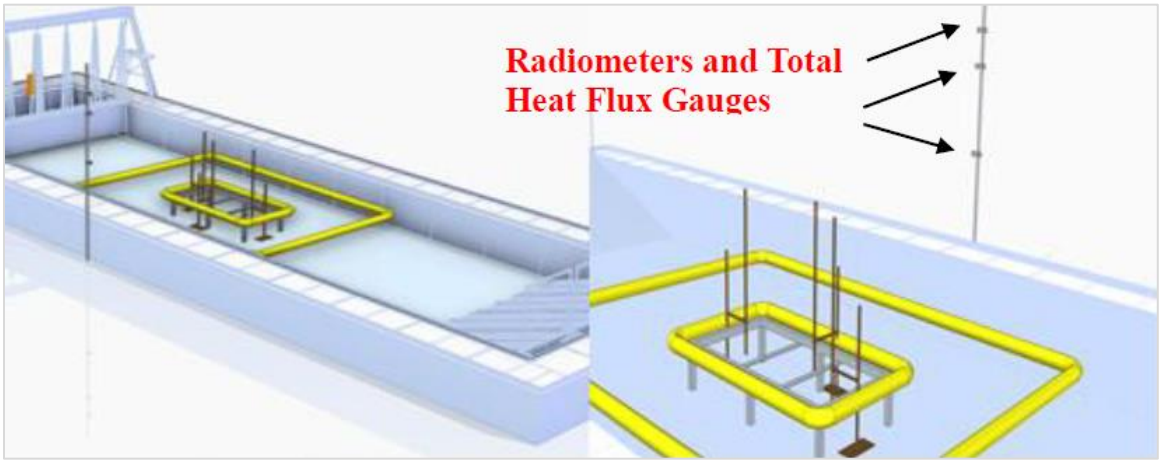

Figure 38. Large-scale ISB heat flux gauge setup.

3.3.1.6 Residue and Water Chemical Analyses

Researchers planned to collect three separate five-milliliter (5 ml) samples for chemical analysis: 1) baseline water prior to oil input, 2) post-burn water from about 15 cm, or six (6) inches (in), below the surface, 3) pre-burn oil and 4) post-burn oil residue.

3.3.1.7 Emissions inside the Smoke Plume

The USCG collaborated with the EPA Office of Research and Development (ORD) to conduct emission sampling and analysis of the large-scale burn smoke plumes. A RDC small, unmanned aerial system (sUAS) carried an EPA sensor package (Kolibri) into the smoke plume during the large-scale burns (Figure 39). The Kolibri sensor measured CO, CO_2, particulate matter less than 2.5 micrometers ($PM_{2.5}$), total carbon/organic carbon/elemental carbon (TC/OC/EC), black carbon (BC), brown carbon (BrC), and volatile organic compounds (VOCs) in the smoke plume. Researchers attempted at least three flights per burn for each of four burns to obtain replicate samples and detectable levels.

Figure 39. RDC's sUAS with EPA's Kolibri sampling system.

3.3.1.8 Ground-based Air Quality Monitoring

Per Special Monitoring of Applied Response Technologies (SMART) protocol, the USCG Gulf Strike Team performed air sampling during ISB of RMG 380 using a Dust track II 8530 (See APPENDIX E). The instrument collected particulates sized 2.5-10.0 microns (µm) in diameter from three different locations around the burn pan. Figure 40 shows the three locations where technicians stationed ground-monitoring instruments. Technicians established ground-monitoring locations in accordance with USCG currently accepted air-monitoring protocols to measure emissions near the source, downwind from the source and near observers (APPENDIX E). The first location is east of the burn pan; the second is northeast of the burn pan and is the furthest away from the pan; and the third location is adjacent to the burn pan.

Figure 40. Locations of ground-based air quality monitoring devices.

3.3.1.9 Visual Documentation

The research team estimated pre-boil over and boil over events by visual and audio observations. However, they did not measure fuel oil and/or water lost via splashing or vaporizing caused by boil over phenomena.

The test team digitally recorded and manually timed the burns to estimate burn rate. Stationary video cameras captured footage around the burn area (Figure 41).

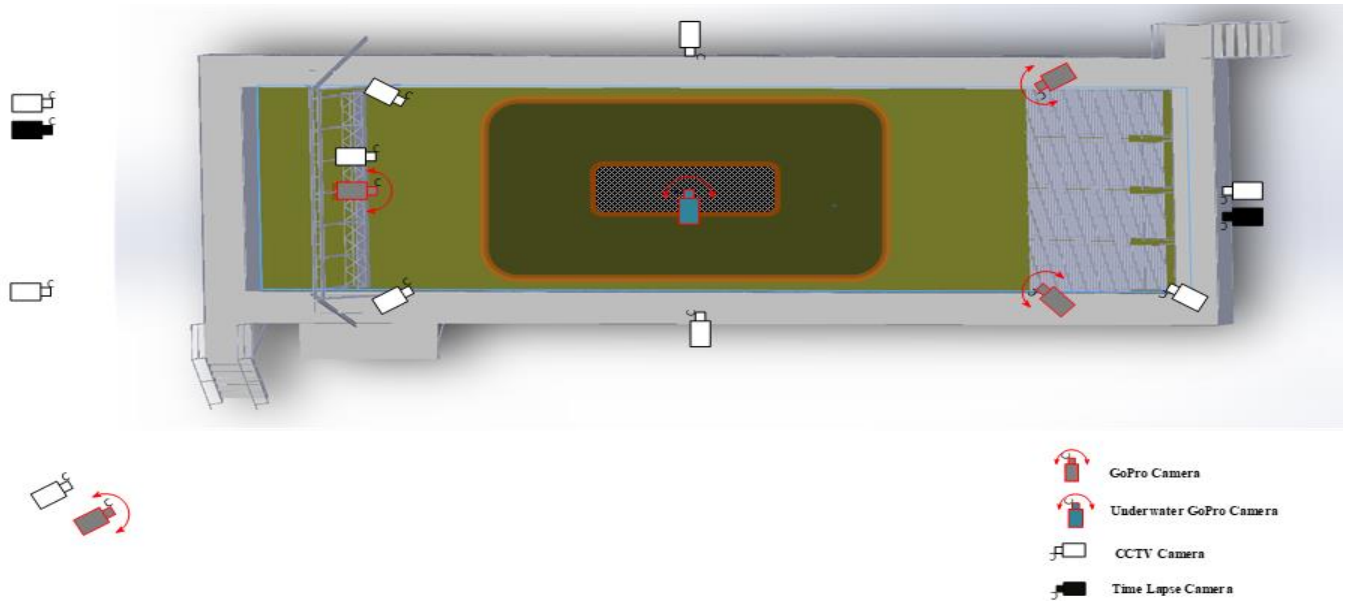

Figure 41. Stationary video placements for large-scale ISB tests.

3.3.2 Large-scale Execution

Table 12 provides details of the large-scale experimental matrix. The first set included two burns with medium crude oil (L1 and L2). The second set included two burns with RMG 380 (L3 and L4). As mentioned in large-scale design, the targeted sustained length of burns was at least 20-30 minutes. Technicians flowed oil as necessary to maintain the target ten millimeters slick thickness for the full burn length. The fuel flow team closely monitored and measured fuel flow rate by weight. Figure 41 shows the ignition of the large-scale ISB.

At the start of the test L1, the test team was adjusting the fuel pump rate and discharged 165kg (22mm slick thickness) of crude oil into the boomed area versus the initial target of only 74kg (10mm slick thickness).

Table 12. Large-scale ISB test matrix and parameters.

Test #	Date	Vegetation Surface Coverage (%)	Oil Type	Oil Mass In (kg)	Vegetation Mass In (kg)	Approximate Burn Time (min:s)	Wind Speed (kn)	Relative Humidity (%)	Ambient Temperature
L1	9/17/2019	0	Medium Crude	758.86	0	28:00	1.9	60	27ºC/80ºF
L2	9/18/2019	50	Medium Crude	654.08	21.71	24:30	2.3	70	28ºC/82ºF
L3	10/21/2019	0	RMG 380	546.13	0	31:00	8.7	75	23ºC/73ºF
L4	10/22/2019	50	RMG 380	560.19	24.45	34:00	8.9	75	23ºC/73ºF

Figure 42. Ignition of large-scale ISB tests using extended torch at JMTF.

3.3.2.1 Small Unmanned Aerial System Set-up and Operation

The pilots and EPA monitors launched and controlled the sUAS from about 30 m outside of the burn site in a sterile cockpit, meaning it was free from radio and other testing activity interference (Figure 43). Two dedicated visual observers, with line of sight on opposite sides of the plume, remained in radio communication with the pilot. The flight plan was to hover in the plume while mounted sensors measured parameters (Figure 44). The sensor package relayed temperature and CO_2 data via real time telemetry to the ground station allowing the EPA scientist direct placement of the sUAS in the heart of the plume. As necessary (one to three times per burn), the sUAS returned to the launch pad for rapid battery or filter swaps. See APPENDIX E for more information about the potential for sUAS emissions measurements during ISB.

Figure 43. sUAS mounted with EPA sensor package (yellow circle) flying in ISB smoke plume.

.

Figure 44. sUAS mounted air monitoring sensor package sampling inside the smoke plume.

3.3.3 Large-scale Test Results

The large-scale tests provided information on burn characteristics for medium crude oil and a heavy oil (RMG 380), including the effect of vegetation (Table 13).

Table 13. Large-scale ISB residue mass, burn efficiencies and burn rates[2].

Test #	Oil Type	Mass In (kg)		Residue Mass Out (kg)		Burn Efficiency (%)	Approximate Burn Duration (min:s)	Burn Rate (mm/min)
		Oil	Vegetation	Inside Primary Boom	Outside Primary Boom			
L1	Medium Crude	759	n/a	8.64	3.31	98.43	28:00	3.59
L2	Medium Crude	654.08	21.71	10.92	2.30	98.04	24:30	3.63
L3	RMG 380	546.13	n/a	7.35	9.16	96.98	31:00	1.90
L4	RMG 380	560.19	24.45	134.24	7.37	75.78	34:00	1.45

3.3.3.1 Large-scale Burn Efficiency

As with the small and mesoscale burns, researchers calculated burn efficiency using Equation 1 (Section 3.2.3.2). Table 13 shows the large-scale burn efficiency summary. The oil feed rate for test L1 was variable and fluctuated due to fuel pump rate adjustments. For test L2, burn efficiency with vegetation was approximately the same as test L1. For the RMG 380 oil, there was a significant difference in burn efficiency between test L3 and test L4. The burn with vegetation (L4) had a burn efficiency reduced by approximately 22%. L4 also had greater residual product inside the primary boom. The bulk of unburned residue inside the burn area was sunken and adhered to cattail stalks below the surface.

[2] At 15ºC, density of crude oil (tests L1 and L2) was 817.1 kg/m3 and of RMG 380 (tests L3 and L4) was 984.9 kg/m3.

3.3.3.2 Flame Spread and Burn rate

The burn rate for RMG 380 was significantly lower than for crude oil. For the crude oil burn, there was no notable change in burn rate with vegetation, however for the RMG 380 test, there was more than 20% reduction in burn rate with vegetation.

For ISB with crude oil without vegetation, the flame spread rapidly throughout the boomed area after ignition. The fire fully involved the burn area within 10s after ignition (Figure 45). The ignition and flame spread rate for crude with vegetation was similar at 6 s. For ISBs with RMG 380, the fire fully involved the burn area after about 200 seconds (Figure 46). The ignition and flame spread rate for RMG 380 with vegetation was similar at 210 s.

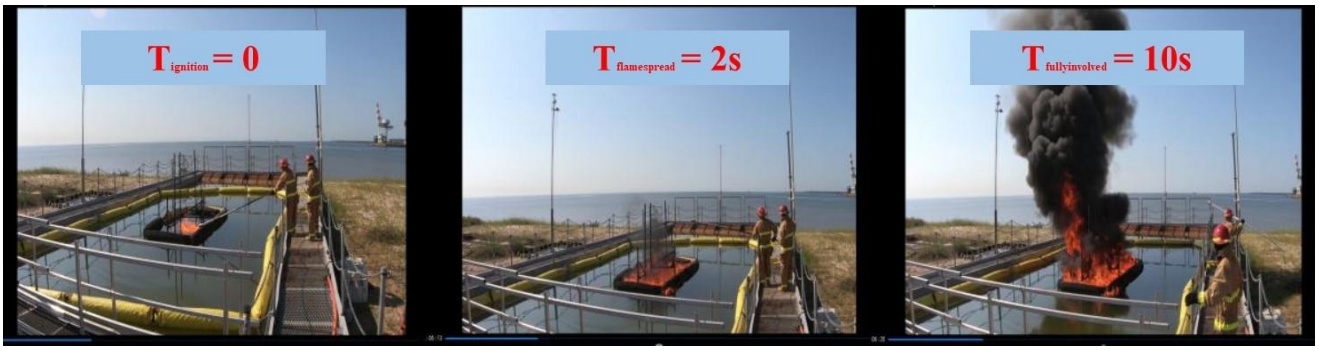

Figure 45. Ignition, flame spread and fully involved times for large-scale crude ISB.

Figure 46. Ignition, flame spread and fully involved times for large-scale RMG 380 ISB.

3.3.3.3 Temperature and Heat Flux

Table 14 shows the temperature, heat flux, and heat release rate summary for the large-scale ISB. The temperature peaked at 900°C for all but the last test (L4). During L4, thermocouples sustained damage resulting in incomplete data.

Table 14. Large-scale ISB temperature/heat flux/heat release rate data summary.

Test #	Description	Approximate Burn time (min:s)	Peak Temperature (°C)	Peak Heat Flux (kW/m²)	Average Heat Flux (kW/m²)	Heat Release Rate (HRR) (MW)
L1	Crude baseline	28:00	900	10	6	13
L2	Crude with vegetation	24:30	900	10	6	n/a
L3	RMG 380 baseline	31:00	900	7.5	4	12.6
L4	RMG 380 with vegetation	34:00	n/a	7	2.5	n/a

For tests L1 and L2, the wind direction was Northwest at a speed of approximately 2 knots. The flames were tilting toward the southeast and away from the heat flux gauges, resulting in uneven contact with the thermocouples trees and heat flux gauges (Figure 47). Heat flux also fluctuated with oil flow rate, as the technicians adjusted the rate to maintain target surface oil thickness. TT3 severely warped after test L2, so the research team removed it from tests L3 and L4.

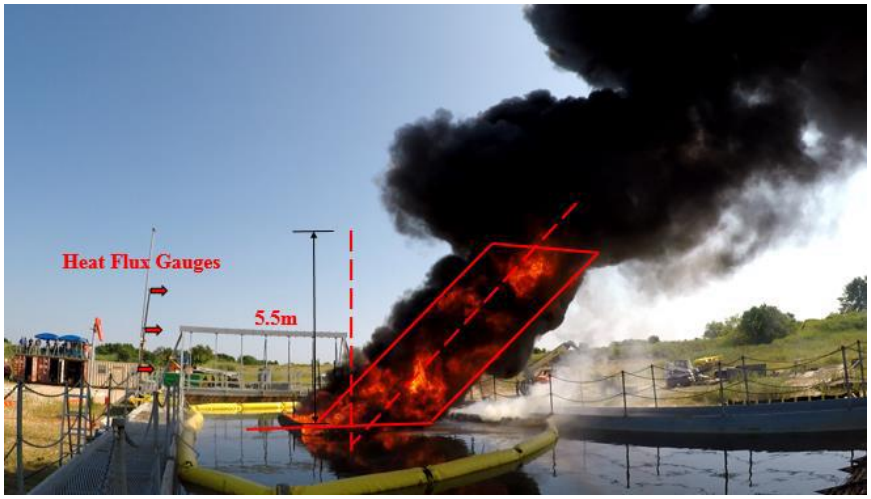

Figure 47. Large-scale flame and plume trajectory affected by wind (L1).

For test L3 and L4, the winds were approximately 8 knots. The winds caused the fire to burn more erratically due to the fanning effect on the fire. The wind speed also kept the flame height and smoke plume low to the surface level resulting in uneven contact with the upper thermocouples (Figure 48). APPENDIX DF contains temperature and heat flux plots from large-scale burns.

Figure 48. Large-scale flame and low smoke layer (L4).

3.3.3.4 Residue and Water Chemical Analyses

Chemists collected samples for laboratory analysis as described above in Sections 3.2.2 and 3.4.1.6 with the exception of test L4. During this test burn only, researchers found sunken residue after the burn. Chemists collected additional samples of the sunken residue, some of which adhered to submerged sections of vegetation.

The EPA and RDC collected separate oil and residue samples, used different analytical instrumentation, and measured different parameters. Researchers from the EPA Office of Research and Development (ORD) conducted chemical analyses on the pre-burn oil and water and the post-burn water and residue for crude and RMG 380 oil. The focus of the EPA chemical analysis was to examine the concentrations of benzene, toluene, ethylbenzene, xylenes (BTEX); alkanes; and PAHs in the pre-burn oil and post-burn residue.

3.3.3.4.1 Residue Samples

Figure 49 shows the results of the chemical analysis for total n- and i-alkanes in the post-burn residue. There was a greater concentration of i-alkanes than n-alkanes in residue from all tests. Test L2 (crude with vegetation) does not have results for alkane concentrations.

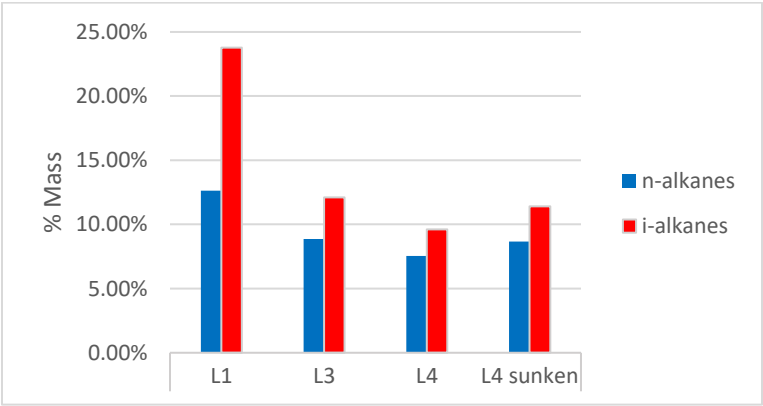

Figure 49. Alkane mass percentages in residue from large-scale ISB of crude (L1 only) and RMG 380.

Table 15 shows the results of EPA ORD analyses of BTEX, alkanes and PAH concentrations in the pre-burn oil and post-burn residue for large-scale ISB tests of crude and RMG 380 oil.

Table 15. Large-scale ISB chemical analysis of oil and residue samples from EPA.

Sample Source	Chemical Component (ng/mg)			
	Short Chain Alkanes	BTEX	Long Chain Alkanes	PAH
Pre-burn crude	26390	104365	48884	8686
L1	33	291	50383	10412
L2	6	159	47767	9833
Pre-burn RMG 380	218987	233735	23853	63635
L3	7074	43161	13346	43926
L4	282	384	4048	17283
L4 sunken	2009	13526	4344	17095

As shown in Table 15, the pre-burn crude oil had a higher ratio of BTEX as compared with the burn residue, where BTEX decreased to negligible numbers. Test L1 (crude without vegetation) post-burn residue had a slight increase in long chain alkanes concentrations as compared with pre-burn oil. Residue from tests L1 and L2 (both crude oil) had greater concentrations of PAHs as compared with the unburned crude oil sample.

Post-burn RMG 380 residue ratios of BTEX, alkanes and PAHs were all lower than in the pre-burn oil. The BTEX concentrations decreased significantly in the RMG 380 residue as compared to the raw oil. Alkane concentrations decreased by 44% in L3 (without vegetation) and 80% in L4 (with vegetation). The PAH concentrations decreased between 30% and 73% in the RMG 380 burn residue as compared with the pre-burn oil. APPENDIX G contains the EPA chemical analysis results.

3.3.3.5 Water Samples

EPA chemists collected pre-burn water from the ISB test pool, prior to adding crude and RMG 380 oil, to measure baseline concentrations of PAH, alkanes, and BTEX. Likewise, they collected post-burn water for comparison after each ISB test. Chemical analysis of post-burn water for tests L1 and L2 (crude oil) showed a significant increase in BTEX concentrations in the post-burn water as compared with pre-burn water (Table 16). For tests L3 and L4, there was an increase (approximately 220 fold) in PAHs and BTEX concentrations in the post-burn water samples as compared with pre-burn water. For both oil types, ISB increased concentrations of oil components in the surrounding water.

Table 16. Large-scale ISB chemical analysis of water samples from EPA.

Water Sample Source	Chemical Component (ng/L)		
	BTEX	Alkanes	PAH
Pre-burn, crude	164	40	9
Post-burn L1	1489	57	42
Post-burn L2	2140	68	39
Pre-Burn, RMG 380	151	6833	1237
Post-burn L3	208968	82265	315655
Post-burn L4	129019	66078	277183

3.3.3.6 Smoke Plume Emissions

Researchers conducted an analysis of the ISB smoke plumes to characterize emissions. Data for black carbon was not available from the first burn, as the initial flights did not use the black carbon instrument due to concerns about the UAS payload.

EPA used the carbon balance method to calculate emission factors. This method used the ratio of the sampled pollutant mass to the sampled carbon mass (determined from CO + CO_2 measurements) and the carbon percentage of the fuel (85%). The resultant emission factors are the mass of pollutant per mass of oil burned (Equation 2).

Equation 2. Emission factors.

$$\text{Emission factor} = Fc \text{ x } \left[\frac{Analyteij}{Cj}\right]$$

Where:
Fc = Carbon fraction in the oil (85%)
$Analyte_{ij}$ = concentration of the target analyte *i* collected from the volume element *j* of the plume.
C_j = concentration of carbon collected from volume element j of the plume

EPA used a modified combustion efficiency (MCE_T) to calculate how well the oil burned (Equation 3).

Equation 3. Modified combustion efficiency.

$$\text{MCET} = \left[\frac{CO2}{CO2 + CO + TC}\right]$$

Where:
MCE_T = modified combustion efficiency including particles
CO_2 = carbon dioxide in the plume in ppm
CO = carbon monoxide in the plume in ppm
TC = total carbon in the particulates

Table 17 shows averaged concentrations of $PM_{2.5,}$ TC, BC and VOCs in large-scale ISB emissions.

Table 17. Averaged concentrations of large-scale ISB emission factors.

Test #	Description	Burn Efficiency (%)	MCE_T	$PM_{2.5}$ (g/kg)	TC (g/kg)	BC (g/kg)	VOC (mg/kg)
L1	Crude baseline	98.43	0.864	117.2	112.2	N/D	2187
L2	Crude with vegetation	98.04	0.825	147.7	156.9	76.3	1587
L3	RMG 380 baseline	96.98	0.816	162.6	150.4	99.17	4828
L4	RMG 380 with vegetation	75.78	0.786	201.7	187.6	89.2	6469

Results of the preliminary smoke plume analysis validated that better combustion efficiency yielded fewer emissions. The test with the lowest burn efficiency (L4) produced the largest concentrations of VOCs and $PM_{2.5}$.

3.3.3.7 Ground-based Air Quality Monitoring

Figure 50, Figure 51, and Figure 52 show the results of ground-based air quality monitoring during large-scale ISB of RMG 380. The particulate matter (PM) concentrations ranged from 0.004 – 0.009 milligrams per cubic meter (mg/m^3). The results at the first and second locations show similar results with a range of PM concentrations between .003 and .005 mg/m^3. The third location adjacent to the burn pan recorded the largest concentration of all measured PM sizes (between .007 and .009 mg/m^3).

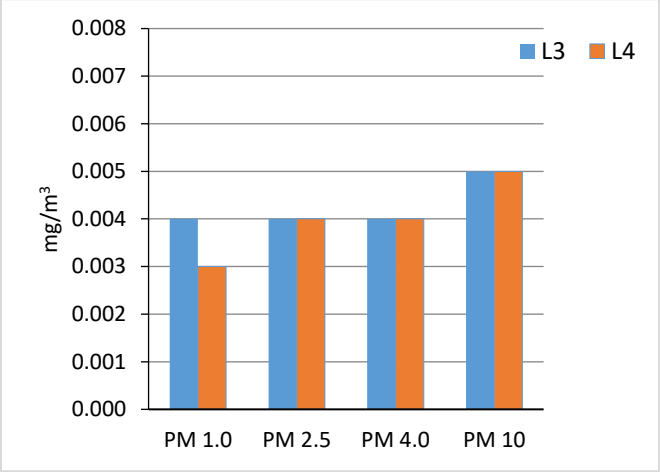

Figure 50. PM size distributions measured by ground-based instruments at location 1.

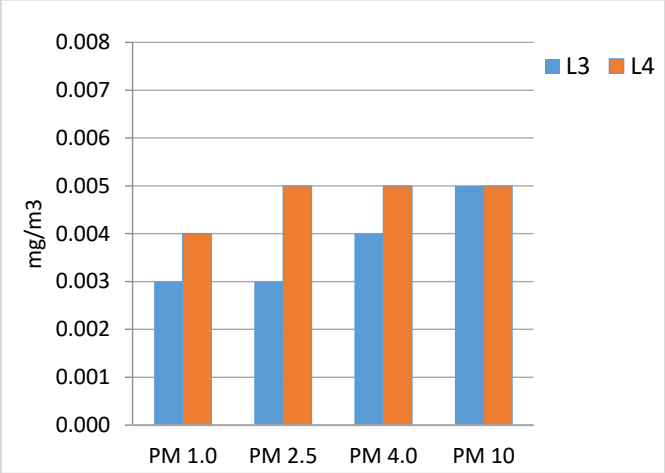

Figure 51. PM size distributions measured by ground-based instruments at location 2.

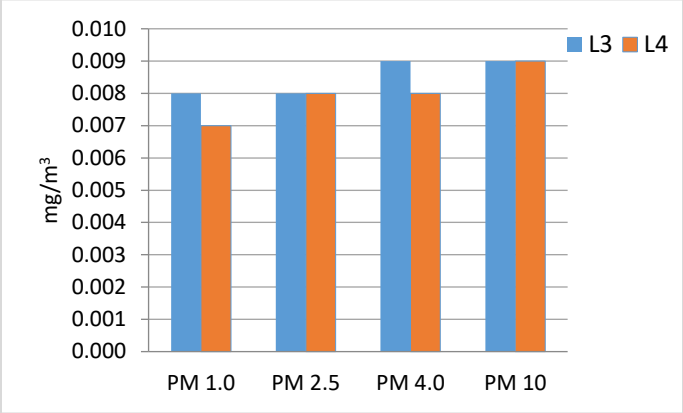

Figure 52. PM size distributions measured by ground-based instrument closest to burn pan.

3.3.3.8 Visual Documentation

More oil splattered outside of the primary burn area during ISB of RMG 380 compared with ISB of crude oil. For both oil types, less product splattered outside of the primary burn area during burns with vegetation compared with those without vegetation.

3.3.4 Large-scale Summary

The large-scale test provided the following results:

- Burn efficiencies for crude oil and RMG 380 without vegetation were similar
- For crude oil tests, vegetation did not measurably affect burn efficiency
- For RMG 380 tests, vegetation did have a significant impact on burn efficiency (approximately 22% lower burn efficiency)
- Peak temperature reached 900°C
- Alkanes and PAHs were more concentrated in crude oil burn residue versus the raw oil
- PAHs and BTEX concentrations increased in post-burn water after crude oil ISB
- Boil over occurred, resulting in an oiled splatter zone beyond the primary containment of the burn area

One burn of each condition at the large-scale is too small a sample to analyze variability. More definitive analysis and comparison of burn characteristics requires additional freshwater ISB at a large-scale (or in open water), and collection of associated residue and emissions data. Ambient test conditions ranged from "temperate" to extremely warm. The range of testing did not include cold or frigid ambient conditions.

4 CONCLUSIONS

4.1 Ignitability

At all scales, ISB tests of RMG 380 in freshwater demonstrated, under ambient conditions, that ten millimeters (10 mm) surface oil thickness was sufficient for ignition and sustained burn. Using diesel fuel as an accelerant did not provide a conclusive change to ignition and burn time. After 24 hours "weathering" at the small-scale, RMG 380 took longer to ignite, but ultimately did ignite and sustain burn, indicating that RMG 380 could possibly sustain ISB under real-world oil spill response times.

Despite having specific gravities relatively close to freshwater, the test iterations showed that all oil types floated when initially introduced into freshwater with and without vegetation. This is fundamentally important, since ISB cannot remove oil submerged in water. These tests did not evaluate the effect of waves, which could have impacts such as formation of emulsions that may less readily ignite and/or more rapidly sink.

4.2 Burn Efficiency

Table 18 shows the summary of burn efficiencies for all ISB tests (averaged for replicate mesoscale tests).

Table 18. Summary of burn efficiencies.

Description	Number of Trials	Burn Efficiency (%)
Small-scale – RMG 380		
Baseline "thick slick"	1	85
Baseline "thick slick" with diesel	1	66
Baseline "thin slick"	2	72
Baseline "thin slick" with diesel	1	58
Mesoscale – Bunker C		
Baseline "thin slick"	4	83
Baseline "thick slick"	2	85
"Thin slick" 50% vegetation	3	77
"Thin slick" 100% vegetation	1	73
"Thick slick" 100% vegetation	1	84
Large-scale – all "thin slick"		
Medium Crude, Baseline	1	98
Medium Crude, 50% vegetation	1	98
RMG 380, Baseline	1	97
RMG 380, 50% vegetation	1	76

Sample sizes were not large enough to conduct regression analyses to statistically evaluate the specific relationship between each variable and burn efficiency. Oil type, oil thickness, the presence of vegetation, and the use of diesel oil accelerant, in various combinations, all appeared to affect ISB burn efficiency in freshwater, within each test group (small-scale, mesoscale, and large-scale). For ISB of "thin slicks" of Bunker C and RMG 380, results suggest that presence of vegetation yielded lower burn efficiency.

Burn efficiencies varied over the range of testing. The large-scale testing, averaging approximately 92% efficiency, more-closely approximated real-world conditions when compared to the small-scale and mesoscale tests. Burns at the smaller scale did not get as hot as the large-scale burns which can affect burn efficiency. The relatively high burn efficiencies in three of the four large-scale tests provide a general expectation of real-world burn efficiencies, for the given types of oil and ambient conditions. As a reference, burn efficiencies estimated from the 2010 Deepwater Horizon spill response in the Gulf of Mexico were on the order of 85% (Stout and Payne, et al., 2016).

4.3 Temperature and Heat Flux

The size of the burn area and presence of vegetation affected ISB temperature and heat flux. Flame temperatures increased from small-scale to mesoscale burns. The mesoscale burn with the lowest efficiency (73%) also recorded the lowest flame temperatures (680°C). The dynamics are not clear. Moist vegetation may have affected air entrainment into the burn. Researchers measured similar peak temperatures (900ºC) at the mesoscale and large-scale. This could indicate that burn behaviors at mesoscale and large-scale were similar. However, plume trajectories during large-scale tests carried fumes and hot gases away from direct effect on the thermocouples. Researchers suspect that large-scale peak temperatures were greater than readings indicated.

4.4 Flame Spread and Burn Rate

The factors that affected flame spread and burn rate were the type of oil, oil slick thickness, and size of the burn area. Mesoscale ISB of Bunker C oil indicated that vegetation did not influence flame spread and burn rates. Burn rates measured for mesoscale ISB of Bunker C oil and large-scale ISB of RMG 380 were similar. Large-scale ISB of medium crude with and without vegetation yielded a higher burn rate than tests with Bunker C and RMG 380. During large-scale ISB with crude, the fire fully involved the burn area within 6-10s after ignition compared to 200s for RMG 380. This significant difference may be due to the greater volatility of the crude oil blend used in the tests as compared to the heavier, residual fuel oils, so that more oil vapors are available for combustion. Note, however, the lowest ambient temperature for any of the tests was 14 C (57 F) in the small-scale tests. Colder temperatures may affect volatility, particularly for initial ignition.

4.5 Burn Residue and Post-Burn Water

4.5.1 Residue Behavior

How much residue remains (burn efficiency), whether or not it floats, how long it floats, and ability to mechanically collect ISB residue are all factors relevant to ISB efficacy. Except for the large-scale RMG 380 burn with vegetation (L4), all measureable unburned residue remained afloat in the freshwater immediately after ISB. This suggests that for ISB of medium crude oil and Bunker C, mechanical collection of burn residue may be effective.

During the small-scale weathering experiment with RMG 380, the residue sank within nine days. ISB of RMG 380 with vegetation left the most unburned residue by mass. The unburned oil may have adhered to the vegetation, or some other interplay between the vegetation and burn activity may have caused the oil to sink before burning completely. The vegetation in test L4, harvested 30 days prior to burning, may have been sufficiently dry to wick the oil downward before being engulfed in flame.

The binding of oil to vegetation observed during test L4 may indicate that mechanical collection of RMG 380 ISB residue in freshwater with vegetation could be just as difficult as mechanical collection of unburned oil spilled in marshland environments. Also, the timeliness of mechanical collection of RMG 380 burn residue in open freshwater is critical as burn residue in the small-scale test sank after several days. Likewise, boil over (which occurred during all ISB test iterations) could spread residue outside any containment and make residue clean-up more difficult.

4.5.2 Chemical Analysis

Response planners need to know the relative makeup of ISB residue with respect to unburned oil. Analytical comparison of raw medium crude oil with residue after ISB revealed near complete removal of light hydrocarbon fractions (short chain alkanes) and BTEX. This is most likely due to the high evaporative properties of crude oil. The concentrations of long chain alkanes and PAHs was greater in medium crude oil residue than the unburned oil. This was foreseeable because heavier alkanes and PAHs evaporate or degrade less readily than lighter oil components. Likewise, in residue after all large-scale ISB iterations, concentration of n-alkanes was lower than i-alkanes, as expected because n-alkanes typically degrade faster than the branched alkanes. Therefore, after ISB, a smaller volume of oil product may remain, yet be more concentrated with these heavier and slower-to-degrade components as compared with the raw oil. Researchers require further information about longer-term fate and toxicity to aquatic ecosystems and human health to draw conclusions about whether the raw oil or burn residue is more harmful. Stakeholders are particularly sensitive to this consideration in the Great Lakes, which are close to population centers (APPENDIX A).

Residue remaining after large-scale ISB of RMG 380 had lower concentrations of BTEX, both short and long chain alkanes, and PAH as compared with the unburned oil. Therefore, although average burn efficiency was lower for RMG 380 than for medium crude oil (i.e., more residue remained), there was a greater reduction in concentrations of certain chemicals known to be harmful to the environment and humans as compared with results of medium crude ISB. Response planners must consider both the volume and relative toxicity of product in the environment when prioritizing clean-up plans. Again, researchers require further toxicity study to evaluate this empirically.

Post-burn water collected immediately after the large-scale ISB of both medium crude and RMG 380 oil contained significantly higher concentrations of BTEX and PAHs as compared with the pre-burn water samples. This indicated that ISB resulted in transfer of these compounds from the oil to water. Based on the tests conducted, it is not clear how this may compare with effects of unburned oil weathering on water over time. Additionally, these tests did not analyze chemical concentrations in post-burn water over time to evaluate if or how quickly residual hydrocarbons dissipated or otherwise changed, and how this may or may not affect biological toxicity.

It was beyond the scope of these ISB tests to evaluate the toxicity of these compounds in a freshwater ecosystem. Researchers require further study in this area to answer the question of whether the burn residue is more harmful or less harmful than unburned oil.

4.6 Smoke Plume Emissions

Large-scale tests provided valuable experience using a sUAS for air emission monitoring during ISB. Preliminary smoke plume analyses from large-scale ISB showed that greater combustion efficiency resulted in lower emissions. The large-scale test with the lowest measured burn efficiency (L4 – RMG 380 with vegetation) produced the highest concentrations of VOCs and $PM_{2.5}$. Overall, ISB of RMG 380 yielded more emissions than ISB of medium crude oil. There was no significant difference in emissions from large-scale ISB of crude oil with or without vegetation. The particulate concentrations in the smoke plume were greatest at the site closest to the burn. Concentrations decreased with increasing distance from burn pan, due to dispersion. The large-scale tests indicate that oil type was a contributing factor in quantity of emissions.

4.7 General Considerations

- ISB may be a viable response option for certain crude oils, Bunker C oil, and RMG 380 in freshwater, within a relatively short period after a spill. For all ISB tests in this report, these oils floated when initially introduced and, in a small-scale test, remained afloat up to 24 hours, without waves. These results could vary with the impact of weathering factors in open water.

- Approximately 10 mm is likely a reasonable target slick thickness for initiation of ISB. In these tests, all oils ignited and sustained burn at this starting surface thickness without need for accelerant. In fact, addition of diesel accelerant to RMG 380 at the small-scale yielded lower burn efficiency measurements versus those burns without accelerant.

- Tests comparing different vegetation coverage percentages indicated that densely present vegetation, particularly among a thinner (approximately 10 mm) slick of heavy oil, may result in lower peak burn temperature and lower burn efficiency. This may mean that ISB is less effective for a thin slick in dense marshland. Tests indicated that burn efficiency, at least for heavy oils, may be less negatively affected by vegetation if the starting slick is thicker (approximately 20 mm).

- Responders must determine if projected burn efficiencies justify the cost versus benefit of ISB. Burn efficiencies under the various test conditions ranged from 58-98%. At the large-scale, average burn efficiency was much higher (in three cases, over 97%). Additional large-scale burns are in order to better quantify and evaluate the variability of these results. Peak burn temperature and heat flux increased with ISB scale. Because these burn characteristics affect other burn outcomes such as residue and emissions factors, response planners should use large-scale results to inform ISB decision-making.

- Responders may expect that volatility of each specific oil type will affect burn behaviors such as burn rate. Oil volatility and its relationship to vapor availability for combustion is a primary consideration for responders in predicting the practicality of ISB. Crude oil ignited and burned faster than Bunker C oil and RMG 380. Responders may consider burn rate to anticipate and prepare for response operations.

- Mechanical collection of residue after ISB of Bunker C oil and crude oil both with and without vegetation, and RMG 380 without vegetation, may feasibly result in near complete oil spill clean-up. All measurable residue from these burns remained afloat immediately following ISB. Small-scale

weathering study of RMG 380 burn residue indicated that mechanical collection should occur within a few days after ISB, before residue begins to sink.

- RMG 380 ISB in vegetation raised issues. There was relatively low burn efficiency (76%) and considerable sunken residue, as well as the highest concentrations of VOCs and $PM_{2.5}$ in emissions. The higher emissions factors likely link to lower combustion efficiency, further devaluing ISB of RMG 380 in vegetation. Mechanical collection of residue after RMG 380 ISB in marshland vegetation, particularly when stalks are dry, may be more difficult than clean-up of the unburned oil.

- Overall, emissions from ISB of RMG 380 were greater than from ISB of crude oil. Use of a sUAS for remote plume monitoring may offer improvements in understanding of different air quality safety considerations, particularly with different ISB parameters, for responders and the public. The capability of sUAS for remote monitoring may necessitate air monitoring protocol revisions to keep up with advances in technology, developments in techniques, and improvements in understanding.

- Various concentrations of hydrocarbons, BTEX and PAHs remained in residue and water post burn. However, researchers require further information about longer-term fate and toxicity to aquatic ecosystems and human health to draw conclusions about whether the raw oil or burn residue is more harmful.

5 REFERENCES

API. (2015). *Field Operations Guide for In-Situ Burning of Inland Oil Spills.* Washington, DC: API Publishing Services. Retrieved from http://www.oilspillprevention.org/~/media/oil-spill-prevention/spillprevention/r-and-d/in-situ-burning/guide-for-isb-of-inland-water-spills.pdf

Arsava, K.S., Lamie, N.J., and Booker, B. (2019). *Mesoscale In-Situ Burn (ISB) Experiments for Oil Spill Response in Freshwater with Vegetation*, U.S. Army Engineer Research and Development Center Cold Regions Research and Engineering Laboratory, USCG RDC Internal Report, 8 November 2019.

DeLaune, R.D., Smith, C.J., Patrick, W.H. Jr., Fleeger, J.W., and Tolley, M.D. (1984). *Effect of Oil on Salt Marsh Biota: Methods for Restoration*, Environmental Pollution (Series A), Vol. 36, pp. 207-227, 1984.

Environmental Canada, Emergencies Science and Technology Division (N.D.). *Bunker C Fuel Oil*. Retrieved on 12 May 2020 from http://www.etccte.ec.gc.ca/databases/oilproperties/pdf/web_bunker_c_fuel_oil.pdf.

Fingas, M. (2011). An overview of in-situ burning. In Oil spill science and technology (pp. 737-903). Gulf Professional Publishing. Elsevier, Boston. IPIECA Guidelines on oil characterization to inform spill planning and decision making

FWS. (1999). *Multi-Species Recovery Plan: Frehswater Marshes and Wet Pariries.* Bethesda, MD: Fish & Wildlife Service Reference Service. Retrieved from https://www.fws.gov/verobeach/MSRPPDFs/FreshMarWetPrairie.pdf

Garo, J., Vantelon, J., and Fernande-Pello, A. (1996). Effect of the fuel boiling point on the boil over burning of liquid fuels spilled on water. *Symposium (International) on Comubustion, 26*(1), 1461-1467.

Gullett, B. K., Aurell, J., Holder, A., Mitchell, W., Greenwell, D., Hays, M., Conmy, R., Tabor, D., Preston, W., George, I., Abrahamson, J.P., Vander Wal, R., Holder, E., (2017). Characterization of emissions and residues from simulations of the Deepwater Horizon surface oil burns. *Marine pollution bulletin*, *117*(1-2), 392-405.

Hu, L. (2017). A review of physics and correlation of pool fire behavior in wind and future challenges.

IARC. (1997). Polychlorinated dibenzo-para-dioxins and polychlorinated dibenzoflurans. *IARC Monographs on the Evaluation of Carcinogenic Risks to Humans, 69*.

Kennedy, M. (2019, November 27). Massive explosion rips through Texas chemical plant. *NPR: National News*, pp. 1-11. Retrieved from Refinery Explosions Raise New Warnings

Kiesling, R.W., S.K. Alexander, and J.W. Webb, “Evaluation of Alternative Oil Spill Cleanup Techniques in a Spartina alterniflora Salt Marsh”, Environmental Pollution, Vol. 55, pp.221-238, 1988.

Mabile, N. (2012) "Controlled in-situ burning: Transition from alternative technology to conventional spill response option." Proc. 35th AMOP Tech. Sem1: 584-605

McCauley, C.A. and Harrel, R.C. (1981). *Effects of Oil Spill Cleanup Techniques on a Salt Marsh*, Proceedings of the 1981 Oil Spill Conference, American Petroleum Institute, Washington, D.C., pp.401-407, 1981.

Mendelssohn, I.A., Lin, Q., Bryner, N.P., Walton, W.D., Twilley, W.H., and Mullin, J.V. (2002). *In-Situ Oil Burning in the Marshland Environment - Recovery and Regrowth of Spartina alterniflora, Spartina patens, and Sagittaria lancifolia Plants*, Proceedings of the Twenty-Fifth Artic and Marine Oil Spill Program Technical Seminar: Environment Canada. pp. 785–802, 2002.

Michel, et al., (2013), Extend and degree of shoreline oiling: Deepwater Horizon oil spill, Gulf of Mexico, USA. PloS one, 8 (6), p. e65087

National Fire Protection Association, NFPA 30 (2015), *Flammable and Combustible Liquids Code*

NOAA. (2006). *SMART at the New Carissa Oil Spill.* U.S. Department of Commerce.

NOAA. (2013). *Shoreline Assessment Manual.* Emergency Response Division, Office of Response and Restoration. Seattle: U.S. Department of Commerce. Retrieved from https://response.restoration.noaa.gov/sites/default/files/manual_shore_assess_aug2013.pdf

NOAA. (2019). *In Situ Burning*. Retrieved from NOAA Office of Response and Restoration: https://response.restoration.noaa.gov/oil-and-chemical-spills/oil-spills/resources/in-situ-burning.html

NRC. (2004). *Fire Dynamics Tools (FDTs): Quantitative Fire Hazard Analysis Methods for the U.S. Nuclear Regulatory Commission Fire Protection Inspection Program.* Washington, DC: U.S. Nuclear Regulatory Commission. Retrieved from https://www.nrc.gov/docs/ML0432/ML043290075.pdf

Phillips, S. (2019). Refinery explosions raise new warnings about deadly chemicals. *NPR: Special Series*, pp. 1-13, 19 July 2019. Retrieved from https://www.npr.org/2019/07/19/742367382/refinery-explosions-raise-new-warnings-about-deadly-chemical

Sharqawy, M. H., Lienhard V, J. H., and Zubair, S. M. (2010). Thermophysical properties of seawater: a review of existing correlations and data. *Desalination and Water Treatment, 16*, 354-380, April 2010.

Stout, S. A., & Payne, J. R. (2016). Chemical composition of floating and sunken in-situ burn residues from the Deepwater Horizon oil spill. *Marine pollution bulletin, 108(1-2),* 186-202.

U.S. Census. (2000). *America 2050 analysis of 2000.*

USCG. (2006). *Special Monitoring of Applied Response Technologies.* Seattle: NOAA OR&R. Retrieved from https://response.restoration.noaa.gov/sites/default/files/SMART_protocol.pdf

(This page intentionally left blank.)

APPENDIX A. ISB GREAT LAKES CONSIDERATIONS

A.1 Proximity to Population Centers

Response industry regulators generally believe ISB smoke plume gases dissipate to acceptable levels relatively quickly (USCG, 2006). But, since particulates in the smoke plume are a public health concern (USCG, 2006), Federal On-Scene Coordinators (FOSC) and Unified Commands need to know *exactly* when and where emissions are and are not safe upon deciding to initiate, continue, or terminate ISB efforts. To date, lack of incentives due to perceived negative effects of ISB smoke plumes on human health has resulted in very little research on the impacts of ISB in freshwater, which tend to be closer to population centers as compared with the offshore environment or brackish marshes along the Gulf of Mexico, where ISB is a relatively common response tactic. The Great Lakes region, in particular, contains several major cities that are the combined home to tens of millions of people (U.S. Census, 2000). Therefore, more scientific data about the safety of ISB is necessary for Great Lakes Regional Response Team (RRT) members to accept it as a response option. Further information about air quality considerations is in APPENDIX B.

A.2 Freshwater

Untested, the question remains if burn rate for a fuel product is different in fresh versus salt water. Burn rate is quantified by heat transfer. Thermal inertia, the tendency of material to resist temperature change, dictates rate of heat transfer. Thermal inertia is the square root of thermal conductivity x density x specific heat. The thermal conductivity – or material's ability to conduct heat – of seawater and pure (fresh) water are very close (Sharqawy, Lienhard V, & Zubair, 2010). Compared with freshwater, salt water has a lower specific heat, which is a measure of heat required to raise the temperature. However, density of saltwater is greater than that of freshwater. So, the calculated thermal inertias of saltwater and freshwater are similar. The tests covered by this report provided real thermal conductivity data to better inform freshwater responders about burn behavior in freshwater. The question remains whether marine and brackish water ISB knowledge is applicable in a freshwater environment.

A.3 Great Lakes and Coastal Wetlands Vegetation

Within the Great Lakes Basin, wetlands support many beneficial ecological functions, as well as economic and cultural values. Great Lakes coastal wetlands play an important role in the Great Lakes ecosystem, providing habitat for many plant and animal species, hydrologic retention, nutrient cycling, shoreline protection, and sediment trapping (EPA, n.d). Great Lakes coastal wetlands improve the Great Lakes water quality by capturing and filtering nutrients and other contaminants from upstream sources. Those nutrients and contaminants are taken up by wetland plants, and prevent increases in algae and plant growth in the Great Lakes, which would otherwise lead to algae blooms and low dissolved oxygen levels (EPA, n.d). Great Lakes stakeholders identified cattails as a common and good proxy for the most likely vegetation that may be encountered during an oil spill in the Great Lakes region. The research team harvested local cattails (*Typha lotifolia*) for testing.

Oil spills can severely damage or disrupt the biodiversity within this specific ecosystem on the Great Lakes, which include rare, threatened, or endangered species, and significantly impact water quality. However, it is difficult to summarize the impacts of crude oil spills on wetlands because of the range of spill conditions

and the importance of other factors. Generally though, the levels of impact from oil correlate with the degree of oiling. Crude oils and heavy refined oils that coat the entire plant, and particularly the leaves, will have the greatest potential impacts. Oiling of only the stems often results in limited mortality. If only the aboveground vegetation is oiled, regrowth is likely during the next growing season, particularly for oiling at the fringe where natural removal processes are relatively fast (Michel et al, 2013).

Impacts are more persistent when oil penetrates into the wetland soils. Persistence increases with deeper penetration, soils high in organic matter, and sites that are sheltered from natural removal processes. Vegetation recovery will occur quicker for spills of any type of oil during the non-growing season, compared with a spill during the growing season (Michel et al, 2013).

Heavy crude oils and heavy refined oil products, such as heavy fuel oil, Bunker C, and intermediate fuel oils (IFO) 180 and 380, are thought to affect marsh vegetation primarily via physical effects from coating and smothering of the vegetation and/or soil surface because they generally have low amounts of acutely toxic compounds (Michel et al, 2013).

APPENDIX B. TEST OIL SPECIFICATION SHEETS

B.1 Medium Crude Oil (37-41 API Gravity)

Report of Analysis

Justin Huemme
427 Commercial Street
merica

Our Reference Number: US290-0038558
Lab Reference Number: 2019-MOBL-001648
Customer Reference Number: Benedette Adewale

Product Description: Petroleum Crude Oil
Location: Mobile, AL, USA, Chickasaw, Alabama, United States
Sample Representing: Petroleum Crude Oil - Submitted USCG
Drawn By: Client

Sample ID: 2019-MOBL-001648-002
Date Sampled: 19-Sep-2019
Date Submitted: 14-Oct-2019
Date Tested: 15-Oct-2019

Method	Property	Result	Units
ASTM D5002	API Gravity @ 60°F	41.6	°API
	Density @ 15ºC	817.1	kg/m³
ASTM D93	Procedure Used	A	
	Corrected Flash Point	< 104	°F
ASTM D5950	Test Interval	3 °C	
	Instrument Model	ISL CPP-5Gs	
	Pour Point	<-30	°C
ASTM D445	Kinematic Viscosity @ 122 ºF/ 50 ºC	1.750	mm²/s
ASTM D240	Gross Heat of Combustion	18386	BTU/lb
	Gross Heat of Combustion	125375	BTU/gal

Results are only representative of the sample tested. All tests have been performed using the latest version unless otherwise indicated. This report shall not be reproduced except in full without written approval of Intertek. Report is subject to our standard Terms and Conditions which can be obtained at our website : http://www.intertek.com/terms
The sample was submitted for testing purposes. Intertek cannot accept liability for the representativeness of the sample.

Signed By: Digitally signed by Thomas Veals DN: cn=Thomas Veals, o=Intertek, ou=Intertek, email=thomas.veals@intertek.com, c=US Date: 2019.10.15 14:02:13 -05'00'
Thomas Veals, Laboratory Manager
Date:

B.2 RMG 380

Report of Analysis

U.S. Coast Guard
Justin Huemme
427 Commercial Street
Boston, MA 02109
United States of America

Our Reference Number: US290-0038558
Lab Reference Number: 2019-MOBL-001648
Customer Reference Number: Benedette Adewale

uct Description: RMG 380
Location: Mobile, AL, USA, Chickasaw, Alabama, United States
e Representing: RMG 380 - Submitted USCG
Drawn By: Client

Sample ID: 2019-MOBL-001648-001
Date Sampled: 19-Sep-2019
Date Submitted: 14-Oct-2019
Date Tested: 15-Oct-2019

Method	Property	Result	Units
ASTM D4052	Density @ 15°C	984.9	kg/m³
	API Gravity at 60 deg F	12.1	°API
ASTM D93	Procedure Used	B	
	Corrected Flash Point	164	°F
ASTM D5950	Test Interval	3 °C	
	Instrument Model	ISL CPP-5Gs	
	Pour Point	-18	°C
ASTM D445	Kinematic Viscosity @ 122 ºF/ 50 ºC	346.3	mm²/s
ASTM D240	Gross Heat of Combustion	18220	BTU/lb
	Gross Heat of Combustion	149757	BTU/gal

Results are only representative of the sample tested. All tests have been performed using the latest version unless otherwise indicated. This report shall not be reproduced except in full without written approval of Intertek. Report is subject to our standard Terms and Conditions which can be obtained at our website : http://www.intertek.com/terms
The sample was submitted for testing purposes. Intertek cannot accept liability for the representativeness of the sample.

Signed By: Digitally signed by Thomas Veals DN: cn=Thomas Veals, o=Intertek, ou=Intertek, email=thomas.veals@intertek.com, c=US Date: 2019.10.15 14:01:28 -05'00'
Thomas Veals, Laboratory Manager
Date:

B3. Bunker C

Bunker C Fuel Oil

Synonyms: Fuel Oil No. 6
Residual/Heavy Fuel Oil

Data from Shell 1999 were taken from MSDS Number 362-100.

For additional fuel specifications refer to ASTM D396.

			Reference ID
API Gravity			
		14.1	API 81
		12.3	EETD 88
Equation(s) for Predicting Evaporation			
Short term (<5 days): $\%Ev = (0.35 + 0.13T)\sqrt{(t)}$			
Long term: $\%Ev = (-0.21 + 0.045T)\ln(t)$			
Where %Ev = weight percent evaporated; T = surface temperature (°C); t = time (minutes)			
			ESD 96
Sulphur (weight %)			
		2.40	API 81
Water Content (weight %)			
		0.1	ESD 96
Flash Point (°C)			
		98	EETD 88
		174	Twardus 80
		>62	Shell 99a
Fire Point (°C)			
		>257	Twardus 80
Density (g/mL)			
	Temperature (°C)		
	0	0.9600	Mackay 82a
		0.9941	EETD 88
	5	0.9760	Mackay 82a
		0.9904	EETD 88
	10	0.9730	Mackay 82a
		0.9867	EETD 88
	15	0.9690	Mackay 82a
		0.9830	EETD 88
		<1.029	Shell 99a
	16	0.9710	API 81
	20	0.9660	Mackay 82a
		0.9788	EETD 88
	25	0.9650	Mackay 82a
		0.9749	EETD 88
	30	0.9718	
Pour Point (°C)			
		15	EETD 88
		6	Mackay 82a
		7	Twardus 80
Dynamic Viscosity (mPa·s or cP)			
	Temperature (°C)		
	0	73500000	Twardus 80
		1037000	ESD 93
	10	26700000	Twardus 80

Bunker C Fuel Oil

			Reference ID
Dynamic Viscosity (mPa·s or cP)			
	Temperature (°C)		
	15	45030	ESD 93
	20	5980000	Twardus 80
	25	3180	Mackay 82a
Kinematic Viscosity (mm²/s or cSt)			
	Temperature (°C)		
	50	211 to 640	Shell 99a
Emulsion Formation			
Evaporation (weight%)			
	Visual stability	entrained	ESD 98
	Viscosity (mPa·s)	110000	
	Complex modulus (Pa)	720	
	Water content (wt %)	26	
Chemical Dispersibility (volume %)			
	Corexit 9500	7	ESD 98
	Corexit 9527	0	EETD 89
	Dasic LTS	0	
	Enersperse 700	0	
Hydrocarbon Groups (weight %)			
	Saturates	24	Mackay 82a
	Aromatics	55	
	Resins	15	
	Asphaltenes	6	
		7	ESD 91
	Waxes	12	
		55	Mackay 82a
Surface Tension (mN/m or dynes/cm)			
	Temperature (°C)		
	0	NM	EETD 88
	15	NM	
	Room temperature	27.0	Twardus 80
Oil/Salt Water Interfacial Tension (mN/m or dynes/cm)			
	Temperature (°C)		
	0	NM	EETD 88
	15	NM	
Oil/Fresh Water Interfacial Tension (mN/m or			
	Temperature (°C)		
	0	NM	EETD 88
	15	NM	
	Room temperature	40.0	Twardus 80
Boiling Point Distribution (weight %)			
	Boiling Point (°C)	Weight %	
	160	1	ESD 94
	180	1	
	200	2	

Bunker C Fuel Oil

				Reference ID
Boiling Point Distribution (weight %)				
	Boiling Point (°C)	Weight %		
	250	5		ESD 94
	300	8		
	350	13		
	400	20		
	450	28		
	500	33		
	550	38		
	600	51		
	650	68		
	700	81		
Boiling Point Distribution (°C)				
	Weight %	Boiling Point (°C)		
	5			ESD 94
	10			
	15			
	20			
	25			
	30			
	35			
	40			
	45			
	50			
	55			
	60			
	65			
	70			
	75			
	80			
	85			
Metals (ppm)				
	Barium	<0.3		Cao 92
	Chromium	<1.5		
	Copper	1.2		
	Iron	35.0		
	Lead	<		
	Magnesium	23.9		
	Molybdenum	<0.6		
	Nickel	8.6		
	Titanium	<0.6		
	Vanadium	42.0		
	Zinc	1.6		
Other Elements (weight %)				
	Nitrogen	0		API 81
Aqueous Solubility (mg/L)				
	22	0	(a)	Suntio 86
	Unknown	2	(a)	Murray 84
	20	6	(b)	Anderson 74

(a) distilled water; (b) salt water

Bunker C Fuel Oil

Acute Toxicity of Water Soluble Fraction (mg/L)	Test Organism		Reference ID
24h LC50	Neanthes arenaceodentata	>6.3	Rossi 76
	Capitaella capitata	>6.3	
	Mysidopsis almyra	6	Anderson 74
	Palaemonetes pugio	3	
	Penaeus aztecus	4	
	Menidia beryllina	4	
	Fundulus similis	4	
	Cyprinodon variegatus	5	
48h LC50	Neanthes arenaceodentata	5	Rossi 76
	Capitaella capitata	1	
	Mysidopsis almyra	1	Anderson 74
	Palaemonetes pugio	3	
	Penaeus aztecus	4	
	Menidia beryllina	3	
	Fundulus similis	2	
	Cyprinodon variegatus	4	
96h LC50	Neanthes arenaceodentata	4	Rossi 76
	Capitaella capitata	1	
	Palaemonetes pugio	3	Anderson 74
	Penaeus aztecus	2	
	Menidia beryllina	2	
	Fundulus similis	2	
	Cyprinodon variegatus	3	

(This page intentionally left blank.)

APPENDIX C. SMALL-SCALE TEMPERATURE AND HEAT FLUX DATA

Figures C-1 to C-8 show the temperature profiles, and heat flux plots for the small-scale burns.

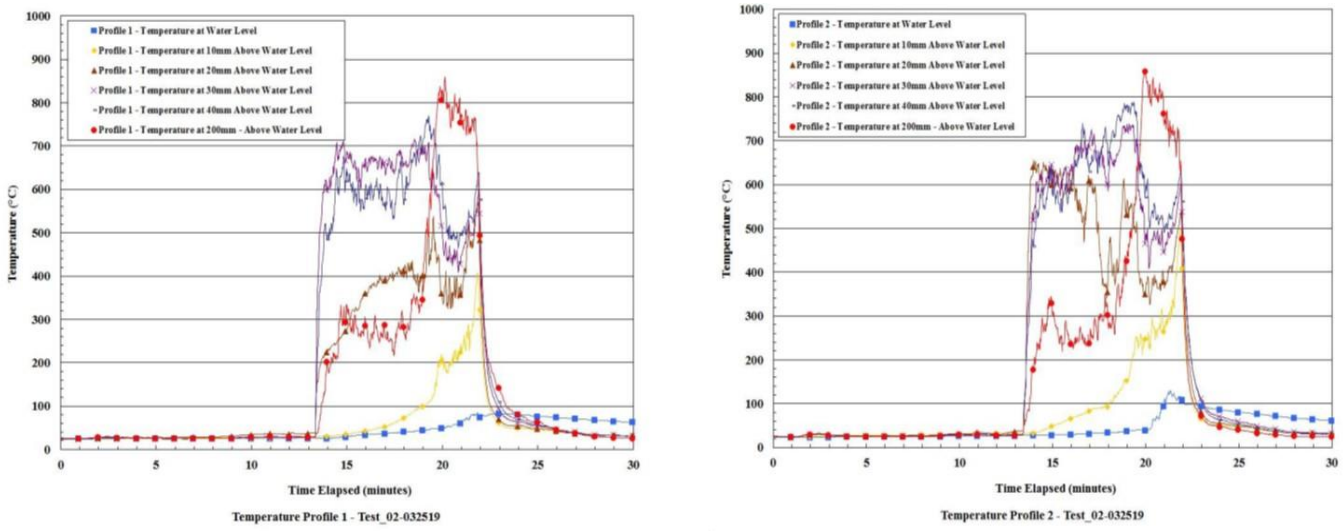

Figure C-1. Test 2 temperature profile 1 and profile 2.

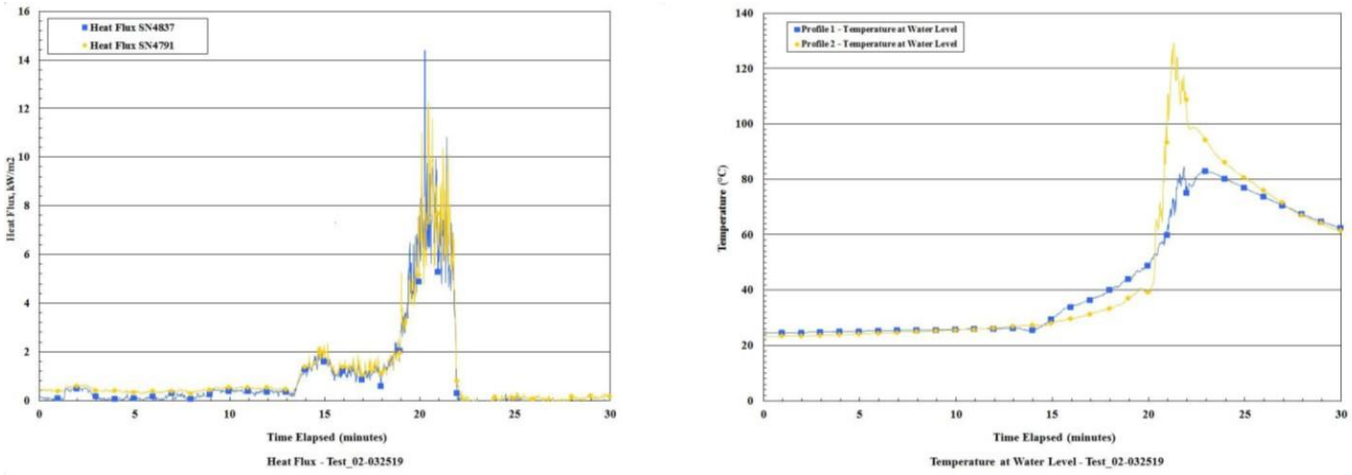

Figure C-2. Test 2 total heat flux measurement and temperature at the water level.

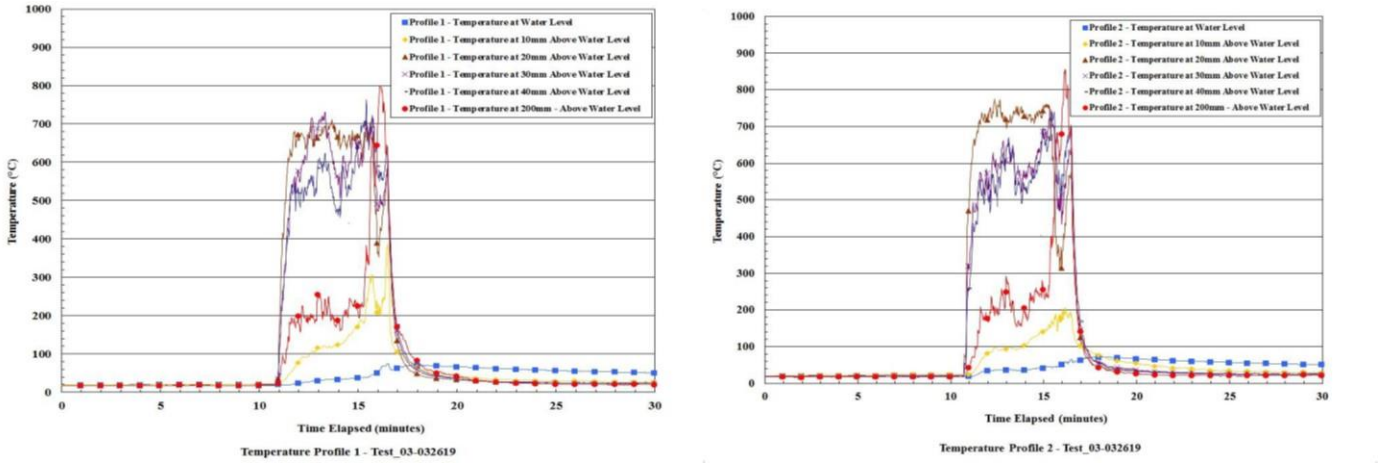

Figure C-3. Test 3 temperature profile 1 and profile 2.

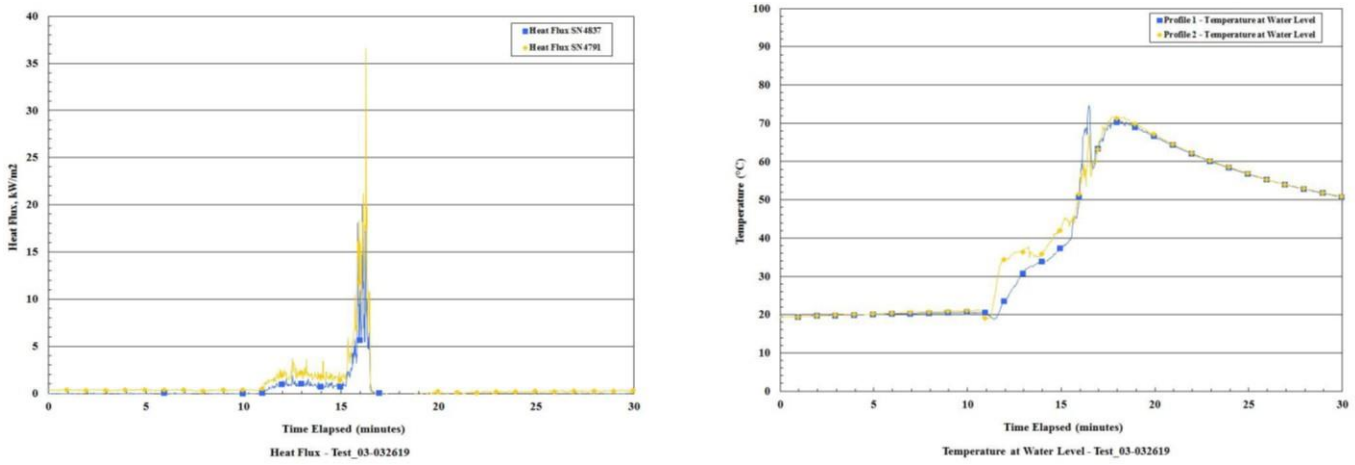

Figure C-4. Test 3 total heat flux measurement and temperature at the water level.

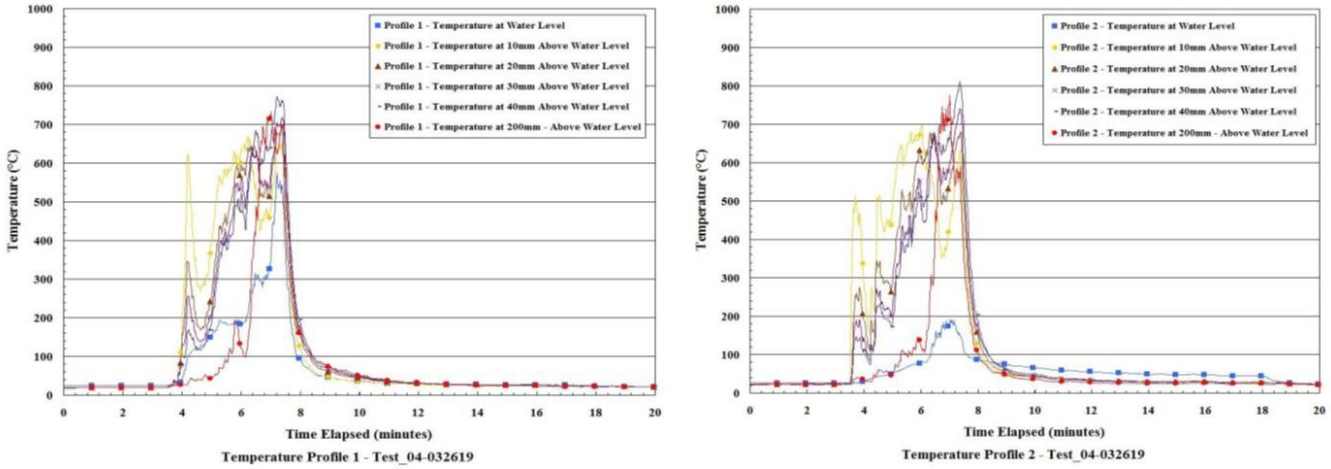

Figure C-5. Test 4 temperature profile 1 and profile 2.

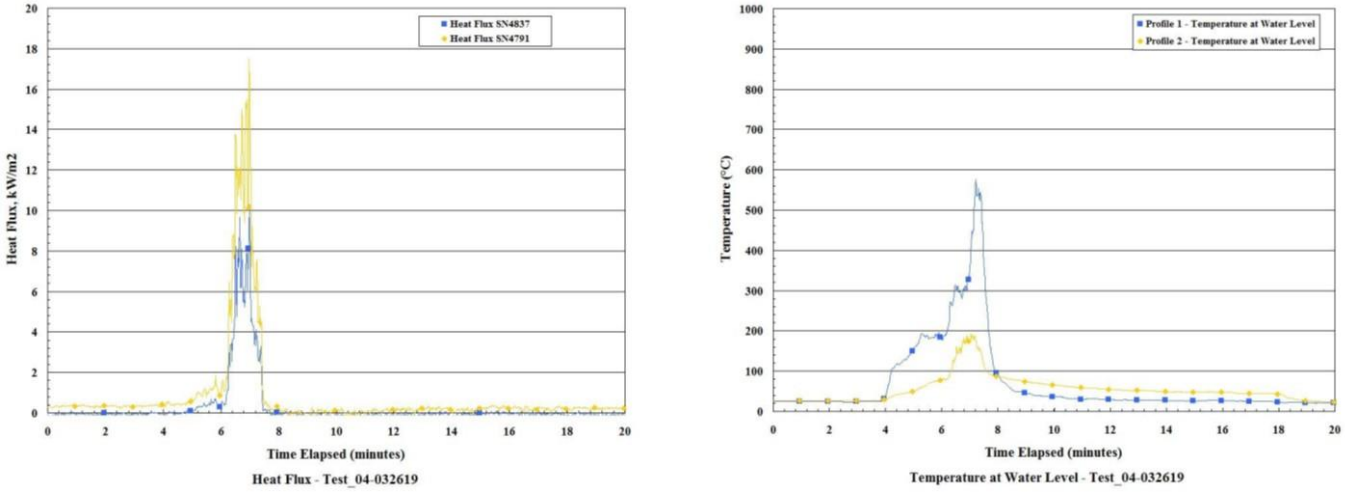

Figure C-6. Test 4 total heat flux measurement and temperature at the water level.

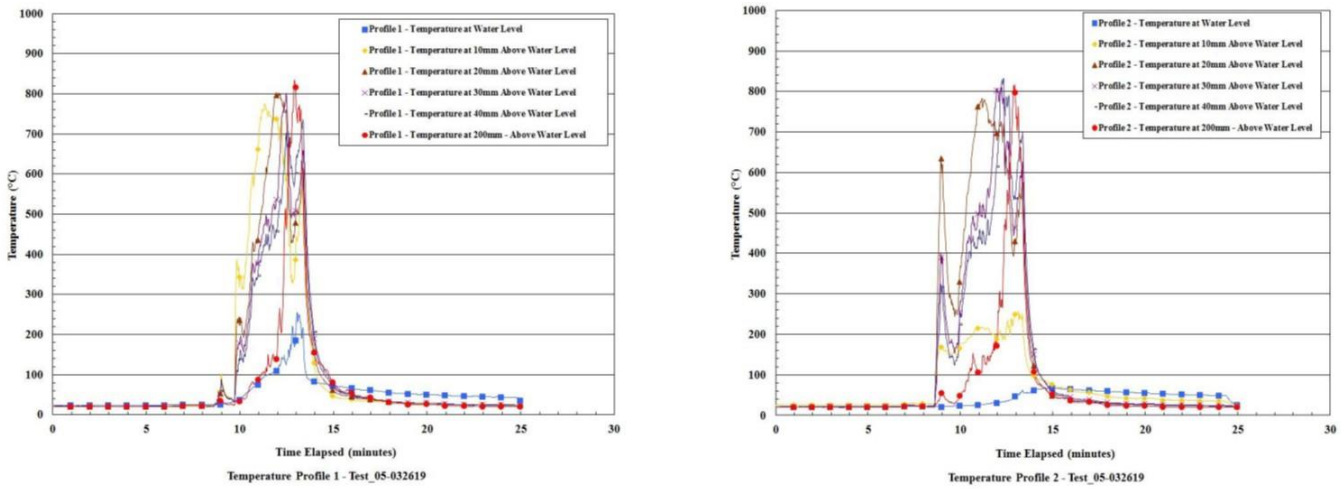

Figure C-7. Test 5 temperature profile 1 and profile 2.

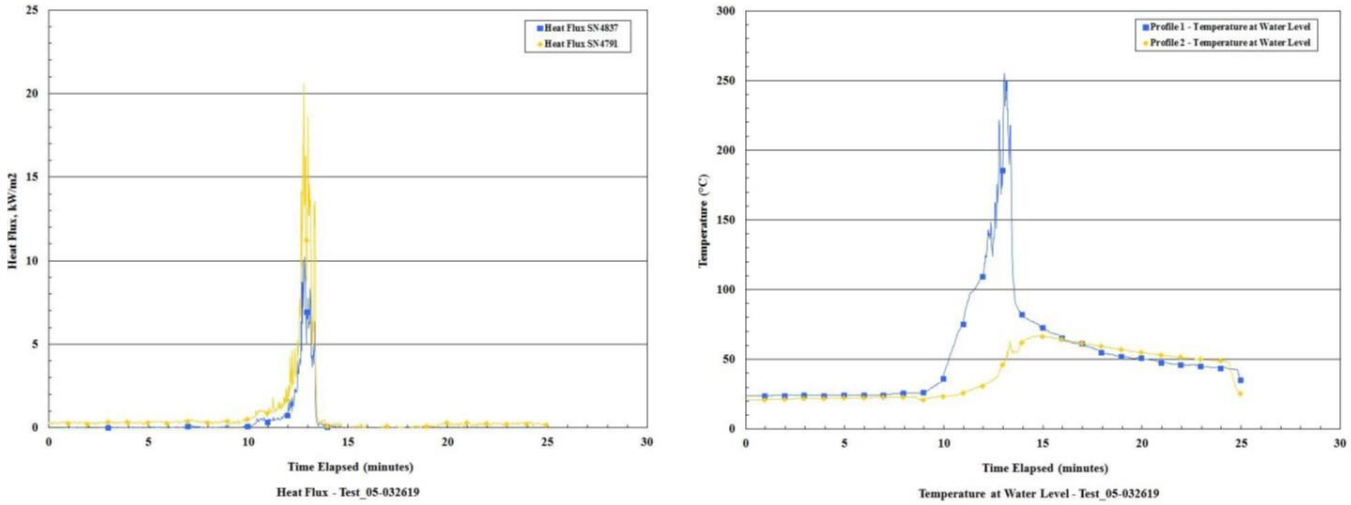

Figure C-8. Test 5 total heat flux measurement and temperature at the water level.

(This page intentionally left blank.)

APPENDIX D. COMPLETE MESOSCALE RESULTS AND OBSERVATIONS

The experimental results are analyzed from the perspective of quantifying the change in heat transfer by the flame to the oil slick because of the vegetation and the influence of the vegetation on the burning efficiency in terms of mass loss rate, flame spread and post burn residue (Arsava et al, 2019).

D.1 Oil Penetration into the Vegetation

The heavy oil was introduced by a custom design spill plate made of polycarbonate. The spill plate was placed on the left side of the burn pan and the oil was poured slowly to achieve an evenly distributed oil slick on water. As a standard procedure, the poured oil was left for 10 minutes before ignition to obtain its final shape. The influence of vegetation on oil penetration was determined by comparing the oil coverage area before ignition. Figure D-1 shows the oil coverage area for different vegetation densities and fuel mass. The boundaries of the oil slick was marked with yellow line.

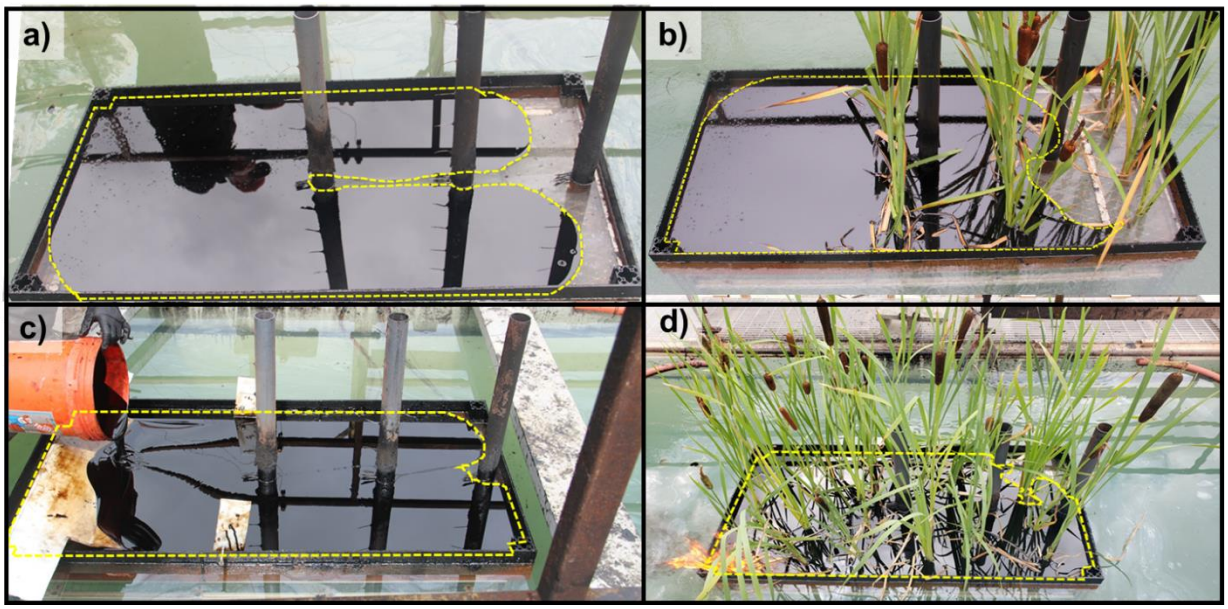

Figure D-1. Oil spread before ignition.

Technicians used the density of Bunker C oil to determine the required mass to achieve a ten-millimeter thick oil slick, which they poured into the burn pan. Calculations assumed even oil coverage over 100 percent of the burn pan surface, which was not exactly the case. The research team based the targeted ten-millimeter slick thickness on Garo et al. (1999), where they showed that the fuel-burning rate is independent of the initial fuel layer thickness for fuel layers thicker than 10 millimeters. As seen from Figure D-1, the high viscous oil, 45030 cP, was not able to spread fully over the burn pan surface and promoted a thicker oil slick. As an example, the oil coverage was about the 87 percent of the burn pan area for the most baseline tests (Figure D-1a) except for the first baseline test. In the first baseline test, the oil coverage was 93 percent due to wind blowing to the NW that helped the oil spread further. With the introduction of 50 percent and 100 percent vegetation coverage, the oil spread decreased to 75 percent (Figure D-1b) and 65 percent of the pan area respectively. For the tests with double oil mass, aiming for approximately 20 mm oil slick

thickness, the oil spread about 99 percent for the baseline case and covered 96 percent of pan area for the 100 percent vegetation coverage.

D.2 Burn Efficiency

Burn efficiency is the ratio of the mass of oil burned to the initial oil mass:

$$Burn\ Efficiency\ (\%) = \left[\frac{Initial\ Oil\ Mass - Residue\ Mass}{Initial\ Oil\ Mass}\right] \times 100 \qquad \text{(E-1)}$$

After each burn, the residue was allowed to cool. Chemists then collected the residue with pre-weighed sorbent pads and then weighed in a garbage bag immediately after. The residue inside and outside of the burn pan was collected and weighted separately. Table D-1 shows the experimentally determined burn efficiencies with varying vegetation coverage and oil mass.

Table D-1. Experimentally determined burn efficiencies.

Test #	Description	Initial Mass (kg)		Residue Mass (kg)		Burn Efficiency (%)
		Oil	Vegetation	Inside Burn Pan	Outside Burn Pan	
M1	Baseline	11.02	n/a	0.63	1.32	82.30
M2	Baseline	10.96	n/a	0.36	0.96	87.96
M3	Baseline	11.22	n/a	0.73	0.91	85.38
M4	50% vegetation	10.95	3.36	2.09	0.89	79.18
M5	50% vegetation	11.09	1.30	1.83	0.95	77.56
M6	50% vegetation + rain	11.02	2.22	2.28	1.07	73.26
M7	Baseline	11.25	n/a	1.16	1.29	78.22
M8	Baseline, double oil mass	22.70	n/a	1.21	2.21	84.93
M9	100% vegetation	11.34	2.80	2.62	1.13	73.48
M10	Baseline, double oil mass	23.10	n/a	1.95	1.29	85.97
M11	100% vegetation, double oil mass	21.75	3.15	2.67	1.25	84.26

The mesoscale experiments demonstrated that the burn efficiency of thin oil slicks decreases with vegetation. As shown in Table D-1, for the baseline tests (M1, M2, M3, and M7) performed with a thin oil slick (approximately 12.7 mm) the average burn efficiency was about 83.46 percent. For the tests with vegetation covering the 50 percent of the burn area (M4 and M5), the burn efficiency reduced to 78.37 percent and decreased further to 73.48 percent for the fully vegetation test (M9). The lack of air entrainment into the combustion zone due to dense vegetation, and high moisture content in the vegetation might be the reasons for the decrease. The least efficient test was Test 6, 50 percent vegetation, due to rain. The water droplets continuously cooled the flame and caused an early extinction. For the tests performed with higher oil mass (M8, M10, and M11), the vegetation did not have any influence on the burn efficiency. The average burn efficiency of these tests was about 85.05 percent. This can be explained by the long burn duration. The vegetation burned in the early stages of the fire and did not have an impact on the burn efficiency.

D.3 Flame Spread

The flame spread rates were determined by using the videos recorded during the tests. The ignition time (t_i), times of 50 percent (t_{50}) and 100 percent (t_{100}) flame coverages, and self-extinction time ($t_{extinguish}$) were

recorded. Table D-2 shows the flame spread rates with varying vegetation coverage and oil mass. Figure D-2 shows the zones used to calculate the flame spread rates in Table D-2.

Table D-2. Flame spread rates.

Test #	Description	Time Passed After Sustained Ignition (min)			Flame Spread Rate (mm/min)	
		t_{50}	t_{100}	$t_{extinguish}$	Through 1st 50% of the Pan Area (Figure E-2)	Through 2nd 50% of the Pan Area (Figure E-2)
M1	Baseline	2.77	3.32	6.40	271.08	1363.64
M2	Baseline	2.03	2.97	5.32	368.85	803.57
M3	Baseline	2.32	3.35	6.28	323.74	725.81
M4	50% vegetation	3.18	4.60	6.90	235.60	529.41
M5	50% vegetation	3.00	4.12	7.07	250.00	671.64
M6	50% vegetation + rain	1.50	2.02	4.40	500.00	1451.61
M7	Baseline	2.08	3.38	5.68	360.00	576.92
M8	Baseline double oil mass	2.18	3.08	11.90	343.51	833.33
M9	100% vegetation	2.10	3.25	6.22	357.14	652.17
M10	Baseline double oil mass	2.22	3.18	12.20	338.35	775.86
M11	100% vegetation, double oil mass	3.05	4.07	13.08	245.90	737.70

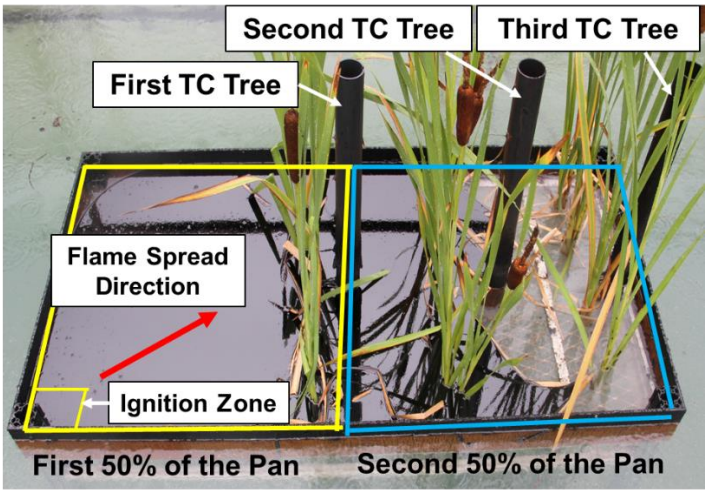

Figure D-2. Picture of the zones used to calculate the flame spread rates in Table D-2.

The results presented in Table D-2 show that the vegetation does not have a significant effect on flame spread. It is observed that the flame spread rates in the second half of the burn pan were about two to three times higher than the spread rates in the first half of the pan. When the flame reaches to the midpoint, the heat feedback from flame to fuel was sufficient enough to heat the oil surface up to a point where its viscosity decreases significantly. Less viscous fuel evaporates faster and allows flame front end to move faster. Figure D-3 is a sketch explaining the faster flame spread in the second half of the burn pan due to increased heat transfer from flame to the oil surface, less viscous oil, and increased m_{oil}.

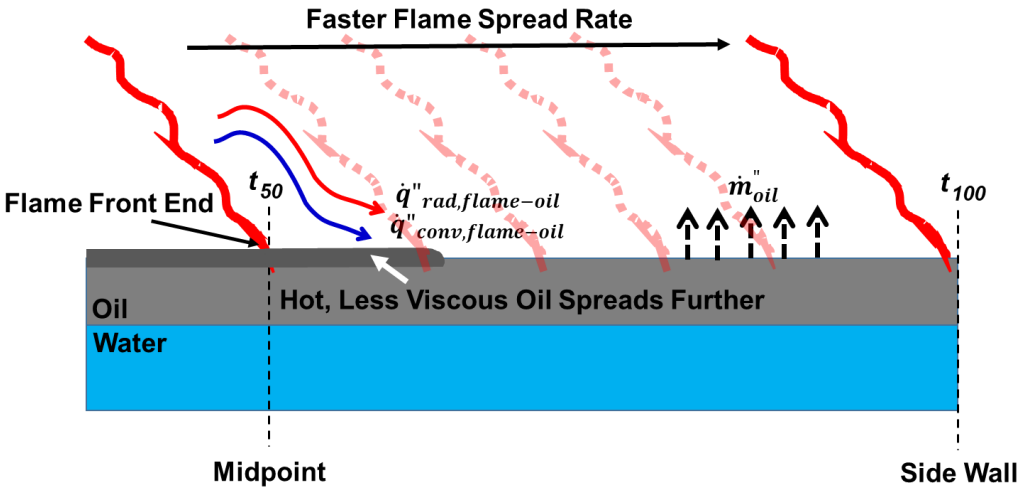

Figure D-3. Sketch of the faster flame spread in the second half of the burn pan.

D.4 Burn Rate

The flame spread analysis demonstrated that it takes between three to four minutes to achieve 100 percent flame coverage. The fuel burnt during this transition time needs to be considered in burn efficiency calculations. In this context, the area integration method is used to calculate the experimental burn efficiencies. The method is described as follows:

1. Determine the time from ignition (t_i) to 50 percent (t_{50}) and 100 percent (t_{100}) flame coverage.
2. Divide the burn pan into two equal zones and then divide the first half (0.75 m x 0.75 m) into equal subsections (n). By assuming the flame spread rate is linear, calculate the burn area for each time interval $\left(\frac{t_{50}}{n}\right)$. As an example, the area of a single subsection ($A_{50\text{-}i}$) of the first zone divided into 10 equal pieces will be 0.05625 m² $\left(\frac{0.75}{10} \times 0.75\right)$. With the ignition, the flame will cover the first section, ($A_{50\text{-}1}$), at $\frac{t_{50}}{10}$. It will spread to the second section at $\frac{t_{50}}{5}$ and the flame coverage area will be 0.1125 m². At t_{50} the cumulative burn area will be $A_{50} = A_{50\text{-}1} + A_{50\text{-}2} \ldots + A_{50\text{-}10}$.
3. Repeat the same procedure for the second half of the pan by keeping the time interval constant. For example, the area of a single section ($A_{100\text{-}i}$) of the second half of the pan divided into 2 equal pieces will be 0.2812 m² $\left(\frac{0.75}{2} \times 0.75\right)$. At $\frac{t_{100}}{2}$ the flame coverage will be $A_{100\text{-}1} = A_{50} +$ 0.2812 m². At t_{100} the cumulative burn area will be $A_{100} = A_{100\text{-}1} +$ 0.2812 m².
4. After full coverage the burn area will remain same,1.125 m², for each time interval $\left(\frac{t_{50}}{10}\right)$ until the flame self-extinguishes ($t_{extinguish}$). At the end, a cumulative burn area is obtained and the burn rate is calculated as follows:

$$Burn\ Rate\ (mm/min) = \left[\frac{Initial\ Oil\ Mass - Residue\ Mass}{Cumulative\ Burn\ Area\ \times\ Time\ interval}\right] \qquad \text{(E-2)}$$

The burn rate calculation of Test M1 is presented in Table D-3 as an example.

Table D-3. Burn rate calculation of Test M1 by area integration method.

Time (sec)	Burn Area (m^2)
0 (t_i)	0
16.62	$A_{50\text{-}1}$ = 0.05625
33.24	$A_{50\text{-}2}$ = 0.1125
49.86	$A_{50\text{-}3}$ = 0.16875
66.48	$A_{50\text{-}4}$ = 0.225
83.1	$A_{50\text{-}5}$ = 0.28125
99.72	$A_{50\text{-}6}$ = 0.3375
116.34	$A_{50\text{-}7}$ = 0.39375
132.96	$A_{50\text{-}8}$ = 0.45
149.58	$A_{50\text{-}9}$ = 0.50625
166.2 (t_{50})	$A_{50\text{-}10}$ = 0.5625
182.82	$A_{100\text{-}1}$ = 0.84375
199.44 (t_{100})	$A_{100\text{-}2}$ =1.125
216.06	1.125
232.68	1.125
249.3	1.125
265.92	1.125
282.54	1.125
299.16	1.125
315.78	1.125
332.4	1.125
349.02	1.125
365.64	1.125
382.26 ($t_{extinguish}$)	1.125
Cumulative Area	**17.4375 m²**

$$Burn\ Rate = \frac{9.07\ kg \Big/ \frac{1000000 \frac{mm^2}{liter}}{0.86 \frac{kg}{liter}}}{17.4375\ m^2 \times 1000000 \frac{mm^2}{m^2} \times 16.62\ sec \Big/ 60 \frac{sec}{min}}$$

$$\boldsymbol{Burn\ Rate\ of\ Test\ 1 = 2.183\ mm/min}$$

Figure D-4 shows the experimental burn rates calculated by the area integration method.

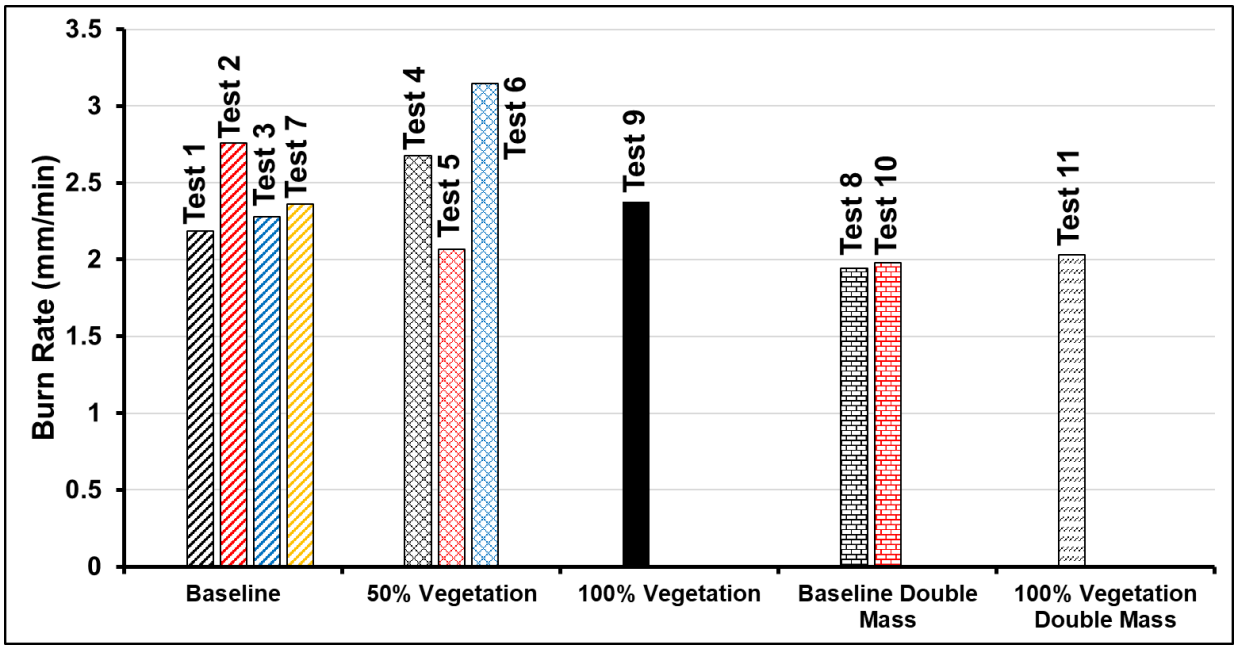

Figure D-4. Experimental burn rates calculated by the area integration method.

As shown in Figure D-4, the average burn rate of the four baseline tests was about 2.4 mm/min, while the average burn rate of the 50 percent and 100 percent vegetation burns (M4 and M5) were 2.37 mm/min and 2.37 mm/min. For the increased fuel mass tests, the burn efficiencies of the baseline and 100 percent vegetation were similar. The results demonstrated that the vegetation does not have an influence on the burn rate.

D.5 Temperature Profiles

It is observed that there was little variations across replicates, therefore data from individual burns (M3, M4, M9, M10, and M11) will be presented from here on. Figure D-5 shows the temperature distribution along the vertical axis of the first TC tree located at the center of the burn pan at different time intervals for the baseline (M3), 50 percent vegetation (M4) and 100 percent vegetation tests (M9). The propane torch was held at the edge of the oil slick for around 30 – 50 s until a steady flame was observed after which the torch was removed. The t_i = 0 s time frame shows the sustained ignition by a propane torch. All temperature results presented in this study are time averaged (20 seconds).

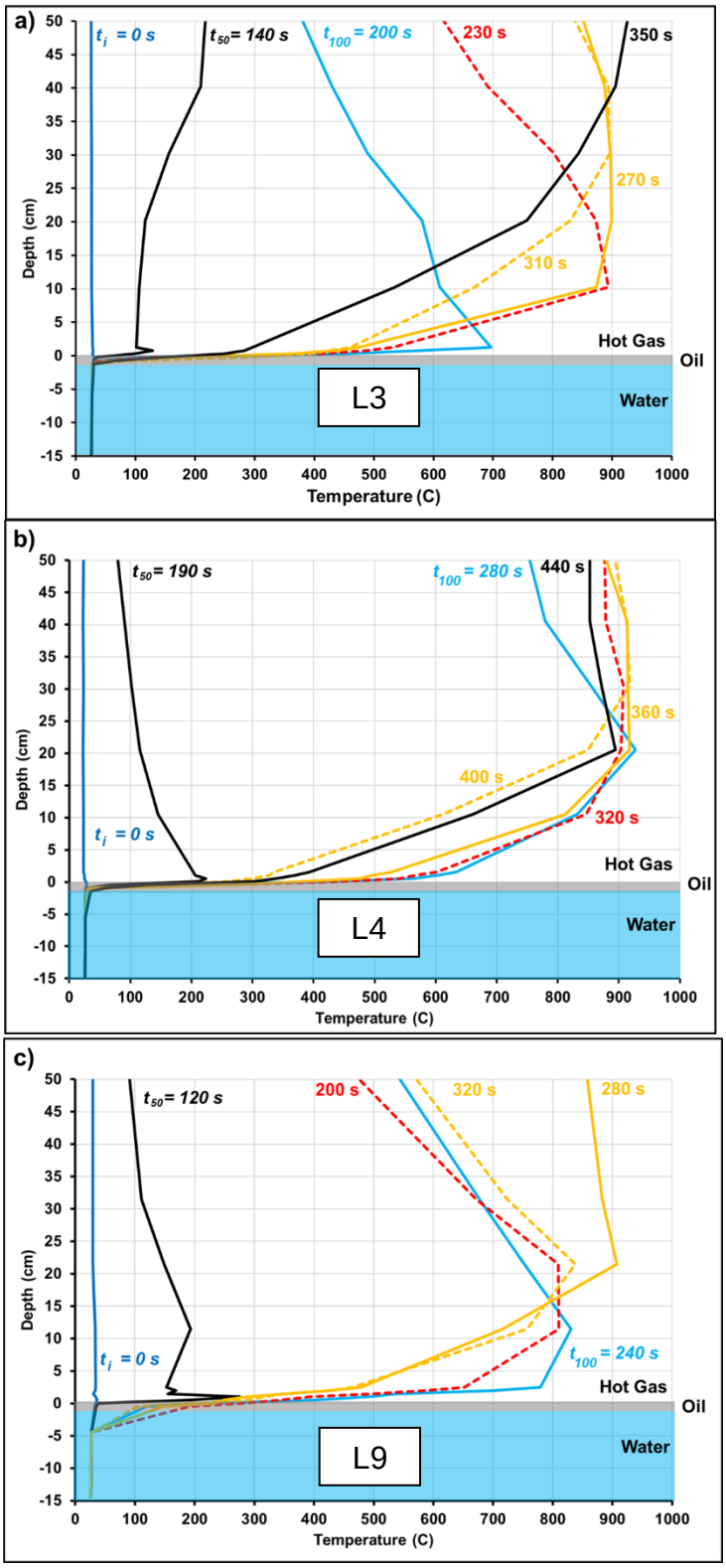

Figure D-5. Temperature profiles of example mesoscale experiments.

Figure D-6 shows the vertical temperature distribution at the center for the baseline (M3), 50 percent (M4) and 100 percent vegetation (M9) cases after 1 minute obtaining 100 percent flame coverage (t_{100}). With an increase in the vegetation coverage, the curves move to the left, the flame temperature lowers, as shown in the Figure D-6.

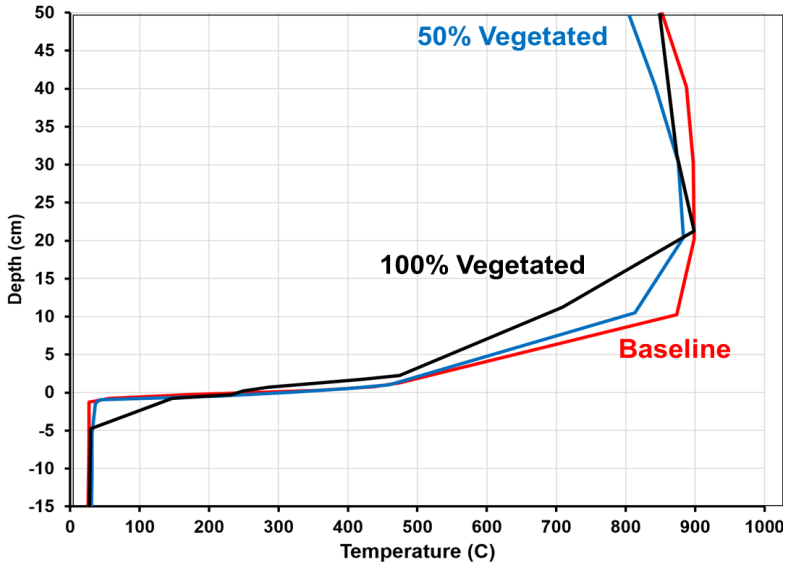

Figure D-6. Temperature profiles at the pan center after 1 minute reaching to the t_{100}.

When the oil surface was covered with 100 percent vegetation, the temperature above ten centimeters of the fuel layer reaches up to 680° C, which is around 200° C lower than the baseline case as shown in Figure D-6. The lower temperature causes a decrease in burning efficiency. When the baseline and 50 percent vegetation cases are compared, it is observed that the hot gas temperature decreased 70° C, while the fuel temperatures did not change significantly. Figure D-7 shows the temperature distribution along the vertical axis of the first TC tree placed at the center of the burn pan at different time intervals for the baseline (M10) and 100 percent vegetation (M11) tests with double oil mass.

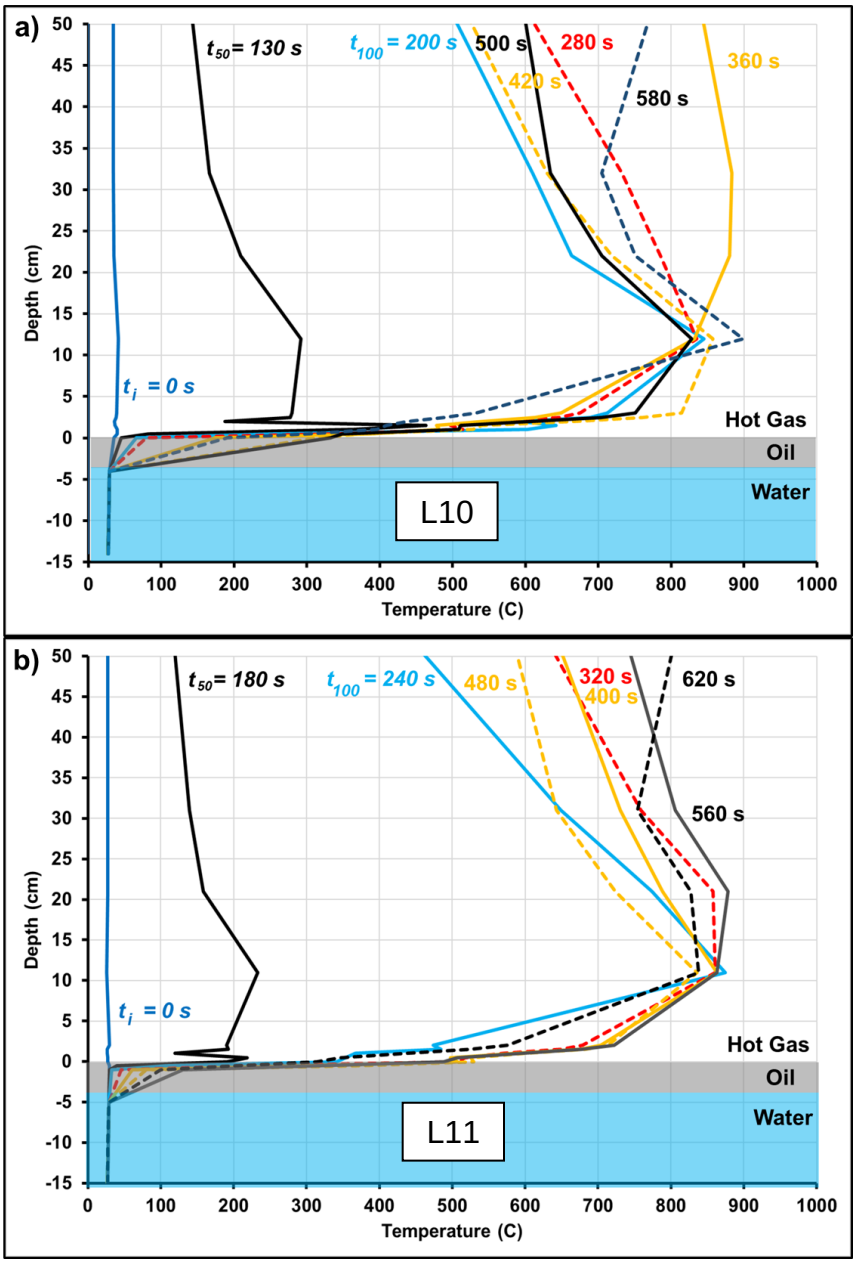

Figure D-7. Temperature profiles of the mesoscale experiments with double oil mass.

It is observed that the vegetation caused lower flame and hot-gas temperatures while the flame was spreading in the first half of the pan. At t_{50}, for the baseline case, the temperature above ten centimeters of the fuel layer (hot-gas zone) reaches up to 290° C, which is about 100° C higher than the fully vegetation case as shown in Figure D-7. After reaching t_{100} + 4 minutes, with the burn of all vegetation, the temperature profiles of the two cases becomes similar.

D.6 Heat Flux Measurements

Radiometers capable of measuring radiative heat flux alone and total heat flux gauges (HFG's) were used to distinguish the contributions from flame radiative and convective heat fluxes. Figure D-8 shows the total

(convective + radiative) and radiative heat flux measurements of the baseline (M3), 50 percent vegetation (M4) and 100 percent vegetation tests (M9).

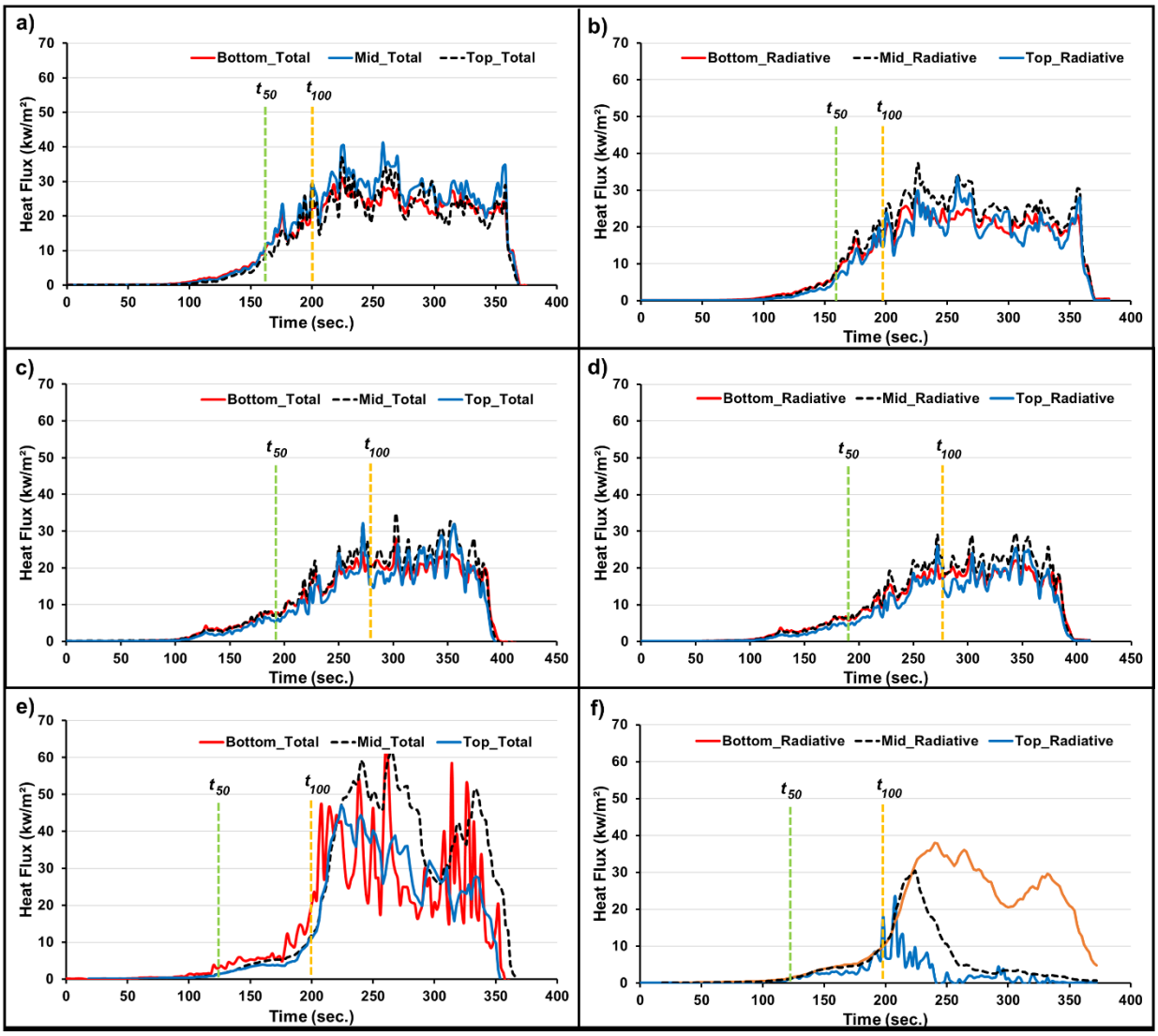

Figure D-8. Heat flux measurements of the mesoscale experiments.

Total heat flux - baseline (M3), b) radiative heat flux - baseline (M3), c) total heat flux - vegetation covering the 50 percent of the burn area (M4), d) radiative heat flux - vegetation covering the 50 percent of the burn area (M4), e) total heat flux - vegetation covering the 100 percent of the burn area (M9), f) radiative heat flux - vegetation covering the 100% of the burn area (M9). Bottom: 30 cm above the fuel layer, mid: 85 cm above the fuel layer, top: 130 cm above the fuel layer.

As expected the difference between the total and radiative heat flux values is not significant. The total HFG's was not able to capture the convective heat since the hot air rises up, while the radiant heat was captured by all gauges since radiation moves in waves in all directions (Figure D-9). When the radiative heat fluxes were compared, both the baseline and the 50 percent vegetation cases emitted about 20 kW/m² of radiant heat (Figure D-8b and Figure D-8d). However, the exposure of oil to the heat flux was different

for the two cases. For the baseline, the exposure of oil to the 0.4 kW/m² heat flux (the fraction of total energy transmitted back to the fuel is about 2 percent) was about 60 seconds longer than the 50 percent vegetation case. The longer exposure can cause an increase in burn efficiency.

For the 100 percent vegetation case, the high wind speed (2.05 m/s, SE -NW direction) tilted the flame towards to the HFG's and caused and increase in the measurements. The average total heat flux measured by the sensors was about 32 kW/m² (Figure D-8e). The radiant heat flux 30 cm above the fuel level (red line) reached an average value of 30 kW/m² (Figure D-8f). However, the tilted flame provided a very low amount of radiative heat feedback to pool surface causing a decrease in burning efficiency.

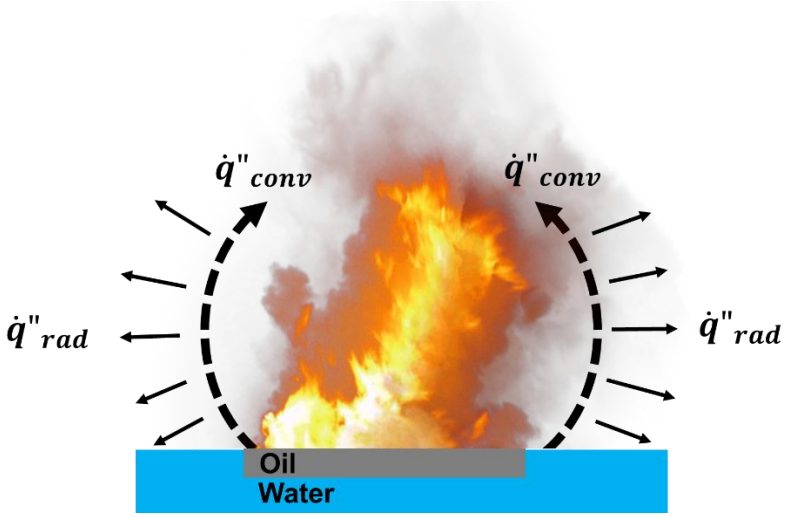

Figure D-9. Heat transfer mechanism from flame to ambient in an ISB.

Figure E-10 shows the total (convective + radiative) and radiative heat flux measurements of the baseline (M10) and 100 percent vegetation (M11) tests with double oil mass.

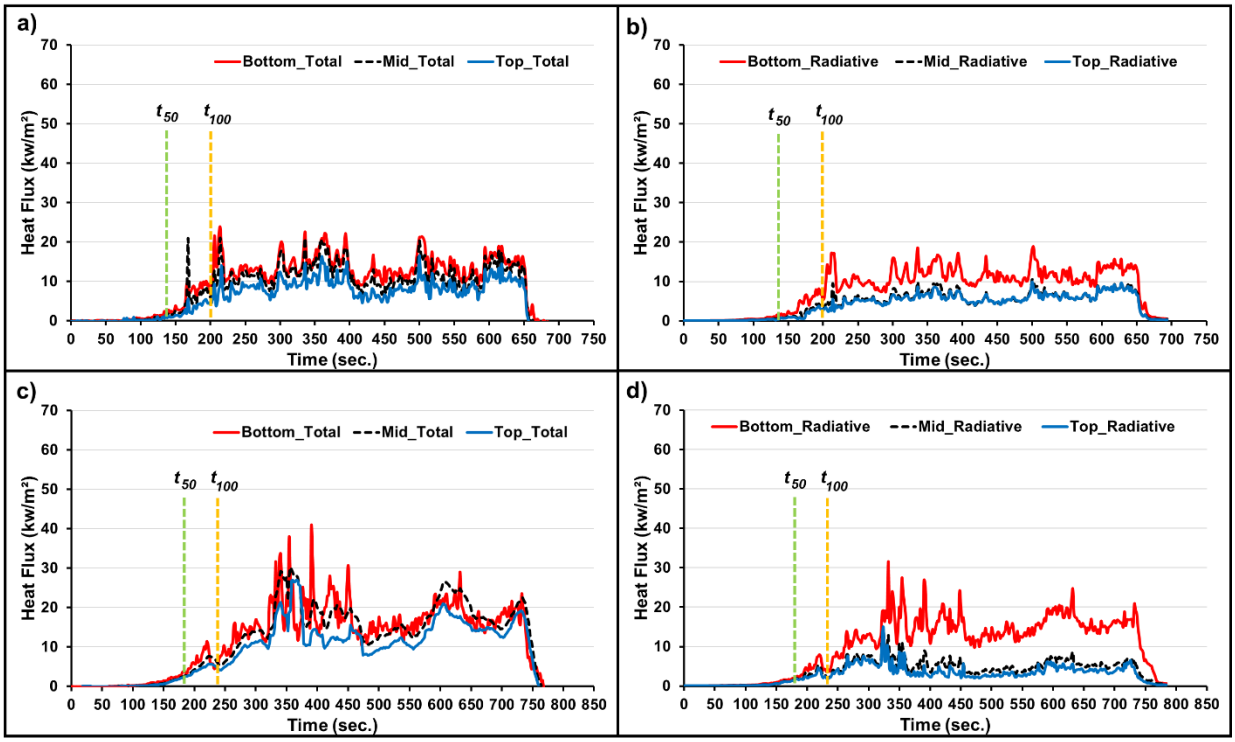

Figure D-10. Heat flux measurements of the mesoscale experiments with double oil mass.

For the 100 percent vegetation double oil mass case, the wind blown from SE to NW direction tilted the flame and caused an increase in the heat flux measurements (Figure D-10 c, d). When the radiant heat emitted by the baseline and the 100 percent vegetation case were compared, there was no significant difference (both emitted about 10 kW/m²).

APPENDIX E. AIR MONITORING

E.1 Air Monitoring Considerations

E.1.1 Special Monitoring of Applied Response Technologies (SMART) Protocol

A benefit of ISB is reduced need for collection, storage, transport and disposal of recovered material – because a large portion of the oil converts to gaseous combustion products (USCG, 2006). But, this brings about a recognized need for air monitoring where there is potential for smoke exposure to humans and/or environmentally sensitive areas (USCG, 2006). Special Monitoring of Applied Response Technologies (SMART) protocol, as described in the National Oil and Hazardous Substances Pollution Contingency Plan, provides the USCG's current guidelines for monitoring ISB smoke plumes. In accordance with this monitoring program, mobile ground teams collect real-time data at sensitive locations such as population centers downwind of the burn using portable air monitoring instruments. The critical question SMART protocol addresses for the FOSC and Unified Command is, "Are particulate concentration trends at sensitive locations exceeding level of concern (LOC), per EPA's National Ambient Air Quality Standard (NAAQS) and National Response Team (NRT) guidelines?" (USCG, 2006). To answer this question, field monitors collect instantaneous concentration readings and calculate time weighted average (TWA). Figure E-1 shows a sample graph of this data from a test burn near Mobile, AL on September 25, 1997. The TWA is an indication of concentration trends and considered a more stable and reliable indicator of exposure to particulates (USCG, 2006).

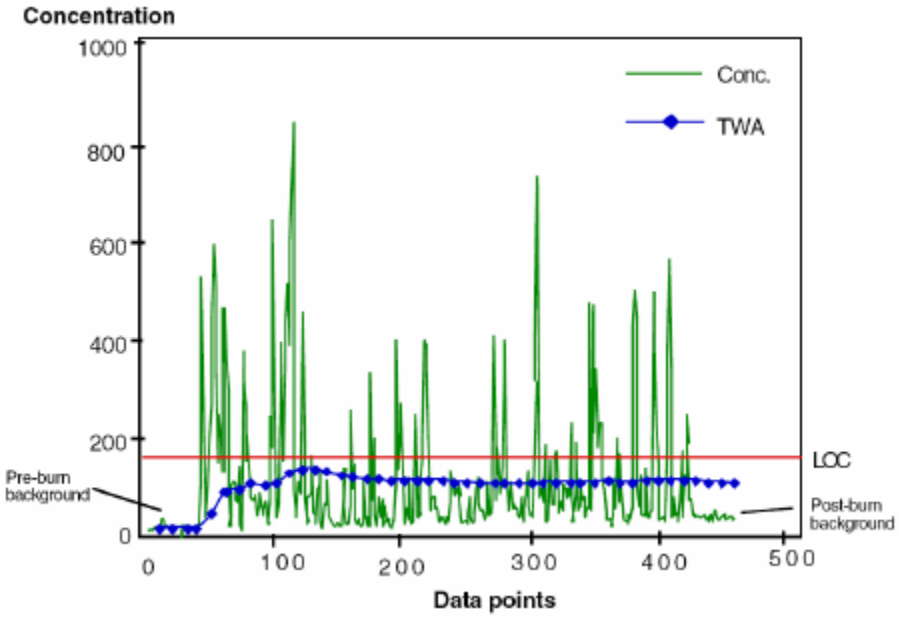

Figure E-1. Sample graph of ISB smoke plume field monitoring data collected via SMART protocol.

LOC is level of concern for particulate concentration; TWA is the time weighted average. Source: *Special Monitoring of Applied Response Technologies* (USCG, 2006).

Air quality measurement uses the principle of light scattering, readings for which monitors convert to weight of particulates in micrograms per cubic meter of air ($\mu g/m^3$) (NOAA, 2006).

E.1.2 Smoke Plume Components

ISB emits a black smoke plume composed of 80-85 percent carbon dioxide (CO_2) and water (H_2O) (USCG, 2006). Polychlorinated dibenzo-*para*-dioxins/dibenzofurans (PCDD/PCDF) are contaminants that persist in the environment and accumulate in animal fat. They are formed as by-products of all combustion processes. According to the World Health Organization (WHO), some PCDD/PCDFs are of carcinogenic risk to humans (IARC, 1997).

As of March 1999 in accordance with EPA's NAAQS, the NRT recommended a conservative upper exposure limit (i.e., LOC) of 150 micrograms of particulates smaller than ten micrograms in diameter (PM_{10}) per cubic meter of air, averaged over one hour (USCG, 2006). When the TWA of particulate concentrations exceeds the LOC in a sensitive area, then the NRT recommends precautionary action (USCG, 2006).

E.2 sUAS Use in Air Emissions Monitoring

E.2.1 Potential for Small Unmanned Aerial System Air Quality Measurements during In-situ Burning

SMART protocol does not directly address the health and safety of spill responders or monitoring personnel (USCG, 2006). Moreover, it requires a team of responders to operate downwind of the burn, in a high risk zone of emissions exposure. USCG, NOAA, EPA, the Center for Disease Control (CDC) and the Bureau of Safety and Environmental Enforcement (BSEE) jointly developed SMART protocol in 2006 to use the best available and operationally practical technology (USCG, 2006). sUAS monitoring necessitates air monitoring protocol revisions to keep up with advances in technology.

During an ISB, the general public may be at risk when the trajectory of smoke plume particulates and emissions at ground level exceed safe levels. Air quality data gathered via sUAS mounted sensors represent emissions factors at varying elevations. Therefore, the data should be modeled with weather or other atmospheric data to most effectively address public health concerns. This is not necessarily an added layer of logistical analysis because current SMART protocol uses real-time monitoring as only one decision-making factor to be paired with smoke modeling, trajectory analysis and visual observations (USCG, 2006). Successful modeling paired with sUAS smoke plume monitoring to assess risks to sensitive areas would eliminate the case-by-case analytical guess - work required to determine best placement of ground monitors (USCG, 2006), since all sUAS monitoring moves with the plume itself. Unless a plume moves directly into a sensitive area, remote monitoring as evaluated in this study would not directly measure emissions in that area.

Another consideration is that current SMART protocol instruments generally provide continuous data logging for at least eight hours (8 h). Each 0.5 h ISB test conducted during this study required three (3) sets of sUAS batteries (two rapid landings for battery change). Battery swaps did not affect data integrity, but a longer burn would require more, fully-charged battery sets.

Table E-1 summarizes a comparison of pros and cons for current SMART protocol and remote monitoring via sUAS identified by this study. Further field tests could better compare the capabilities of existing methods for air monitoring during ISB with remote air monitoring potential.

Table E-1. Pros and cons for current SMART protocol and remote monitoring via sUAS.

Factor	Current SMART Protocol	Remote Monitoring via sUAS
Spill Responder Health and Safety	⊗ Not addressed	✓ Responders not required to operate downwind
Monitoring Location	✓ Measures emissions at ground-level directly in sensitive areas	✓ Monitoring location does not require case-by-case evaluation
Data Logging Endurance	✓ Instruments generally provided data logging for at least 8 hours	⊗ Frequent battery changes needed

(This page intentionally left blank.)

APPENDIX F. LARGE-SCALE TEMPERATURE AND HEAT FLUX DATA

F.1 Temperature and Heat Flux Plots from Large-scale Crude Oil Burns

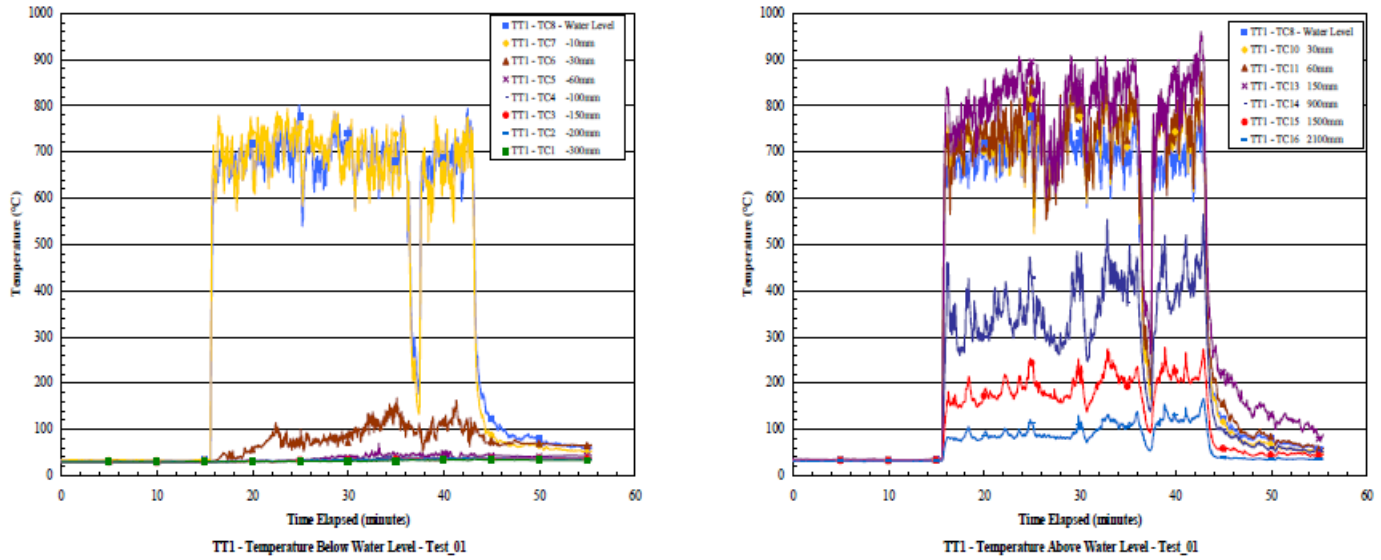

Figure F-1. Large-scale test L1 (crude oil baseline), thermocouple tree 1.

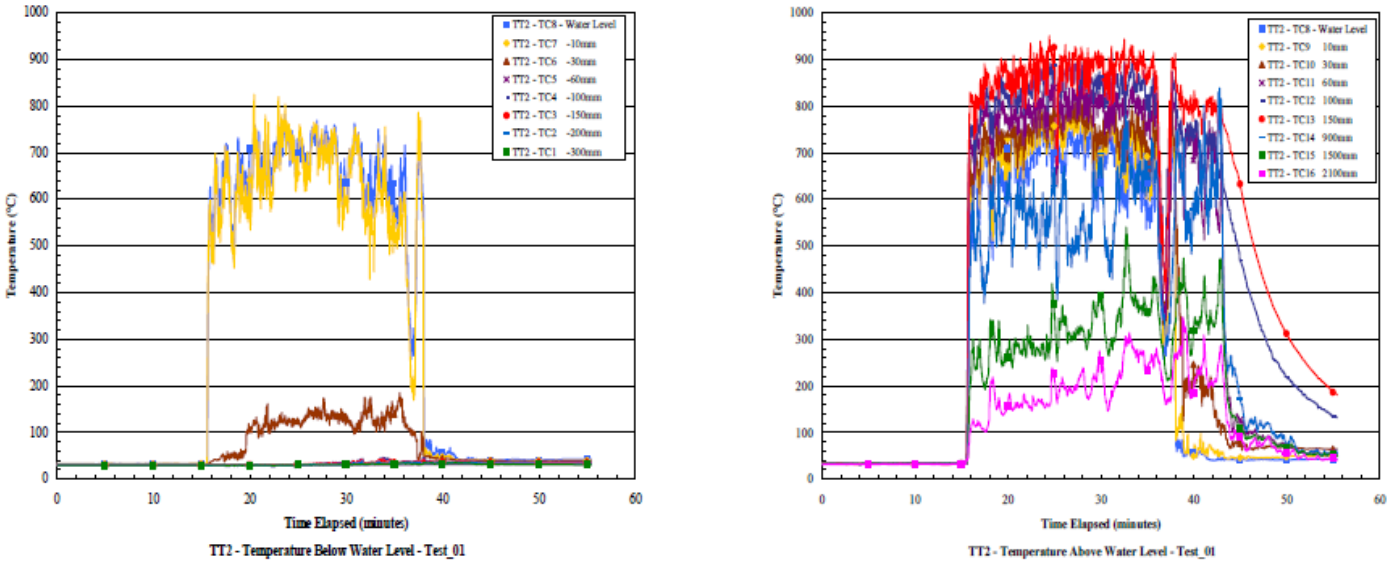

Figure F-2. Large-scale test L1 (crude oil baseline), thermocouple tree 2.

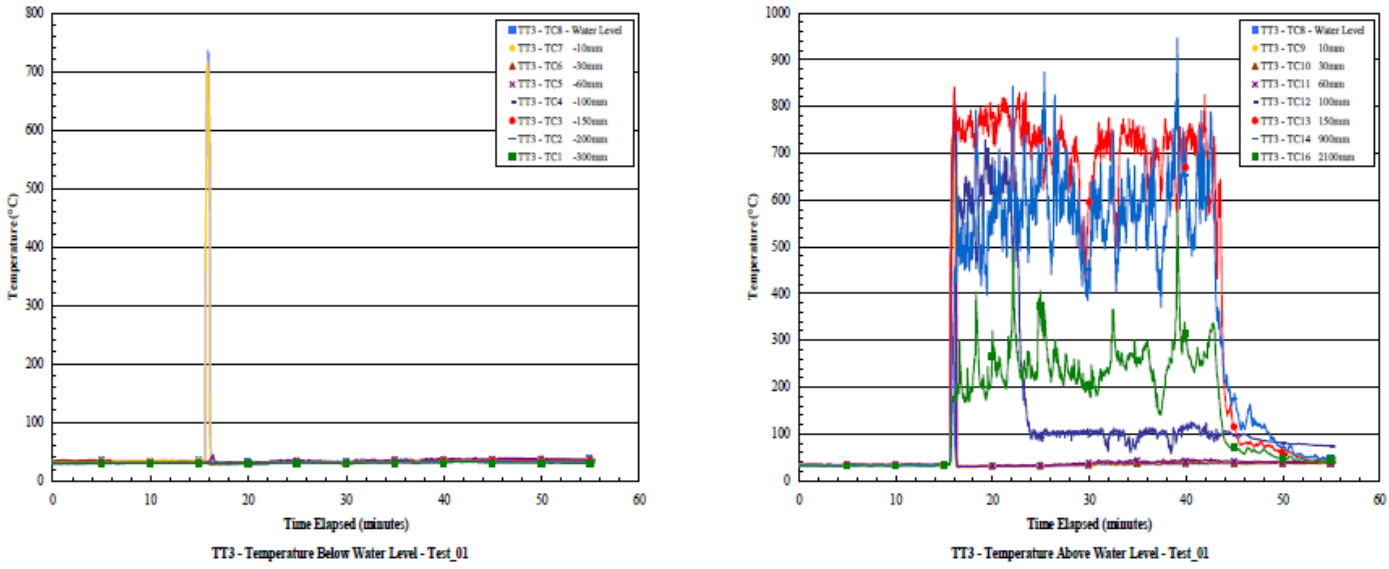

Figure F-3. Large-scale test L1 (crude oil baseline), thermocouple tree 3.

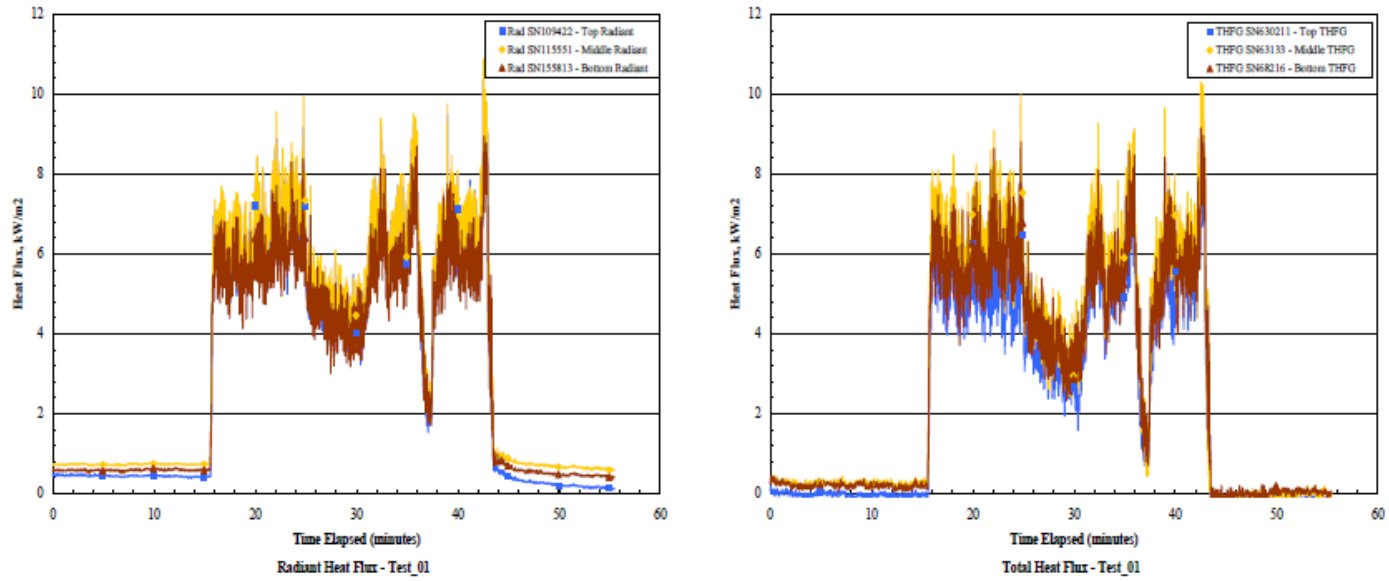

Figure F-4. Large-scale test L1 (crude oil baseline), radiant and total heat flux measurements.

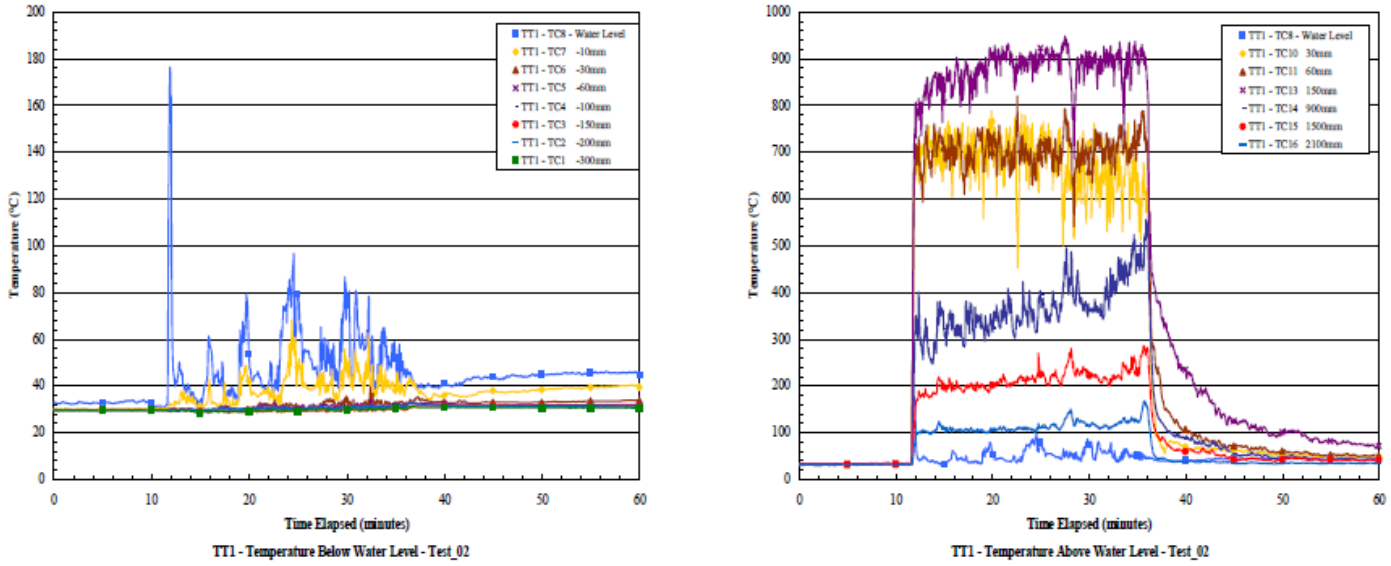

Figure F-5. Large-scale test L2 (crude oil with vegetation), thermocouple tree 1.

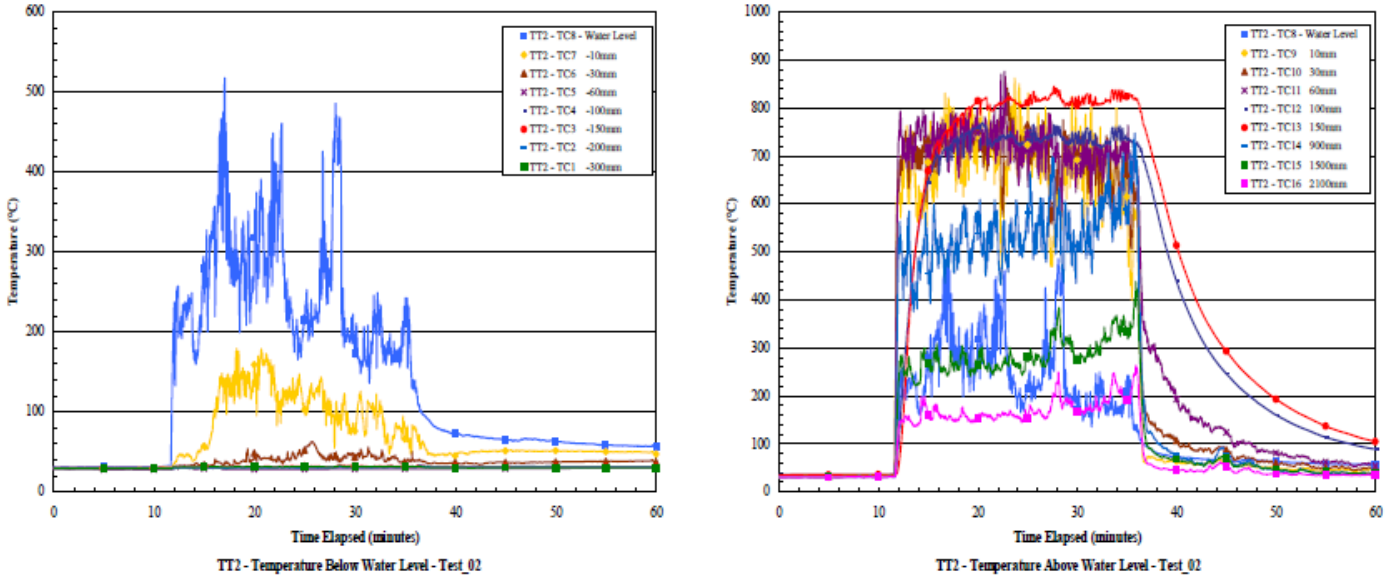

Figure F-6. Large-scale test L2 (crude oil with vegetation), thermocouple tree 2.

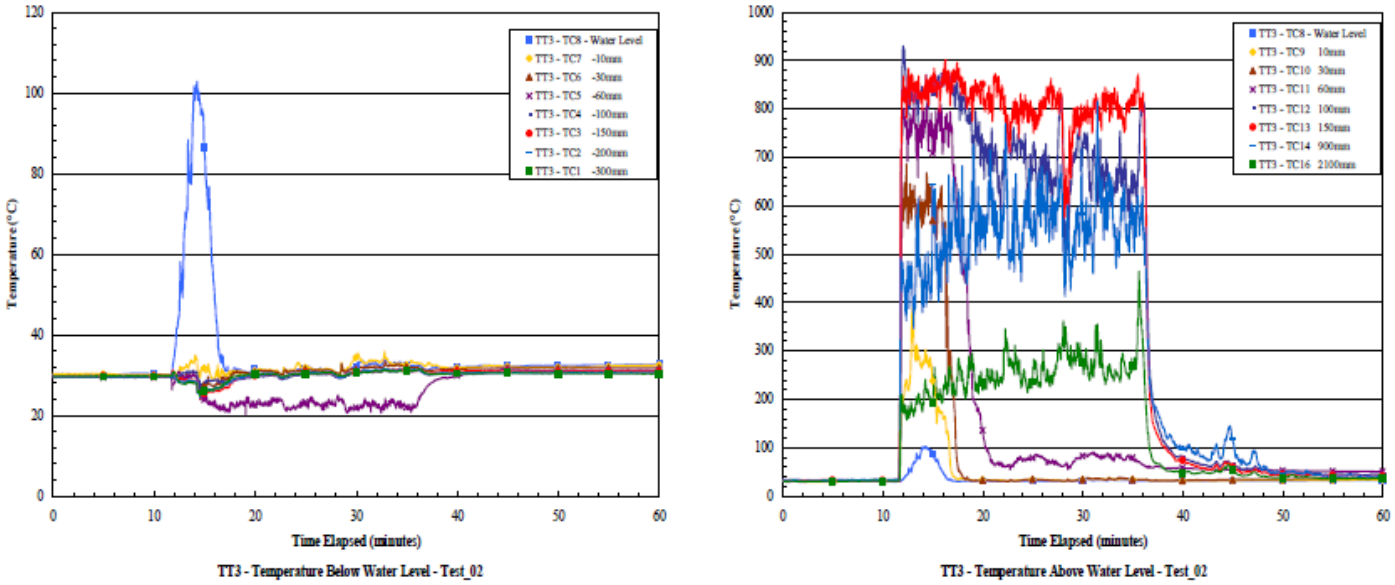

Figure F-7. Large-scale test L2 (crude oil with vegetation), thermocouple tree 3.

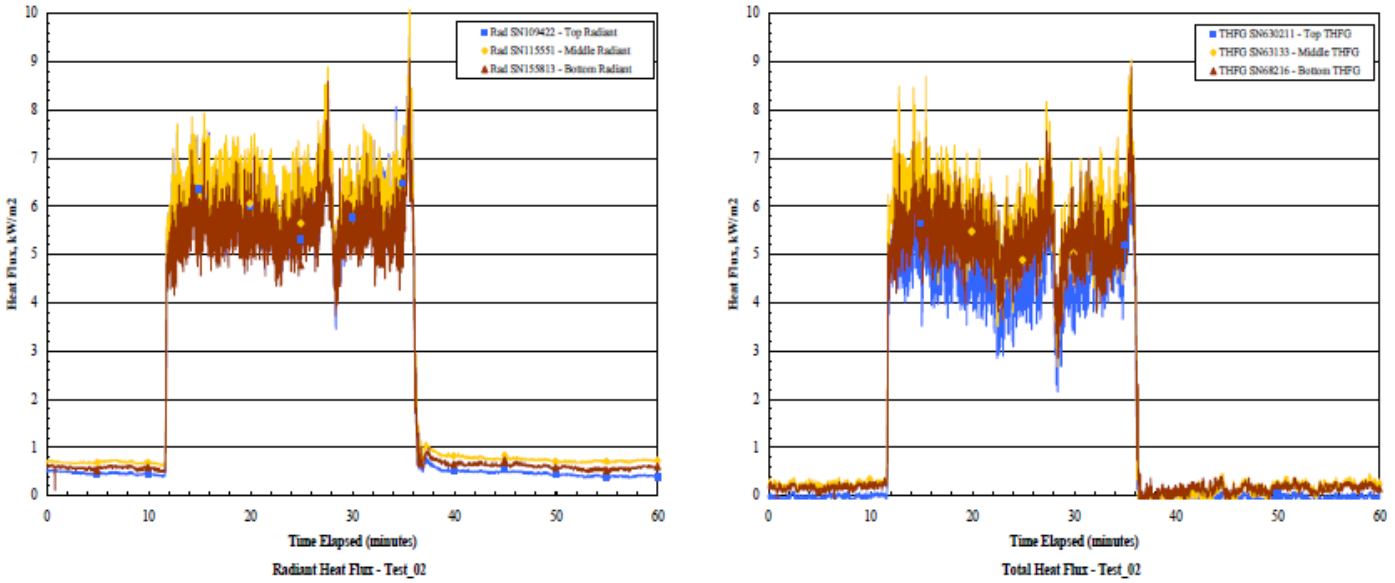

Figure F-8. Large-scale test L2 (crude oil with vegetation), radiant and total heat flux measurements.

F.2 Temperature and Heat Flux Plots from Large-scale RMG 380 Burns

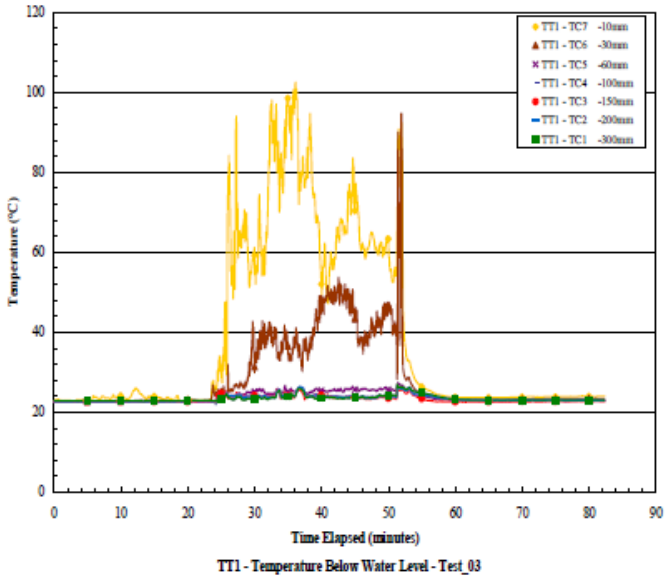

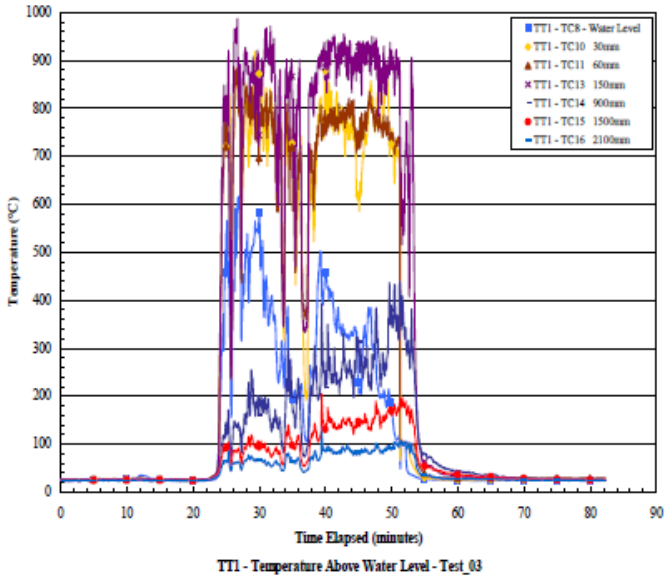

Figure F-9. Large-scale test L3 (RMG 380 baseline), thermocouple tree 1.

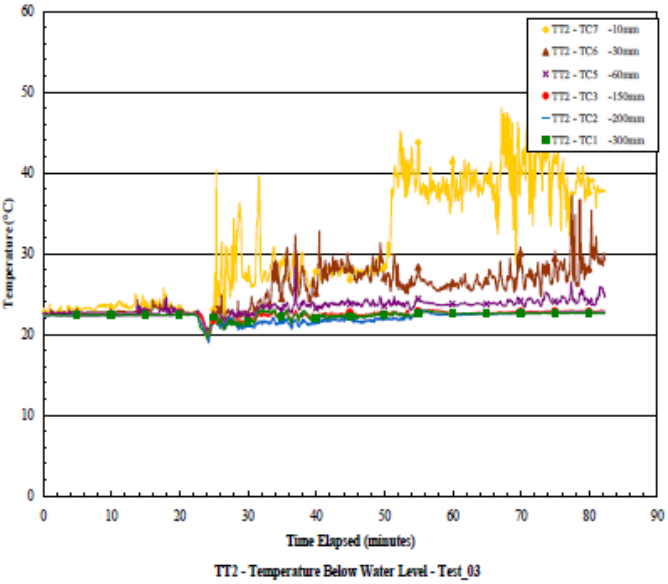

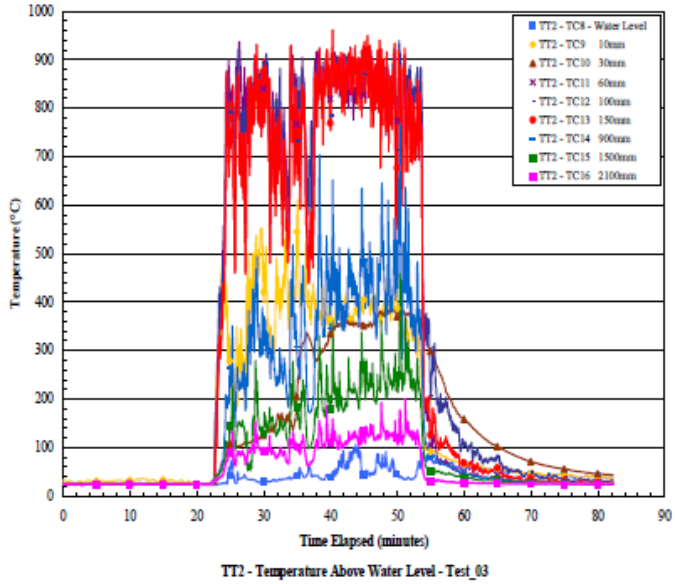

Figure F-10. Large-scale test L3 (RMG 380 baseline), thermocouple tree 2.

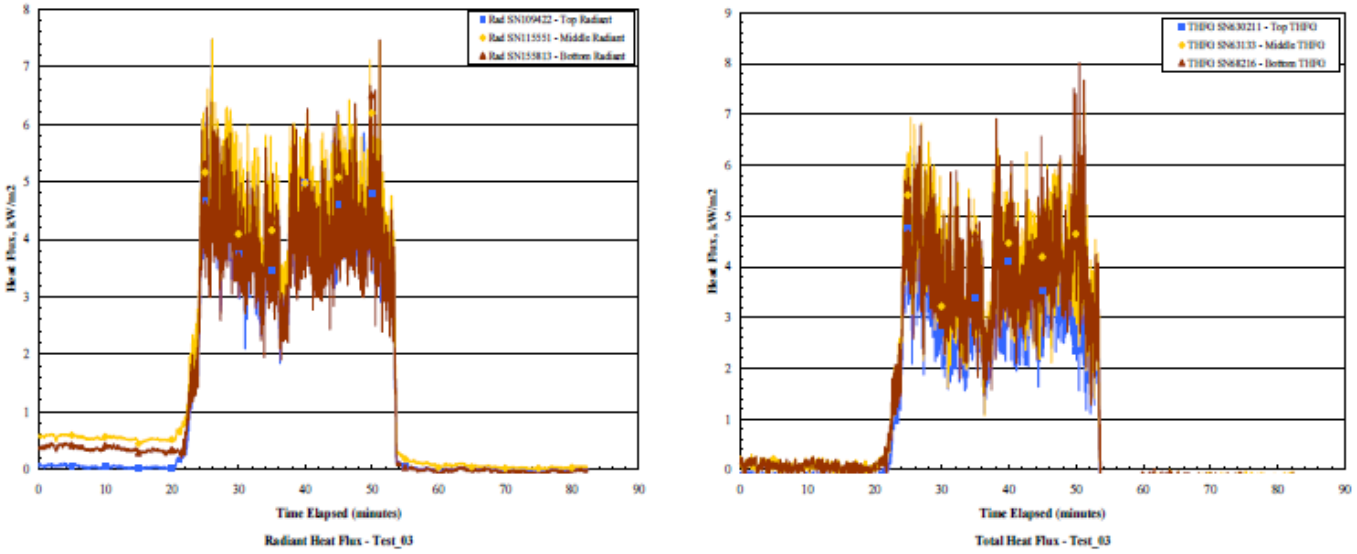

Figure F-11. Large-scale test L3 (RMG 380 baseline), radiant and total heat flux measurements.

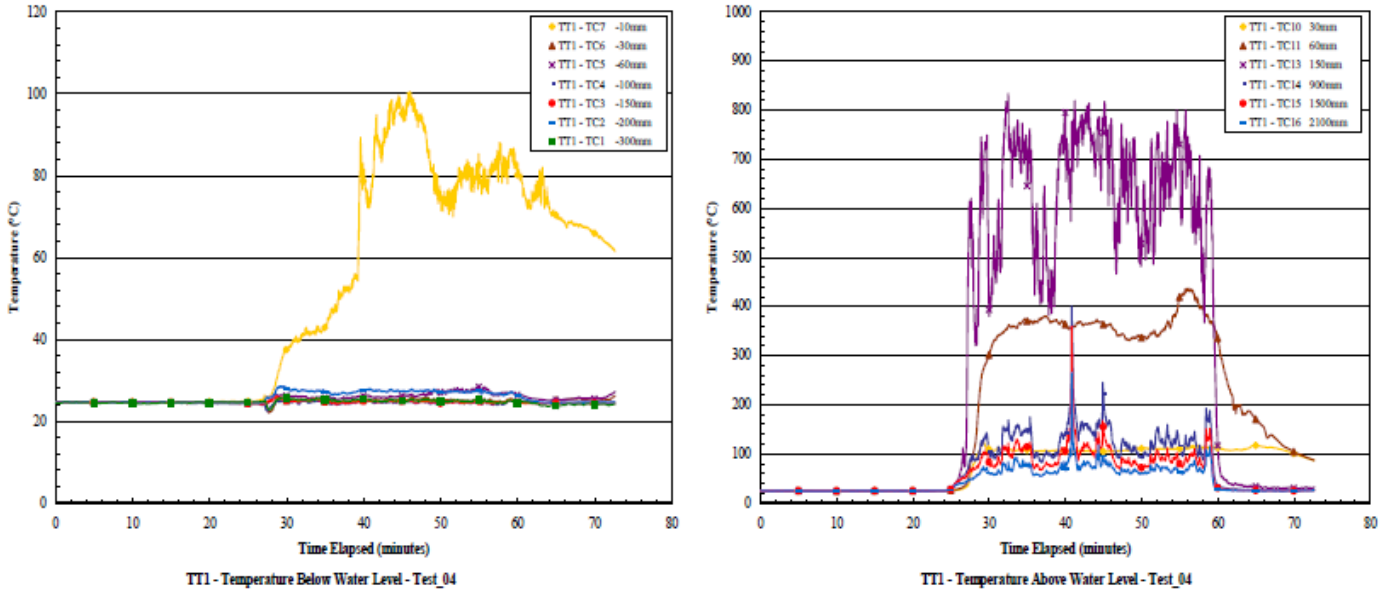

Figure F-12. Large-scale test L4 (RMG 380 with vegetation), thermocouple tree 1.

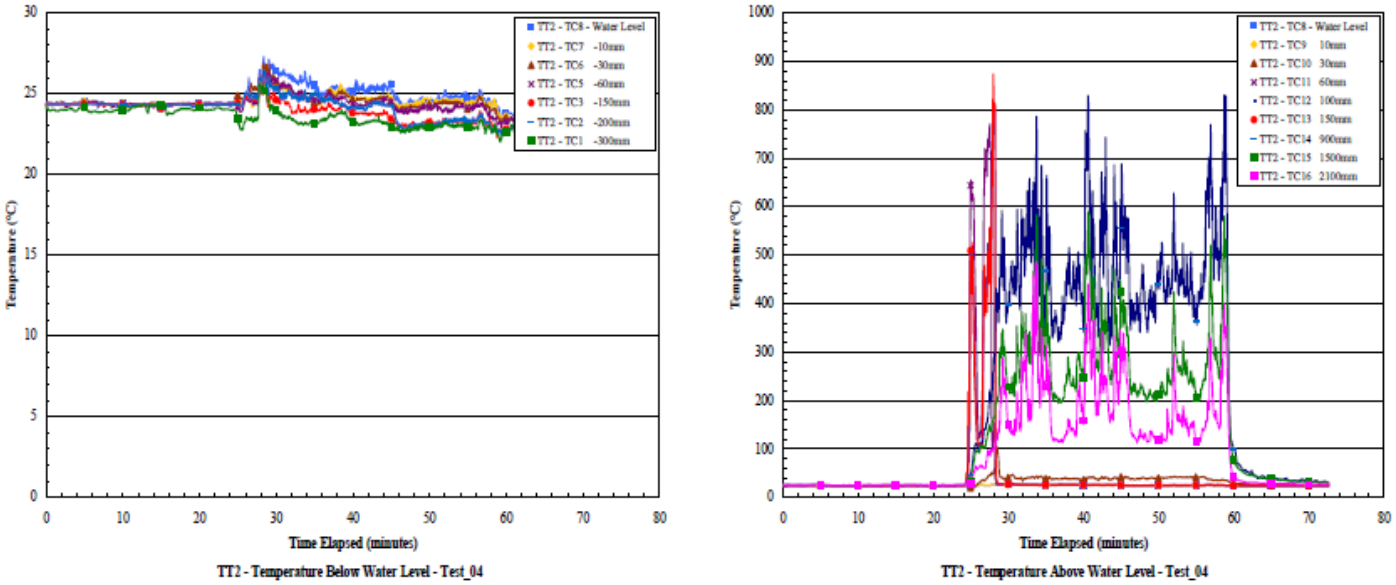

Figure F-13. Large-scale test L4 (RMG 380 with vegetation), thermocouple tree 2.

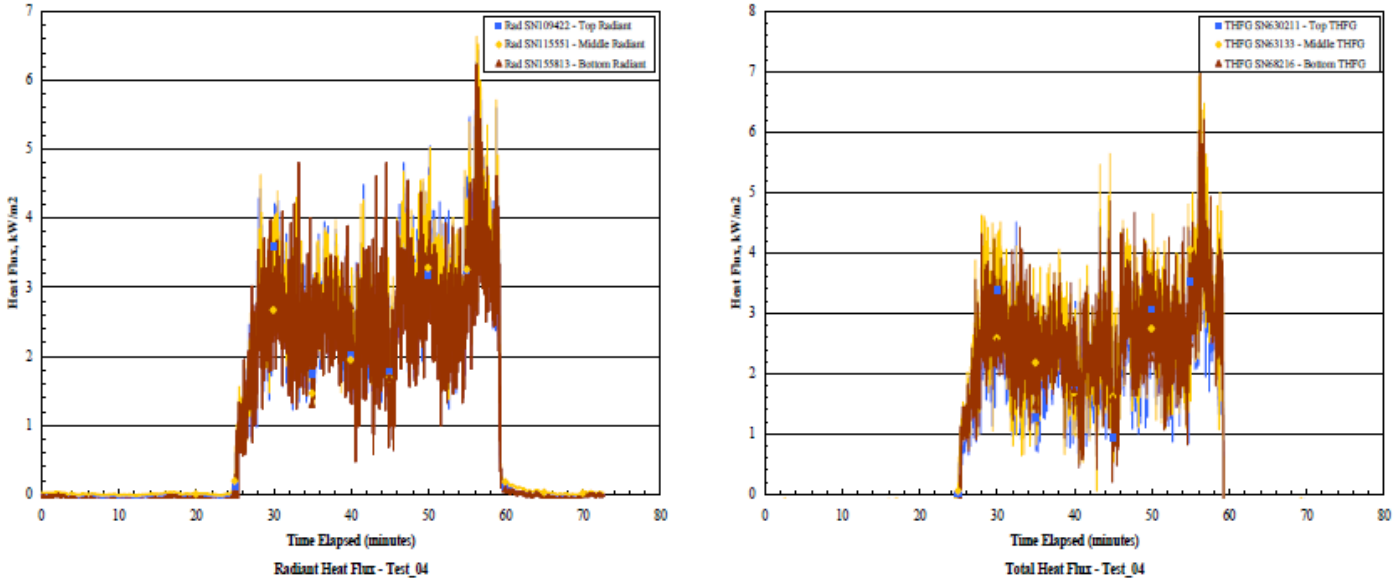

Figure F-14. Large-scale test L4 (RMG 380 with vegetation), radiant and total heat flux measurements.

(This page intentionally left blank.)

APPENDIX G. EPA RESIDUE AND WATER TOXICITY ANALYSIS

U.S. EPA Oil and Water Sample Hydrocarbon Chemistry Results with U.S. Coast Guard from the September 17-18 and October 22, 2019 Mobile Alabama In Situ Burn of Light Oil and RMG 380 oil (Mace Barron, Robyn Conmy, Devi Sundaravadivelu, Beth Moso, U.S. EPA, Office of Research and Development, Pegasus Technical Services, Inc.)

G.1 Crude Oil

Introduction

In collaboration with the U.S. Coast Guard (USCG), U.S. Environmental Protection Agency (EPA) staff collected oil and water samples from the in situ burn (ISB) of light oil at Little Sand Island, Mobile, Alabama. Samples were collected by EPA Office of Research and Development staff for subsequent quantification of petroleum hydrocarbons, with the results to be shared with USCG.

Sample Collection, Processing and Analysis

Samples were collected September 17 and 18, 2019, and included: pre-burn light oil, post burn oil residue (water surface, collection pads), and pre- and post-burn water samples. Samples were collected under chain of custody in pre-cleaned glass jars, stored on ice, and shipped to the EPA hydrocarbon analytical facility.

Samples were extracted and analyzed following EPA Standard Operating Procedures and the Quality Assurance Project Plan. Analytes included BTEX (benzene, toluene, ethylbenzene, xylenes), PAHs (polycyclic aromatic hydrocarbons and alkyl homologs), TPH (total petroleum hydrocarbons), alkanes (aliphatic hydrocarbons of 4 to 35 carbons), and hopanes (a conserved biomarker of petroleum).

- The analysis of volatile organic compounds (VOCs) was conducted using an Agilent 7890A Gas Chromatograph (GC) with a 5975C mass selective detector (MSD) with Triple Axis Detector and CombiPal autosampler (CTC Analytics) following modified EPA Method 524.3. Alkanes (C4-C9) and BTEX analytes were summed to compute ΣC4-C9 and ΣBTEX, respectively, and VOCs were computed from the sum of ΣC4-C9 and ΣBTEX.
- Alkanes (ΣC10-35) and PAHs were quantified using an Agilent 6890N GC with an Agilent 5975 MSD and an Agilent 7683 series autosampler, equipped with a DB-5 capillary column by J&W Scientific (30 m, 0.25 mm I.D., and 0.25 mm film thickness) and a splitless injection port as per EPA NRMRL-LMMD-34-0 SOP. Alkanes (C10-C35 normal aliphatics, and branched alkanes [pristine and phytane]) and PAHs (including 2-4 ring compounds and their alkylated homologs (i.e., C0-C4 naphthalenes, C0-C4 phenanthrenes, C0-C3 fluorenes, C0-C4 dibenzothiophenes, C0-C4 napthobenzothiophenes, C0-C4 pyrenes and C0-C4 chrysenes)) were summed to compute total alkane and PAH concentrations, respectively.
- The light oil used for the burn experiment (pre-burn oil-1) was used to prepare a six-point calibration curve for TPH quantification. An Agilent 7890B GC equipped with a flame ionization detector (FID) and 7693 autosampler following modified EPA Method 8015B.

Results Summary

Table G-1 summarizes the results of EPA oil and water samples collected from the ISB of the light oil.

Table G-1. Summary of crude oil chemical analysis.

Summary of petroleum hydrocarbons[A] in samples from the U.S. Coast Guard September 17 and 18 in situ burn of light oil, Little Sand Island, Mobile, Alabama.						
Sample Identification	**TPH**	**ΣC4-C9**	**ΣBTEX**	**ΣC10-35**	**ΣPAH**	**Hopane**
Oil sample units	**mg/mg**	**ng/mg**	**ng/mg**	**ng/mg**	**ng/mg**	**ng/mg**
Burn-1-Pad	1.378	80	235	32244	6487	62
Burn-1-Residue	1.841	33	291	50383	10412	94
Burn-2-Pad	1.736	144	438	49605	10032	92
Burn-2-Residue-Rep1	1.909	6	159	47767	9833	81
Burn-2-Residue-Rep2	1.890	22	281	53963	11437	106
Pre-burn oil-1	-	26390	104365	21600	3774	9
Pre-Burn oil-2	-	7746	21471	2127	465	1
Sample Identification	**TPH**	**ΣC4-C9**	**ΣBTEX**	**ΣC10-35**	**ΣPAH**	**Hopane**
Water sample units	**mg/L**	**ug/L**	**ug/L**	**ug/L**	**ug/L**	**ug/L**
Pre-burn Water-0917	<0.0001	0	9	3	2	0.018
Pre-burn Water-0918	<0.0001	7	123	52	27	0.442
Pre-burn Water-0919	1.355	16	280	32	10	0.132
Pre-burn Water-0920	0.381	12	164	40	9	0.157
Post-burn Water-0917	9.616	78	1489	57	42	0.160
Post-burn Water-0918	8.585	96	2140	68	39	0.250
A: TPH (total petroleum hydrocarbons); ΣC4-C9 (sum of detected alkanes with 4 to 9 carbons); BTEX (benzene, toluene, ethylbenzene, xylenes), ΣC10-C35 (sum of detected alkanes with 10 to 35 carbons); PAHs (polycyclic aromatic hydrocarbons and alkyl homologs); Hopane (geochemical biomarker of petroleum hydrocarbons).						

G.2 RMG 380 Oil

Samples were taken from two burns of RMG oil that were performed by USCG: Burn 1 (first burn; no vegetation); Burn 2 (second burn; vegetation present). Details of the ISBs are available in the USCG full report, including description of oil source, ISB facility, burn conditions (i.e., oil pumping rate, duration, temperatures, vegetation presence-absence, sample collection methods, etc).

Sample Collection, Processing and Analysis

Samples were collected October 22, 2019, and included: pre-burn RMG oil, post-burn oil residue (water surface, collection pads, sunken oil), and pre- and post-burn water samples. Water samples were collected by submersing the vessel below the water surface. Fresh oil samples were collected by direct dispensing from the source container. Residue samples were collected by either skimming floating oil, collection of

oiled pads, or scraping from the bottom of the burn facility. Samples were collected under chain of custody in pre-cleaned glass jars, stored on ice then refrigerated, and then shipped on ice to the EPA hydrocarbon analytical facility.

Extraction and Analyses

Samples were extracted and analyzed following EPA Standard Operating Procedures and the Quality Assurance Project Plan. Analytes included BTEX (benzene, toluene, ethylbenzene, xylenes), PAHs (polycyclic aromatic hydrocarbons and alkyl homologs), TPH (total petroleum hydrocarbons), alkanes (aliphatic hydrocarbons of 4 to 35 carbons), and C_{30}-αβ hopane (considered to be a conserved biomarker of petroleum).

The analysis of volatile organic compounds (VOCs) was conducted using an Agilent 7890A Gas Chromatograph (GC) with a 5975C mass selective detector (MSD) with Triple Axis Detector and CombiPal autosampler (CTC Analytics) following modified EPA Method 524.3. Alkanes (C4-C9) and BTEX analytes were summed to compute ΣC4-C9 and ΣBTEX, respectively, and VOCs were computed from the sum of ΣC4-C9 and ΣBTEX.

Table G-2. Description of samples of RMG 380 oil.

Description of samples collected by U.S. EPA during the October 22, 2019, in situ burn of RMG oil	
Sample[A]	**Description**
Water Samples	
Pre-burn water	Clean water from the ISB test pool prior to RMG oil addition
Post-burn 1 water	Pool water after the first ISB of RMG oil
Post-burn 2 water	Pool water after the second ISB of RMG oil
Pre-burn oil (Replicate A, B)	Separate samples of unburned RMG oil from the source tank.
Burn 1 RMG Samples	
Burn 1-ResidueA, Burn 1-ResidueB	Separate samples of burn residues floating on the water surface from the first ISB of RMG oil.
Burn1 collection pad	Burn residues collected on oleophilic pads.
Burn 2 RMG Samples	
Burn 2-ResidueA, Burn 2-ResidueB	Separate samples of burn residues floating on the water surface from the second ISB of RMG oil.
Burn 2 sunken oil	Sunken oil residues collected from pool bottom after second burn.
A. No collection pads in Burn 2.	

Alkanes (ΣC10-35), PAHs and hopane were quantified using an Agilent 6890N GC with an Agilent 5975 MSD and an Agilent 7683 series autosampler, equipped with a DB-5 capillary column by J&W Scientific (30 m, 0.25 mm I.D., and 0.25 mm film thickness) and a splitless injection port as per EPA NRMRL-LMMD-34-0 SOP. Alkanes (C10-C35 normal aliphatics, and branched alkanes [pristine and phytane]) and PAHs (including 2-4 ring compounds and their alkylated homologs (i.e., C0-C4 naphthalenes, C0-C4 phenanthrenes, C0-C3 fluorenes, C0-C4 dibenzothiophenes, C0-C4 napthobenzothiophenes, C0-C4 pyrenes and C0-C4 chrysenes) were summed to compute total alkane and PAH concentrations, respectively.

The RMG oil used for the burn experiment (Pre-Burn Oil replicate A) was used to prepare a six-point calibration curve for TPH quantification. An Agilent 7890B GC equipped with a flame ionization detector (FID) and 7693 autosampler was used for analysis following modified EPA Method 8015B.

Results Summary

Table G-3 summarizes the results of EPA oil and water samples collected from the ISB of the RMG oil.

In situ burning of RMG oil increased concentrations of oil components in both the first (Burn 1) and second burn (Burn 2) water samples, and decreased concentrations of oil components in the residue samples compared with pre-burn source oil.

Table G-3. Summary of RMG 380 oil chemical analysis.

Summary of petroleum hydrocarbons[A] in samples from the U.S. Coast Guard October 22, 2019, in situ burn of RMG oil, Little Sand Island, Mobile, Alabama.						
Sample Identification[B]	ΣC4-C9	ΣBTEX	alkanes	PAHs	Hopane	TPH
Water sample units	ng/L	ng/L	ng/L	ng/L	ng/L	mg/L
Pre-burn Water	479	151	6833	1237	54	6
Post-Burn 1 Water	18214	208968	82265	315655	440	11
Post-Burn 2 Water	6912	129019	66078	277183	383	10
Sample Identification[B]	ΣC4-C9	ΣBTEX	alkanes	PAHs	Hopane	TPH
Oil sample units	ng/g	ng/g	ng/mg	ng/mg	ng/mg	mg/mg
Burn 1-ResidueA	7074	43161	13346	43926	51	0.55
Burn 1-ResidueB	14229	67123	14159	41517	47	0.57
Burn 1-Collection Pad	30252	104109	14391	41124	47	0.75
Burn 2-ResidueA	221	290	3701	16070	42	0.28
Burn 2-ResidueB	282	384	4048	17283	41	0.33
Burn 2-Sunken Oil	2009	13526	4344	17095	26	0.26
Pre-Burn-Oil (replicate A)	218987	233735	23853	63635	69	-
Pre-Burn-Oil (replicate B)	78045	282740	24094	64001	66	-
A: TPH (total petroleum hydrocarbons); ΣC4-C9 (sum of detected alkanes with 4 to 9 carbons); BTEX (benzene, toluene, ethylbenzene, xylenes), ΣC10-C35 (sum of detected alkanes with 10 to 35 carbons); PAHs (polycyclic aromatic hydrocarbons and alkyl homologs); Hopane (geochemical biomarker of petroleum hydrocarbons). B: See Table 1 for sample descriptions.						

Disclaimer

The U.S. Environmental Protection Agency (EPA) through its Office of Research and Development analyzed the samples and summarized the data described herein under contract with Pegasus Technical Services. It has been subjected to the Agency's review, but this dataset is distributed solely for the purpose of data sharing with the US Coast Guard. It has not been formally disseminated to the public by EPA. It does not represent and should not be construed to represent any agency determination or policy. Any mention of trade names, products, or services does not imply an endorsement by the U.S. Government or EPA. The EPA does not endorse any commercial products, services, or enterprises. The contractor role did not include establishing Agency policy.